Tracking climate signals in tropical trees

New insights from Indonesian stable isotope records

Doctoral thesis

Karina Schollän

Helmholtz-Centre Potsdam
GFZ German Centre for GeoSciences

Faculty of Science
University of Potsdam, Germany

Institut für Erd- und Umweltwissenschaften
Mathematisch-Naturwissenschaftliche Fakultät
Universität Potsdam
und
Sektion 5.2 Klimadynamik und Landschaftsentwicklung
Helmholtz-Zentrum Potsdam – Deutsches GeoForschungsZentrum GFZ

Tracking climate signals in tropical trees

New insights from Indonesian stable isotope records

DISSERTATION

zur Erlangung des akademischen Grades
"doctor rerum naturalium" (Dr. rer. nat.)
in der Wissenschaftsdisziplin Paläoklimadynamik

eingereicht in Form einer publikationsbasierten Arbeit
an der Mathematisch-Naturwissenschaftlichen Fakultät
der Universität Potsdam

von
Karina Schollän

Potsdam, Februar 2014

Principal supervisor:

apl. Prof. Dr. Achim Brauer
Universität Potsdam
Helmholtz-Zentrum Potsdam, Deutsches GeoForschungsZentrum GFZ

Second supervisor:

Dr. Gerhard Helle
Helmholtz-Zentrum Potsdam, Deutsches GeoForschungsZentrum GFZ

Published online at the
Institutional Repository of the University of Potsdam:
URL http://opus.kobv.de/ubp/volltexte/2014/7194/
URN urn:nbn:de:kobv:517-opus-71947
http://nbn-resolving.de/urn:nbn:de:kobv:517-opus-71947

“Trees are poems that earth writes upon the sky.”

Khalil Gibran, Sand and Foam (1926)

Dedicated to the ones I love.

In memory of my grandfathers.

Abstract

The tropical warm pool waters surrounding Indonesia are one of the equatorial heat and moisture sources that are considered as a driving force of the global climate system. The climate in Indonesia is dominated by the equatorial monsoon system, and has been linked to El Niño-Southern Oscillation (ENSO) events, which often result in severe droughts or floods over Indonesia with profound societal and economic impacts on the populations living in the world's fourth most populated country. The latest IPCC report states that ENSO will remain the dominant mode in the tropical Pacific with global effects in the 21st century and ENSO-related precipitation extremes will intensify. However, no common agreement exists among climate simulation models for projected change in ENSO and the Australian-Indonesian Monsoon. Exploring high-resolution palaeoclimate archives, like tree rings or varved lake sediments, provide insights into the natural climate variability of the past, and thus helps improving and validating simulations of future climate changes.

Centennial tree-ring stable isotope records | Within this doctoral thesis the main goal was to explore the potential of tropical tree rings to record climate signals and to use them as palaeoclimate proxies. In detail, stable carbon ($\delta^{13}C$) and oxygen ($\delta^{18}O$) isotopes were extracted from teak trees in order to establish the first well-replicated centennial (AD 1900-2007) stable isotope records for Java, Indonesia. Furthermore, different climatic variables were tested whether they show significant correlation with tree-ring proxies (ring-width, $\delta^{13}C$, $\delta^{18}O$). Moreover, highly resolved intra-annual oxygen isotope data were established to assess the transfer of the seasonal precipitation signal into the tree rings. Finally, the established oxygen isotope record was used to reveal possible correlations with ENSO events.

Methodological achievements | A second goal of this thesis was to assess the applicability of novel techniques which facilitate and optimize high-resolution and high-throughput stable isotope analysis of tree rings. Two different UV-laser-based microscopic dissection systems were evaluated as a novel sampling tool for high-resolution stable isotope analysis. Furthermore, an improved procedure of tree-ring dissection from thin cellulose laths for stable isotope analysis was designed.

The most important findings of this thesis are: I) The herein presented novel sampling techniques improve stable isotope analyses for tree-ring studies in terms of precision, efficiency and quality. The UV-laser-based microdissection serve as a valuable tool for sampling plant tissue at ultrahigh-resolution and for unprecedented precision. II) A guideline for a modified method of cellulose extraction from wholewood cross-sections

and subsequent tree-ring dissection was established. The novel technique optimizes the stable isotope analysis process in two ways: faster and high-throughput cellulose extraction and precise tree-ring separation at annual to high-resolution scale. III) The centennial tree-ring stable isotope records reveal significant correlation with regional precipitation. High-resolution stable oxygen values, furthermore, allow distinguishing between dry and rainy season rainfall. IV) The $\delta^{18}O$ record reveals significant correlation with different ENSO flavors and demonstrates the importance of considering ENSO flavors when interpreting palaeoclimatic data in the tropics.

The findings of my dissertation show that seasonally resolved $\delta^{18}O$ records from Indonesian teak trees are a valuable proxy for multi-centennial reconstructions of regional precipitation variability (monsoon signals) and large-scale ocean-atmosphere phenomena (ENSO) for the Indo-Pacific region. Furthermore, the novel methodological achievements offer many unexplored avenues for multidisciplinary research in high-resolution palaeoclimatology.

Keywords

oxygen and carbon stable isotopes, tree rings, multi-parameter approach, UV-laser microdissection, cellulose cross-sections, *Tectona grandis*, tropics, dendroclimatology, seasonal rainfall variability, ENSO flavors

Zusammenfassung (German Abstract)

Die tropischen Gewässer um Indonesien sind eine der äquatorialen Wärme- und Feuchtigkeitsquellen, die als treibende Kraft des globalen Klimasystems betrachtet werden können. Das Klima in Indonesien ist geprägt durch das Australisch-Indonesische Monsunsystem. Weiterhin besteht eine Verknüpfung mit El Niño-Southern Oszillation (ENSO) Ereignissen, die oft zu schweren Dürren oder Überschwemmungen in der Region mit tiefgreifenden gesellschaftlichen und wirtschaftlichen Folgen führen. Der neueste IPCC-Bericht legt dar, dass ENSO auch in den nächsten 100 Jahren das vorherrschende Klimaphänomen im tropischen Pazifik bleiben wird. Ferner wird davon ausgegangen, dass sich die ENSO-bezogenen Niederschlagsextrema intensivieren werden. Wenig Übereinstimmung herrscht jedoch bislang zwischen den Klimasimulationsmodellen in Bezug auf die voraussichtlichen Veränderungen von ENSO und dem Australisch-Indonesischen Monsunsystem. Hochaufgelöste Paläoklima-Archive, wie z.B. Jahrringe oder warvierte Seesedimente, geben Auskunft über die natürliche Klimavariabilität der Vergangenheit und können somit dazu beitragen, die Computersimulationen der künftigen Klimaentwicklung zu verbessern und zu validieren.

Hundertjährige stabile Jahrring-Isotopenchronologien | Das Hauptziel dieser Doktorarbeit war es, dass Potenzial von tropischen Jahrringen zur Aufzeichnung von Klimasignalen herauszustellen und deren Evaluierung als Paläoklimaproxys. Im Detail wurden stabile Kohlenstoff- ($\delta^{13}C$) und Sauerstoff- ($\delta^{18}O$) Isotopenverhältnisse in Teakbäumen analysiert, und die ersten gut replizierten hundertjährigen (AD 1900-2007) stabilen Isotopenchronologien aus Java (Indonesien) erstellt. Dabei wurden verschiedene klimatische Einflussgrößen getestet, ob diese signifikante Korrelationen mit den Jahrringparametern aufzeigen. Weiterhin wurden hochaufgelöste intra-annuelle Sauerstoffisotopenzeitreihen erstellt, um den Transfer des saisonalen Niederschlagssignals in den jeweiligen Jahrring zu bemessen. Die ermittelte Sauerstoff-Isotopenchronologie wurde anschließend auf mögliche ENSO Signale hin untersucht.

Methodische Errungenschaften | Ein zweites Ziel dieser Arbeit war es neue Verfahren zur Analyse stabiler Isotope in Baumjahrringen zu entwickeln und zu optimieren. Zwei verschiedene UV-Lasermikrodissektions-Systeme wurden getestet als neues präzises Präparationswerkzeug für stabile Isotopenstudien. Darüber hinaus wurde eine verbesserte Methode für die Probenaufbereitung stabiler Isotopenmessungen anhand von Zellulose-Dünnschnitten entwickelt.

Die wichtigsten Ergebnisse dieser Doktorarbeit sind: I) Die hier vorgestellten neuartigen Techniken zu Probenvorbereitung verbessern die Analyse stabiler Isotope für Jahrringstudien in Hinsicht auf Präzision, Effizienz und Qualität. Es wurde gezeigt, dass die UV-Lasermikrodissektion eine wertvolle Technik ist, um die Beprobung von Pflanzengewebe in höchster Auflösung und beispielloser Präzision durchzuführen. II) Es ist gelungen, einen Leitfaden für ein modifiziertes Verfahren der Zelluloseextraktion an Gesamtholz-Dünnschnitten und der anschließenden Jahrringaufbereitung zu erstellen. Diese neuartige Methode optimiert die Analyse stabiler Isotopenzeitreihen in zweierlei Hinsicht: schnellere und effiziente Zelluloseextraktion und präzise Trennung der Jahrringsequenzen in inter-annueller bis intra-annuelle Auflösung. III) Die hundertjährigen stabilen Jahrring-Isotopenchronologien weisen signifikante Korrelationen mit dem regionalen Niederschlag auf. In den hochaufgelösten stabilen Sauerstoffisotopenwerten spiegelt sich deutlich das Niederschlagssignal der Trocken- und der Regenzeit wieder. IV) Die stabile Sauerstoffisotopenzeitreihe zeigt signifikante Korrelationen mit verschiedenen ENSO Phasen. Dies betont, dass die verschiedenen ENSO Phasen bei der Interpretation von tropischen Paläodaten zu berücksichtigen sind.

Die Ergebnisse der Dissertation zeigen, dass saisonal aufgelöste stabile Sauerstoffisotopenchronologien von indonesischen Teakbäumen ein geeigneter Proxy für mehrhundertjährige Rekonstruktionen der regionalen Niederschlagsvariabilität (Monsun-Signale) und großräumiger Ozean-Atmosphären-Systeme (ENSO) für den Indopazifik ist. Darüber hinaus bieten die neuartigen methodischen Errungenschaften viele neue Ansätze für multidisziplinäre hochaufgelöste Studien in der paläoklimatologischen Forschung.

Stichworte

Stabile Sauerstoff- und Kohlenstoffisotope, Jahrringe, Multiparameter Ansatz, UV-Lasermikrodissektion, Zellulose-Dünnschnitte, *Tectona grandis*, Tropen, Dendro-klimatologie, saisonale Niederschlagsvariabilität, ENSO Phasen

Table of Contents

Abstract		I
Zusammenfassung (German Abstract)		III
List of Figures		VII
List of Tables		VIII
List of Abbreviations		IX
List of Publications		X
Thesis at a glance		XI
Chapter 1	General Introduction	1
	Preface to Chapter 2	7
Chapter 2	UV-laser-based microscopic dissection of tree ring – a novel sampling tool for $\delta^{13}C$ and $\delta^{18}O$ studies (*New Phytologist,* 2014)	9
	Preface to Chapter 3	29
Chapter 3	Tree-ring dissection from cellulose thin sections – an improved procedure of sample preparation for stable isotope analysis in tree rings (*Manuscript in preparation*)	31
	Preface to Chapter 4	47
Chapter 4	Multiple tree-ring chronologies (ring width, $\delta^{13}C$ and $\delta^{18}O$) reveal dry and rainy season signals of rainfall in Indonesia (*Quaternary Science Reviews*, 2013)	49
	Preface to Chapter 5	73
Chapter 5	ENSO flavors in a tree-ring $\delta^{18}O$ record of *Tectona grandis* from Indonesia (*Clim. Past Discussions*, 2014)	75
Chapter 6	Synthesis	89
Chapter 7	Appendix	97
Chapter 8	References	125
Eidesstattliche Erklärung / Declaration of Academic Honesty		i
Curriculum Vitae		iii
Acknowledgements / Danksagung		iv

List of Figures

FIGURE 1.1 | Map of the observed temperature and precipitation changes in Southeast Asia of the last 110 years..... 3
FIGURE 1.2 | Thesis structure as a flow chart. 6
FIGURE 2.1 | Possible steps of wood sample preparation and high-precision sampling using UV-laser-based microscopic dissection systems 13
FIGURE 2.2 | Schematic examples of different dissected wood tissues from several tree species for cutting process with an UV-laser microscopic dissection system. 15
FIGURE 2.3 | Microscopic image of a teak (*Tectona grandis*) cross-section..... 18
FIGURE 2.4 | Comparison between $\delta^{13}C$ values from resin-extracted wood and cellulose of ray parenchyma and xylem tissue in tree rings of an oak sample. 19
FIGURE 2.5 | Intra-annual $\delta^{18}Owd$ variations from teak (*Tectona grandis*) collected in the eastern part of Central Java, Indonesia and corresponding precipitation data. 20
FIGURE 2.6 | Seasonal variations of wood density and stable isotope ratios of a pine tree (*Pinus strobus*) from northwestern Germany for 1977 and corresponding daily temperature, precipitation and relative humidity data. 21
FIGURE 2.7 | Non-linear seasonal growth increments and longevity of cells during the vegetation period for conifers at temperate sites 25
FIGURE 3.1 | Scheme of the cellulose extraction from wholewood cross-sections..... 36
FIGURE 3.2 | Tree-ring dissection technique using cellulose cross-sections..... 37
FIGURE 3.3 | FTIR Spectra of untreated wholewood, resin extracted wholewood, holocellulose of wood samples and α-cellulose standards……...…40
FIGURE 3.4 | Comparison between $\delta^{13}C$ and $\delta^{18}O$ values from cellulose of two teak trees using the standard method of cellulose extraction and the cross-section method……....41
FIGURE 3.5 | Tree species that have been tested for cellulose extraction on wholewood cross-
sections……42
FIGURE 4.1 | Map showing the location of the study site in a lowland rain forest in the eastern part of Central Java (07°52'S, 111°11'E). 53
FIGURE 4.2 | Mean monthly rainfall and temperature at the study site derived from a regional mean of different stations for rainfall (1900-2002) and gridded climate data for temperature……...54
FIGURE 4.3 | Tree-ring series of ring width, $\delta^{13}C$ and $\delta^{18}O$ 58
FIGURE 4.4 | Correlations of TRW, $\delta^{13}C_{TR}$ and $\delta^{18}O_{TR}$ chronologies with monthly and seasonal rainfall (1900-2002). 61
FIGURE 4.5 | A conceptional model of oxygen isotope fractionation and the seasonal cycle of rainfall in the tropics. 66

FIGURE 4.6 | Comparison of the influence of different rainfall conditions during dry and rainy season on the tree-ring $\delta^{18}O$ values. ‘’+‘’ and ‘’-’’ represent below or above average rainfall amount for corresponding season. 68
FIGURE S4.1 | Map of Central/Eastern Java indicating the study site and climate stations with rainfall data……...70
FIGURE S4.2 | Annual rainfall data from climate stations…….70
FIGURE 5.1 | Regression coefficients (mm day-1 °C) of precipitation on the Warm Pool (WP) and the Cold Tongue (CT) El Niño index. 80
FIGURE 5.2 | Time series of the tree-ring $\delta^{18}O$ chronology and the January to February time-averaged indices of Warm Pool (WP) El Niño and La Niña 84
FIGURE 5.3 | Probability density function of tree-ring $\delta^{18}O$ variability from different ENSO types……..85
FIGURE 5.4 | Spectral analysis of the tree-ring $\delta^{18}O$ chronology from 1900 to 2007 and Wavelet coherence transform comparing shared frequency between tree-ring $\delta^{18}O$ record and Warm Pool (WP) El Niño index and La Niña index for 1900 to 2007…….86

List of Tables

TABLE 2.1 | Comparison of the characteristics of the two UV-laser-based microscopic dissection systems tested. 27
TABLE 4.1 | Descriptive statistics for the tree-ring width (TRW), $\delta^{13}C_{TR}$ and $\delta^{18}O_{TR}$ chronologies. 59
TABLE 4.2 | Pearson correlation coefficients between tree-ring parameters and rainfall data for different time periods 60
TABLE S4.1 | Climate stations with rainfall data used for calculating of regional rainfall mean (REG)..... 71
TABLE 5.1 | Classification into ENSO flavors and phase based on $Jan_{n+1}Feb_{n+1}$ values .. 81
TABLE 5.2 | Correlation values between the annually resolved $\delta^{18}O_{TR}$ record and climate months of different ENSO flavors 82

List of Abbreviations

Institutes, agencies and projects

GFZ	German Research Centre for Geosciences, Germany
GNIP	Global Network of Isotopes in Precipitation
IAEA	International Atomic Energy Agency
IPCC	Intergovernmental Panel on Climate Change
CRU	Climate Research Unit
GPCC	Global Precipitation Climatology Centre

Definitions and parameters

$\delta^{13}C$	Stable carbon isotopes
$\delta^{13}C_{TR}$ / $\delta^{13}C_{wd}$	$\delta^{13}C$ value of tree ring from resin extracted wood material
$\delta^{13}C_{cel}$	$\delta^{13}C$ value of tree-ring holocellulose
$\delta^{18}O$	Stable oxygen isotopes
$\delta^{18}O_{TR}$/ $\delta^{18}O_{wd}$	$\delta^{18}O$ value of tree ring from resin extracted wood material
$\delta^{18}O_{cel}$	$\delta^{18}O$ value of tree-ring holocellulose
$\delta^{18}O_{Pre}$	$\delta^{18}O$ value of precipitation
TRW	Tree-ring width
ENSO	El Niño–Southern Oscillation
CT El Niño	Cold Tongue El Niño
WP El Niño	Warm Pool El Niño

Analytical standards and techniques

VSMOW	Vienna Standard Mean Ocean Water
VPDB	Vienna Pee Dee Belemnite
IRMS	Isotope ratio mass spectrometry
CRDS	Cavity ring-down spectroscopy

Other abbreviations

a.s.l.	above sea level
DNLY	Donoloyo Cagar Alam (Donoloyo), tree-ring sampling site located in Central Java, Indonesia (07°52'S, 111°11'E)

List of Publications

MANUSCRIPT 1:

Schollaen, K., Heinrich, I., Helle, G. (2014). UV-laser-based microscopic dissection of tree rings – a novel sampling tool for $\delta^{13}C$ and $\delta^{18}O$ studies.
New Phytologist, 201 (3), 1045-1055, doi:10.1111/nph.12587

MANUSCRIPT 2:

Schollaen, K., Baschek, H., Helle, G. Tree-ring dissection from cellulose thin sections - an improved procedure of sample preparation for stable isotope analysis in tree rings.
Manuscript in preparation for publication

MANUSCRIPT 3:

Schollaen, K., Heinrich, I., Neuwirth, B., Krusic, P.J., D´Arrigo, R.D., Karyanto, O., Helle, G. (2013). Multiple tree-ring chronologies (ring width, $\delta^{13}C$ and $\delta^{18}O$) reveal dry and rainy season signals of rainfall in Indonesia.
Quaternary Science Reviews, 73, 170-181

MANUSCRIPT 4:

Schollaen, K., Karamperidou, C., Krusic, P.J., Cook, E.R., Helle, G. (2014). ENSO flavors in a tree-ring $\delta^{18}O$ record of *Tectona grandis* from Indonesia.
Clim. Past Discuss., *10, 3965-3987*

Further publications:

Schollaen, K. and G. Helle (2013). Testing the influence of graphite and gypsum markings on stable isotope values ($\delta^{13}C$, $\delta^{18}O$) in tropical tree rings. *TRACE* Vol. 11, Proceedings of the DENDROSYMPOSIUM 2012: 85-87.

Schollaen, K., Heinrich, I. and G. Helle (2013). A novel approach for the preparation of high-resolution stable isotope records from tropical tree rings. *TRACE* Vol. 11, Proceedings of the DENDROSYMPOSIUM 2012: 71-76.

Hennig [Schollaen], K., Helle, G., Heinrich, I., Neuwirth, B., Karyanto, O. and M. Winiger (2011). Toward multi-parameter records (ring width, $\delta^{13}C$, $\delta^{18}O$) from tropical tree-rings - A case study on *Tectona grandis* from Java, Indonesia. *TRACE* Vol. 9, Proceedings of the DENDROSYMPOSIUM 2010: 158-165.

Thesis at a glance

MANUSCRIPT 1: UV-laser-based microscopic dissection of tree rings – a novel sampling tool for $\delta^{13}C$ and $\delta^{18}O$ studies

Rationale Evaluation of UV-laser-based microscopic dissection systems as a novel sampling tool for stable isotope studies.

Methods The system was utilized for high-resolution isotopic analyses ($\delta^{13}C/\delta^{18}O$) on thin wood cross-sections from different tree species.

Results The applications demonstrate that the introduced method allows for sampling plant tissue at ultrahigh resolution and unprecedented precision.

Conclusions The technique facilitates sampling for stable isotope analysis like combined tree eco-physiological, wood anatomical and dendroclimatological studies.

Author´s contributions: I developed the study idea and the experimental design, collected the data and carried out laboratory experiments, performed the data analysis and interpretation and wrote the manuscript. *I. Heinrich* contributed to the data interpretation and reviewed the manuscript. *G. Helle* provided guidance and help in constructing the study design, contributed to the data interpretation and reviewed the manuscript.

MANUSCRIPT 2: Tree-ring dissection from cellulose thin sections – an improved procedure of sample preparation for stable isotope analysis in tree rings

Rationale To establish a fast and precise method for preparing tree-ring samples for IRMS by tree-ring dissection from thin cellulose cross-section.

Methods Cellulose extraction process was conducted in a custom teflon device.

Results The new methodology makes sample homogenization obsolete and enables high-throughput stable isotope analysis that can be applied to a large number of coniferous and deciduous tree species.

Conclusions The cellulose extraction method combined with subsequent tree-ring dissection is an important approach to optimize stable isotope analysis in two ways: faster and costumer friendly cellulose extraction and precise tree-ring separation at inter- to intra-annual scale.

Author´s contributions*:* I and *H. Baschek* developed the experimental design and carried out the sample preparation and cellulose extraction procedure. *H. Baschek* provided help with the stable isotope measurements. I performed the validation of the method (FTIR spectrometry, comparison with standard methods) and wrote the manuscript. *H. Baschek* and *G. Helle* helped with writing and editing of the manuscript at various stages.

MANUSCRIPT 3: Multiple tree-ring chronologies (ring width, $\delta^{13}C$ and $\delta^{18}O$) reveal dry and rainy season signals of rainfall in Indonesia

Rationale Evaluation of the influence of rainfall variability on multiple tree-ring parameter of teak (*Tectona grandis*).

Methods Stable isotope analysis were conducted to obtain $\delta^{13}C/\delta^{18}O$ records. Intra-annual $\delta^{18}O_{TR}$ profiles were investigated by using UV-laser dissection. Furthermore climate-proxy relationships were assessed.

Results $\delta^{13}C/\delta^{18}O$ records reveal significantly higher rainfall signals than tree-ring widths. $\delta^{18}O$ responds to peak dry and rainy season rainfall, where high-resolution $\delta^{18}O$ values can distinguish seasonal rainfall variability.

Conclusions The $\delta^{18}O$ record is a valuable proxy for high-resolution multi-centennial reconstruction of seasonal rainfall variability over Indonesia.

Author´s contributions*:* I developed the structure and objectives of this study, the experimental design, carried out field sampling and laboratory experiments, performed the data analysis and interpretation and wrote the manuscript. *I. Heinrich* helped with the data analysis and provided valuable reviews at various stages of the manuscript. *B. Neuwirth* and *P. Krusic* reviewed the manuscript. *R. D´Arrigo* provided additional wood sample material. *O. Karyanto* enabled sampling and provided logistical support during the field campaign. *G. Helle* provided guidance and help during the field campaign, contributed to the interpretation of the results and reviewed the manuscript at various stages.

MANUSCRIPT 4: ENSO flavors in a tree-ring $\delta^{18}O$ record of Tectona grandis from Indonesia

Rationale To investigate ENSO signals in an Indonesian tree-ring $\delta^{18}O$ record.

Methods Statistical analysis were conducted to define ENSO-proxy relationships and to test for temporal stability.

Results A clear influence of Warm Pool El Niños was revealed while no clear signal of Cold Tongue El Niños was found.

Conclusions The $\delta^{18}O$ record indicate potential for generating reconstructions of different ENSO flavors for the East Pacific region and demonstrates the importance of considering ENSO flavors when interpreting palaeoclimatic data.

Author´s contributions*:* I developed the study idea and the experimental design, performed the data analysis and interpretation and wrote the manuscript. *C. Karamperidou* helped with the performance of Figure 1 and provided valuable assistance with statistical analysis, interpretation of results and reviews at various stages of the manuscript. *E. Cook* and *P. Krusic* provided a programme for Kalman filter analysis, helped with data discussion and contributed valuable comments and improvements to the final draft of the manuscript. *G. Helle* had helpful comments on a final version of the manuscript.

Chapter 1

General Introduction

1.1. Introduction and scientific rationale

A global warming in the climate is unequivocal and since the 1950s many of the observed changes are unprecedented over decades to millennia. Thus, the atmosphere and ocean have warmed, the amounts of snow and ice have diminished, sea level has risen and the concentrations of greenhouse gases have increased (IPCC, 2013). This is one of the key statements of the IPCC Fifth Assessment Report, emphasizing that global climate change has increasingly become a matter of public concern. Moreover, observed precipitation changes reveal that wet regions get wetter and dry regions get dryer as it has been observed since the second half of the 20th century. Additionally, extreme weather and climate events became more frequent (IPCC, 2013).

These significant changes in the climate system are also observed in Southeast Asia (FIGURE 1.1A/B), the most populous region of Asia, where changes in the strength, timing or distribution of the monsoon can result in severe floods or droughts, crop failures and famines. Thus the capacity to accurately predict changes in future monsoon variability is of great societal interest. However, hydroclimate predictions at regional to global scale tend to be biased to higher values due to an incomplete spatial coverage of observational records (Wan et al., 2013). Especially over the Australian Maritime Continent (AUSMC) monsoon region (FIGURE 1.1C) including the Indonesian Archipelago where long-term precipitation datasets are scarce (Figure 3 in Wan et al., 2013), the agreement among models simulating monsoon circulation changes is low (FIGURE 1.1D).

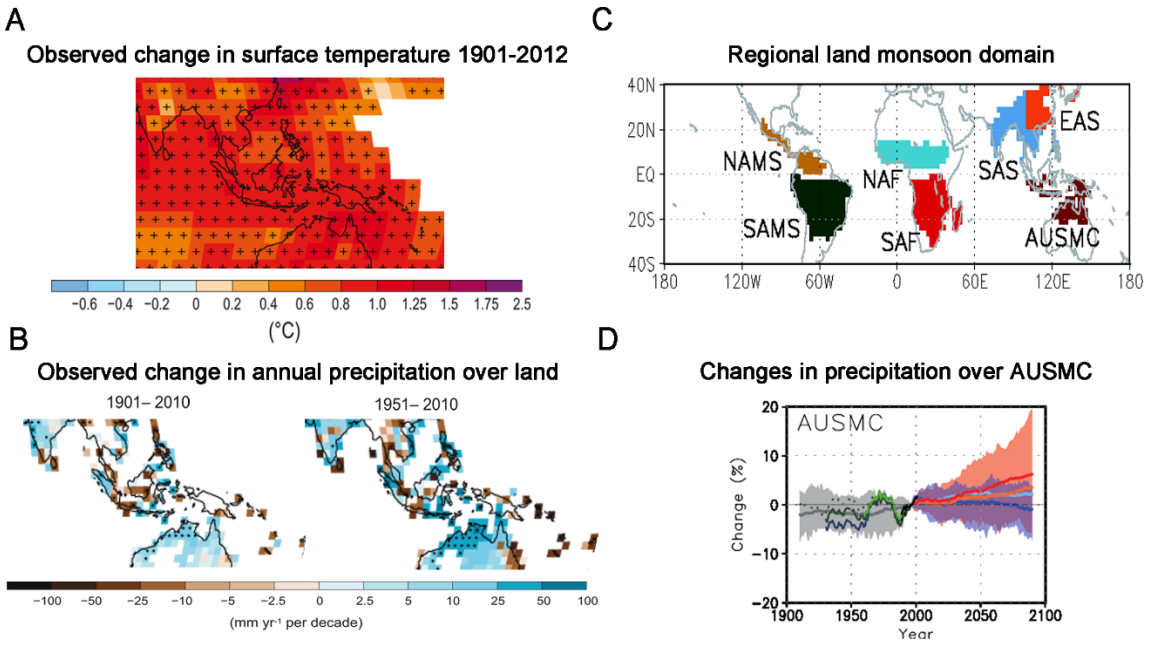

FIGURE 1.1 | Map of the observed temperature (A) and precipitation (B) changes in Southeast Asia of the last 110 years derived from the HadCRUT4 dataset (IPCC, 2013, Figure SPM.1) and the GPCC dataset (IPCC, 2013, Figure SPM.2) , respectively. (C) Regional land monsoon domain

based on 26 CMIP5 multi-model mean precipitation (IPCC, 2013, Figure 14.3) and (D) changes in precipitation indices over the Australian-Maritime-Continent (AUSMC) monsoon region based on CMIP5 multi-models (IPCC, 2013, Figure 14.4).

The reconstruction of palaeoclimate helps to improve and validate the capability of climate models to simulate future climate changes. Palaeoclimate information has been preserved in natural archives like ice cores, speleothems, corals, terrestrial and marine sediments or in tree rings. High-resolution palaeoclimate records focus on climate proxies at seasonal to annual resolutions. These proxy records may extend back continuously from the present, or provide discrete windows into the past, to shed light on high-frequency climate dynamics (e.g. modes of variability, abrupt climate changes, climate system feedbacks) on timescales beyond the length of instrumental records (Hughes, 2011). In particular, palaeoclimate archives help to place contemporary climate variability in a long-term perspective and provide quantitative information on the Earth-system response to forcing mechanisms (IPCC, 2013).

The Indonesian maritime continent is the region of highest convective activity in the world and a centre of heat fluxes that are essential to the global climate system. By choosing tropical tree-ring records from Indonesia for climate investigations, this thesis aims to improve the understanding of tropical climate variability and may help to characterize large-scale ocean-atmosphere phenomena such as the El Niño Southern Oscillation (ENSO) system that has global influence through atmospheric teleconnections affecting weather variability worldwide. Dendroclimatological studies from this region carry a great potential to provide land-based rainfall proxy records and thus may help to improve the capacity to more accurately predict changes in future monsoon variability over the Australian Maritime Continent.

1.2. Objectives and approaches

The overall aim of this thesis was to explore the potential of tree-ring stable isotope records from Indonesia as climate proxies. To date only a few palaeoclimate studies enlighten our understanding of climate variability in the Indonesian region using proxy archives such as corals, speleothems or tree-ring widths. In this thesis, I present the first well-replicated centennial stable isotope records ($\delta^{13}C/\delta^{18}O$) for Java, Indonesia derived from teak trees. Therefore, a study site with a rather weak climate signal in the tree-ring width chronology (D'Arrigo et al., 2006) was selected in order to test if tree-ring stable isotopes provide a better climate signal and/or give additional insights into tropical climate dynamics.

The specific **research objectives** are:

- Establishment of centennial well-replicated multiple tree-ring chronologies (ring-width, $\delta^{13}C$, $\delta^{18}O$) from Java, Indonesia (*Chapter 4*),
- Assessment of statistical and mechanistic relationships between tree-ring records and climate variables for the 20th century (*Chapter 4*),
- Establishment of highly resolved intra-annual $\delta^{18}O$ data to assess the transfer and timing of precipitation signals into the tree rings of teak (*Chapter 2 and Chapter 4*) and
- Investigation of ENSO signals in the annual tree-ring $\delta^{18}O$ record (*Chapter 5*).

Stable isotope records from tree rings are valuable palaeoclimate proxies (e.g. Helle and Schleser, 2004b; McCarroll and Loader, 2004), however, the sample preparation is still labour intensive and the accurate preparation of intra-seasonally resolved datasets is still challenging. Thus, a second aim of this thesis was to assess the applicability of novel techniques which facilitate and optimize high-resolution and high-throughput stable isotope analysis of tree rings.

Hence, **methodological approaches** of this thesis are:

- Assessing the usefulness of UV-laser microdissection microscopes as a high-resolution sampling tool for stable isotope research (*Chapter 2*) and
- Establishment of an improved procedure of sample preparation for high-throughput stable isotope analysis of tree rings (*Chapter 3*).

1.3. Thesis structure

This thesis is organized as a "cumulative thesis" consisting of four manuscripts that are published, ubmitted or in preparation for publication in ISI-listed peer-reviewed journals. A short overview about the manuscripts, including the contribution of the authors, is given in section "Thesis at a glance".

Chapter 1 presents a general introduction presenting the scientific rationale and objectives of this thesis. *Chapter 2-5* contain the manuscripts which can be divided into two parts: methodological approaches (*Chapter 2-3*) and research papers (*Chapter 4-5*) (FIGURE 1.2). A *preface* prior to Chapter 2-5 provides introductory remarks for each of the following manuscripts and ensures an adequate transition between them.

The methodological manuscripts introduce novel approaches which facilitate and optimize the sampling for stable isotope analyses while the research manuscripts focus on tracking climate signals in tree-ring records from Indonesia applying the methods established. The research papers contain a detailed description of the study site and the climate characteristics as well as the material and methodology applied.

Chapter 6 gives a synthesis of the most important findings presented in the manuscripts and highlights the accomplished scientific advances. It also offers avenues for future research. The appendix (*Chapter 7*) includes three additional manuscripts (*Appendix A-C*) that have been published in international peer-reviewed proceedings, and the tree-ring data (*Appendix D*) presented in this thesis. The references are listed in *Chapter 8*.

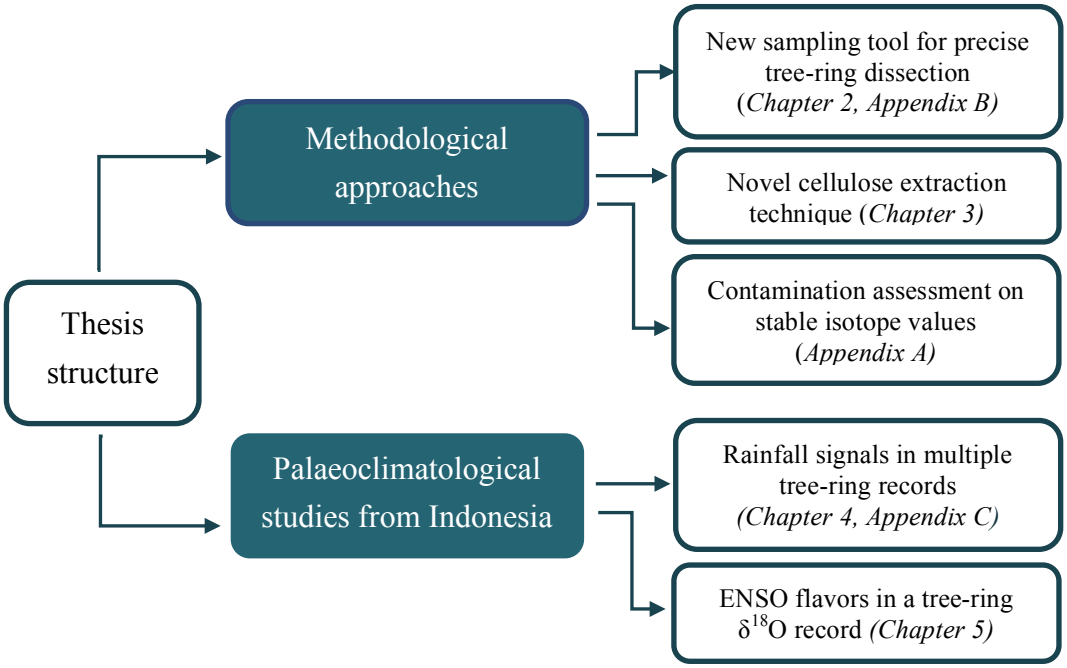

FIGURE 1.2 | Thesis structure as a flow chart. The chapters dealing with the different topics are indicated. A short manuscript overview can be seen in section "Thesis at a glance".

Preface to Chapter 2

Trees assimilate carbon from the atmosphere, take hydrogen and oxygen from soil water to grow and to form wood layers. The stable isotope ratios of the three elements are stored in the, generally annual formed, tree-rings and carry signals that can be interpreted in terms of past climate because isotope ratios are climatically controlled by the trees water and gas exchange budgets (Gagen et al., 2011). Robust mechanistic models do exist describing how carbon, hydrogen and oxygen are fractionated during photosynthesis by plants. This mechanistic understanding on the leaf level is being used to interpret climate signals from stable isotope ratios of tree rings (Barbour, 2007; Farquhar et al., 1982; Helle and Schleser, 2004b; McCarroll and Loader, 2004; Roden et al., 2000; Sternberg, 2009).

Stable isotope in tree rings are high-resolution palaeoclimate proxies that can be resolved from inter-annual to intra-annual scale. Recent advances in analytical methodology make tree-ring stable isotope measurements viable for non-specialist laboratories (Boettger et al., 2007; McCarroll and Loader, 2004; Saurer et al., 1998). However, sample preparation in general and particularly for stable isotope analysis aiming to resolve intra-seasonal climate and environmental information from tree rings is still labour intensive. Accurate preparation of high-resolution samples is likewise required and challenging

.

In the following chapter a novel sampling tool for high-resolution tree-ring stable isotope studies is presented. This sampling system was tested on different tree species and was particularly applied to exploring seasonal climate signals in $\delta^{18}O$ values of teak samples from the study site of this thesis (Java, Indonesia).

Chapter 2

UV-laser-based microscopic dissection of tree rings – a novel sampling tool for $\delta^{13}C$ and $\delta^{18}O$ studies

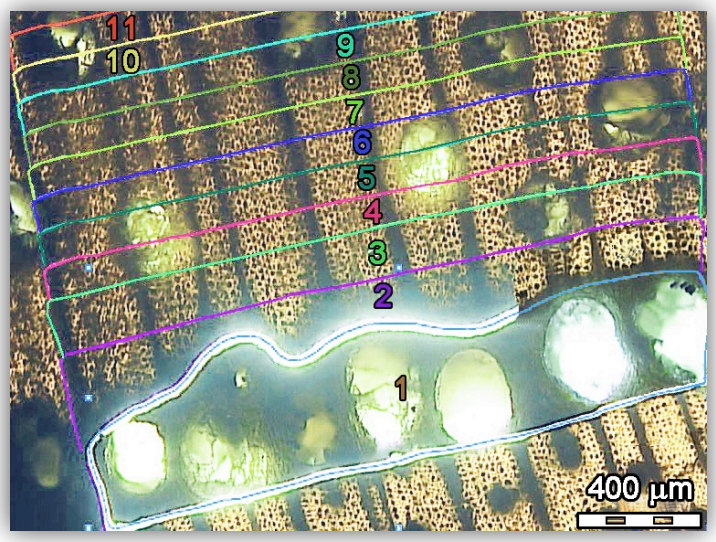

UV-laser dissection of a teak (*Tectona grandis*) cross-section
(Author´s picture: photograph taking during cutting process)

This chapter was published in:

New Phytologist, 2014, V. 201 (3), p. 1045-1055, doi:10.1111/nph.12587

Authored by Karina Schollaen, Ingo Heinrich and Gerhard Helle

GFZ - German Research Centre for Geosciences, Section 5.2 Climate Dynamics and Landscape Evolution, Telegrafenberg, 14473 Potsdam, Germany

Abstract

UV-laser-based microscopic systems were utilized to dissect and sample organic tissue for stable isotope measurements from thin wood cross-sections.

We tested UV-laser-based microscopic tissue dissection in practice for high-resolution isotopic analyses ($\delta^{13}C/\delta^{18}O$) on thin cross-sections from different tree species. The method allows serial isolation of tissue of any shape and from millimeter down to micrometer scale. On-screen pre-defined areas of interest were automatically dissected and collected for mass spectrometric analysis.

Three examples of high-resolution isotopic analyses revealed that: in comparison to $\delta^{13}C$ of xylem cells, woody ray parenchyma of deciduous trees have the same year-to-year variability, but reveal offsets that are opposite in sign depending on whether wholewood or cellulose is considered; high-resolution tree-ring $\delta^{18}O$ profiles of Indonesian teak reflect monsoonal rainfall patterns and are sensitive to rainfall extremes caused by ENSO; and seasonal moisture signals in intra-annual tree-ring $\delta^{18}O$ of white pine are weighted by non-linear intra-annual growth dynamics.

The applications demonstrate that the use of the UV-laser-based microscopic dissection allows for sampling plant tissue at ultrahigh resolution and unprecedented precision. This new technique facilitates sampling for stable isotope analysis of anatomical plant traits like combined tree eco-physiological, wood anatomical and dendroclimatological studies.

Keywords: *dendroclimatology, high-precision sampling, high-resolution stable isotope analysis, plant physiology, tree rings, UV-laser microdissection, wood anatomy*

2.1. Introduction

Stable isotope analyses (hydrogen (H), nitrogen (N), carbon (C), oxygen (O)) on organic tissue are widely used in plant physiological, ecological and climatological research (e.g. Brienen et al., 2012; Dawson et al., 2002; Ehleringer et al., 1993; Heinrich et al., 2013; Helle and Schleser, 2004b; Hietz et al., 2011; Schleser et al., 1999a; Treydte et al., 2006; Werner et al., 2012; West et al., 2010; Ziegler, 1995). State of the art isotope ratio mass spectrometry (IRMS) and cavity ring-down spectroscopy (CRDS) allow precise determination of stable isotope ratios on minimal sample amounts and large numbers of samples. However, accurate preparation of small samples in large numbers is challenging, as this still has to be done manually in most of the research areas. Despite the high precision and accuracy of modern analytical devices, data quality very much depends on the skills and motivation of the person responsible for sample preparation. This applies in particular to inter- and intra-annual stable isotope studies of woody tissue attempting to extract valuable seasonal climatic and environmental information (e.g. Leavitt and Long, 1982; Loader et al., 1995; Schollaen et al., 2013; Treydte et al., 2006) or assessing plant eco-physiological processes (e.g. Gessler et al., 2009; Helle and Schleser, 2004a; Krepkowski et al., 2013; Schubert and Jahren, 2011) from annual growth rings or parts thereof. Furthermore, high-precision dissection is crucial in studies using high-resolution stable isotope data for the identification of anatomically non-distinct annual rings in tropical trees (e.g. Evans and Schrag, 2004; Pons and Helle, 2011; Verheyden et al., 2004a).

Different methods exist for the dissection of wood tissue from tree rings for stable isotope measurements. One common method has been to divide wood segments or cores by cutting tangential slices, utilizing fixed-blade sledge and rotary microtomes (Barbour et al., 2002; Helle and Schleser, 2004a; Loader et al., 1995; Ogée et al., 2009; Ogle and McCormac, 1994; Pons and Helle, 2011; Poussart et al., 2004; Verheyden et al., 2004a) or scalpel/razor blades (e.g. Managave et al., 2010b; Roden et al., 2009). With a microtome, wood slices down to ~10 μm thickness can be achieved (Helle and Schleser, 2004a). Another high-resolution sampling method is by collecting wood dust from a series of small wood holes in radial direction utilizing twist drills (Fichtler et al., 2010; Gebrekirstos et al., 2009; Walcroft et al., 1997), robotic micromilling techniques (Dodd et al., 2008; Wurster et al., 1999) or an UV-laser ablation system in combination with isotope ratio mass spectrometry (LA-C-GC-IRMS), first described in Schulze et al. (2004). Accurate sample adjustment, as well as unambiguous identification of tree rings is normally provided by visual inspection using a microscope or digital camera. After dissection, wood samples are ground to a fine powder and either cellulose is extracted or bulk wood samples are used for stable isotope analysis. The latter is the case for the UV-laser ablation method where dust is ablated from a wood core or segment in an airtight chamber flushed with helium. From

the ablation chamber wood dust is directly transferred into a combustion oven and converted to CO_2. Subsequently, $\delta^{13}C$ is measured by an isotope ratio mass spectrometer that is coupled online to the UV-laser ablation and preparation system. Various studies used this method to analyse the intra-annual $\delta^{13}C$ in tree rings responding to carbohydrate storage and remobilization, as well as short-term climatic effects in conjunction with wood density variability (Intra-annual Density Fluctuations, IADFs) (e.g. Battipaglia et al., 2010; De Micco et al., 2012; Skomarkova et al., 2006). The spatial resolution of a UV-laser shot is 40 µm (Schulze et al., 2004) to 150 µm (De Micco et al., 2012). The widths of the holes caused by the mechanical drills can vary from 500 µm (Gebrekirstos et al., 2009) to 800 µm (Fichtler et al., 2010) up to 1.5 mm (Walcroft et al., 1997) depending on the diameter of the drill. Robotic micromilling generally requires a minimum path width of 400 µm for increment core samples, whereas individual path widths of <100 µm are possible (Dodd et al., 2008).

Different drawbacks exist for the dissection methods mentioned before. For the methods using blades or microtomes, wood samples must have straight-line ring structure boundaries in tangential and transversal direction, as samples are cut in parallel linear segments. However, ring width and curvature of growth rings are rarely strictly parallel and fibre or vessel angles vary under natural conditions as well as depend on species-specific wood anatomical characteristics. Thus, often only a limited number of consecutive tree rings per sample is suitable for high-precision intra-annual stable isotope measurements when applying these dissection methods. Generally, cross-contamination during cutting, milling and other preparatory steps can not be excluded especially when quality control by electronic image documentation is not implemented. For the methods drilling wood holes, straight-line boundaries in transversal direction are less important, but differences in vertical direction can be problematic, depending on the drill depth and the deviation of wood fibre or vessel orientation from the vertical direction (FIGURE 2.1B). LA-C-GC-IRMS systems are presently confined to carbon isotope analysis. Aerosol transfer of wood dust between the ablation chamber and the combustion furnace requires a rather high helium consumption and transfer capillaries may clog up sometimes.

The need for methodological improvements to facilitate fine dissection of irregular and narrow shapes has emerged lately, we assessed a novel method to dissect wood tissue from tree rings using UV-laser-based microdissection microscopes of Leica (LMD7000, Leica Microsystems GmbH, Wetzlar, Germany) and Zeiss (PALM MicroBeam, Carl Zeiss Microscopy GmbH, Jena, Germany). UV-laser-based microscopic dissection systems are being applied widely in biomedical (e.g. Fend and Raffeld, 2000), animal (e.g. Bayona-Bafaluy et al., 2005) and also in plant research (e.g. Abbott et al., 2010; Nelson et al., 2006). However, to our knowledge, this is the first time it has been utilized to precisely dissect plant tissue for stable isotope research. Laser-based microscopic dissection uses an UV-laser beam to isolate tissues of interest from thin sections of samples. We describe the

design and handling of the two different UV-laser microdissection microscopes. Advantages and constraints are discussed on the basis of high-resolution stable isotope analyses on woody plant material of deciduous and coniferous trees from temperate and tropical climate zones. Variability of the new sub-seasonal C and O stable isotope data was evaluated with respect to seasonal changes of climatic conditions and wood growth dynamics. Furthermore, we tested whether $\delta^{13}C$ in the woody ray parenchyma and in xylem cells of a deciduous tree is different.

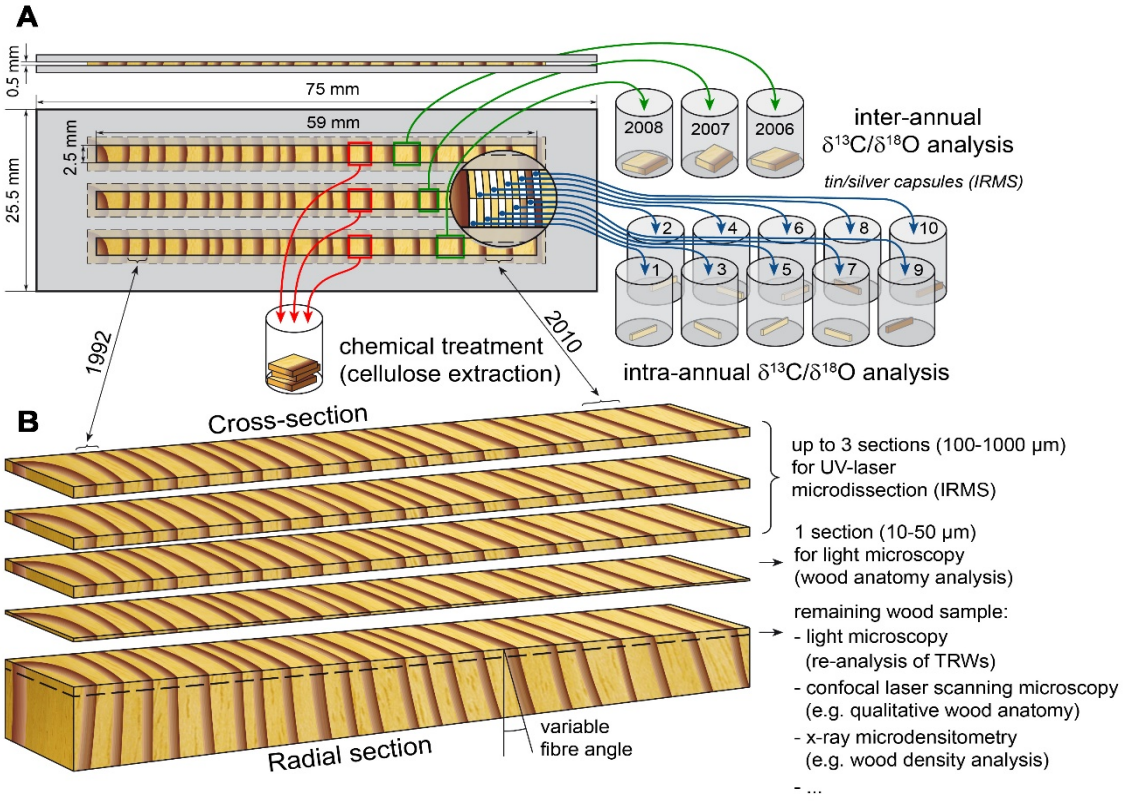

FIGURE 2.1 | Possible steps of wood sample preparation and high-precision sampling using UV-laser-based microscopic dissection systems. (A) Top view and profile of a metal frame slide with wood cross-sections used for gravity-assisted collection (LMD7000, Leica). Up to three cross-sections of 59-mm length can be mounted between two metal frames. For stable isotope analyses it is possible to cut serial sections at inter- to intra-annual resolution or even to pool sample material, e.g. for cellulose extraction. To avoid material loss the dissection of tissue can be alternatingly shifted. (B) Schematic view of sample preparation with a wood segment in radial and cross-section. The use of cross-sections diminishes difficulties of cross-contamination when sampling tree rings with tight curvatures, non-parallel boundaries, varying fibre and vessel angles and/or changing tree-ring width in radial direction. The dissection of wood cross-sections ranging in thickness from 100 µm to a maximal 1000 µm is possible. Remaining wood sample can be used for multidisciplinary approaches, e.g. combining high-resolution stable isotope analysis, quantitative wood anatomy, ring width or wood density analysis.

2.2. Material and Methods

UV-laser-based microscopic dissection

UV-laser microdissection microscopes were used as a precise tool for dissecting different wood samples in stable isotope studies. We tested two different UV-laser microdissection microscopes of Leica (LMD7000, software v6.7.1.3952, Leica Microsystems GmbH) and Zeiss (PALM MicroBeam, software v4.5.0.9, Carl Zeiss Microscopy GmbH). We followed a preparation scheme containing five steps:

1. manual preparation of thin wood cross-sections (max. 1000 µm thickness) with a microtome or a high precision saw,
2. microscopic identification and pen-screen selection of tissues of interest,
3. automatic UV-laser-based microscopic dissection of inter-or intra-annual wood sections,
4. semi-automatic sample collection into tin or silver capsules by gravity or forceps, optional chemical treatment (e.g. cellulose extraction) and
5. stable carbon (C) and oxygen (O) isotope analysis via conventional Isotope Ratio Mass Spectrometry (IRMS) coupled online to a combustion or pyrolysis furnace.

UV-laser-based microscopic dissection enables selection of relevant plant cells/tissues on screen by pen, while nonrelevant tissues (e.g. resin ducts, wood rays) may not be selected or be removed (FIGURE 2.2A/D) prior to sampling. Any size and area can be dissected, which is important for precise dissection of asymmetric tree rings or parts thereof as shown for example by lobate growth (FIGURE 2.2A), intra-ring density fluctuations (FIGURE 2.2B) or wedging tree rings (FIGURE 2.2C). Furthermore, it is possible to cut serial sections or even to pool sample material, for example if the weight of the dissected tissue from one thin section is not sufficient for a stable isotope measurement. Sample material from the same array of wood cells can be identified unambiguously on a second or third cross-section and may be pooled for chemical treatment, like cellulose extraction prior to IRMS analysis (FIGURE 2.1A).

In general, wood samples of 100 µm to 1000 µm thickness can be dissected without any major constraints (FIGURE 2.1B). Dissection samples of up to 1000 µm thickness are achieved by cutting iterations and adjustment of the z-focus of the UV-laser beam. The use of cross-sections thinner than 100 µm normally results in insufficient amount of material for present-day combustion/pyrolysis systems normally coupled to IRMS. Taking thin sections, however, has the advantage that part of the wood sample is left intact, providing the opportunity for reanalysis of ring widths or allowing other investigations as for example quantitative wood anatomy or wood density measurements. Furthermore, the risk of cross contamination of various tissues is diminished, for example when studying narrow

tree rings that have non-parallel boundaries and/or have varying fibre and vessel angles (FIGURE 2.1B).

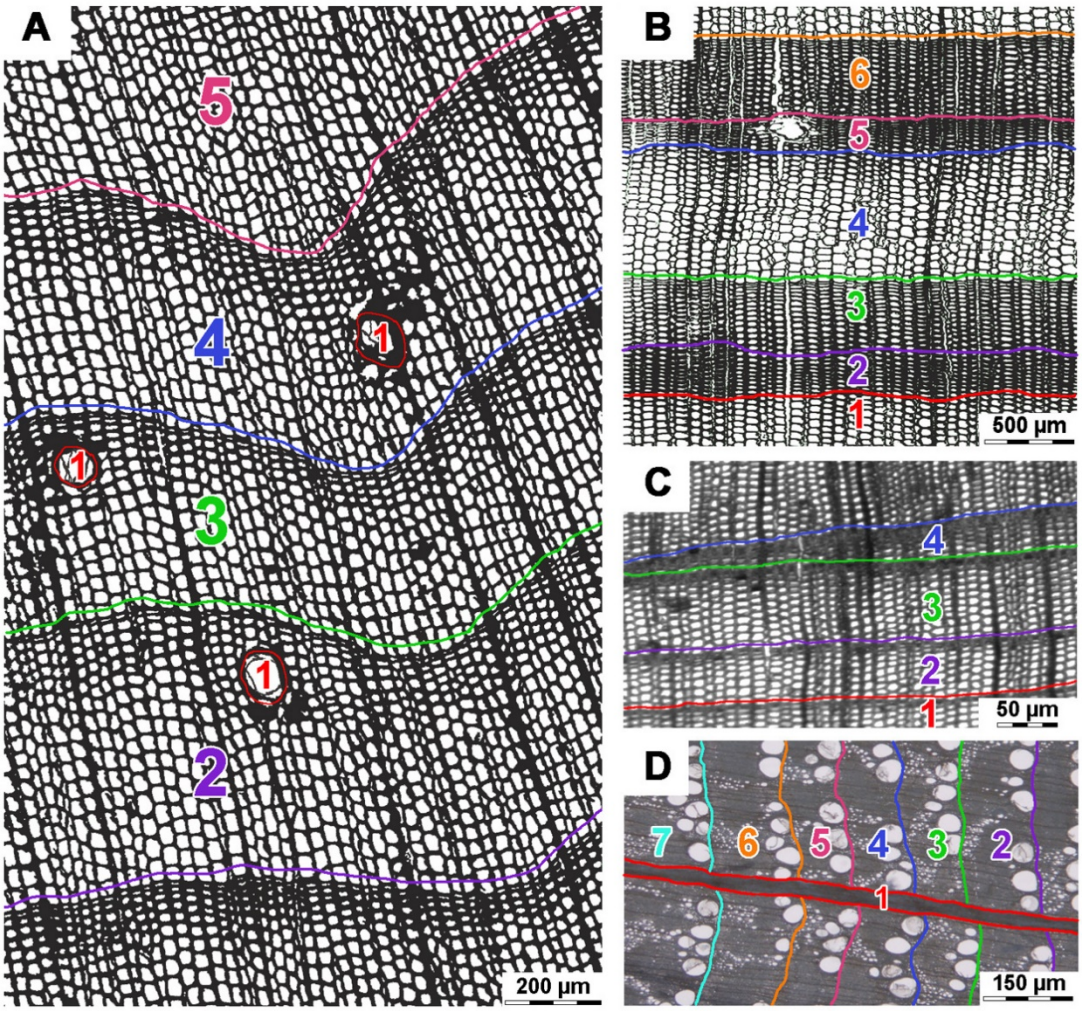

FIGURE 2.2 | Schematic examples of different dissected wood tissues from several tree species for cutting process with an UV-laser microscopic dissection system. Nonrelevant tissues (e.g. resin ducts, wood rays) can be removed before stable isotope analysis and any size and area can be dissected. (A) Cross-section of Pinus sylvestris. Resin ducts and asymmetric growth rings can be easily dissected; (B) Cross-section of Pinus sylvestris. Density fluctuations within tree rings are dissected (nos 2 and 5); (C) Cross-section of Juniperus excelsa. Tree rings are marked, including wedging rings; (D) Cross-section of Quercus robur. Wood ray (no 1) is marked together with tree rings.

Sample material

In order to test the UV-laser-based microscopic dissection method in practice we focused on three applications. In the first experiment, we tested whether the $\delta^{13}C$ values in xylem cells of an oak sample (*Quercus robur* L.) differ from the $\delta^{13}C$ values in ray cells in order to assess potential influences of ray parenchyma on the isotope variability of tree-ring sequences. Therefore, an oak tree was sampled at the Telegrafenberg Hill in Potsdam,

northeastern Germany (52°23'N, 13°04'E; 94 m above sea level (a.s.l.)). Germany is characterized by a warm, temperate and humid climate of the mid-latitudes with weakening oceanic influences from the northwest to the southeast. In the second and third example, we dissected wood tissues to analyse high-resolution intra-annual $\delta^{18}O$, $\delta^{13}C$ and wood density data. The material selected comprises wood of coniferous and broad-leaf trees from two study sites differing in climatic conditions. The sampling site of the coniferous tree (*Pinus strobus* L.*)* is located in St. Arnold, northwestern Germany (52°13'N, 7°23'E; 56 m a.s.l.), having similar climatic conditions as the site of the first example. The sampling site of the broad-leaf tree is located in lowland rain forest in the eastern part of Central Java, Indonesia (07°52'S, 111°11'E; 380 m a.s.l.). An increment core of 5 mm in diameter of a living teak tree (*Tectona grandis* L.) was chosen from a collection that was gathered during a field campaign in 2008 (Schollaen et al., 2013). At this study site, the climate is characterized by a distinct dry season from June to September and a rainy season from October to May (FIGURE 2.5B). The growing season for teak in this region generally lasts from the beginning of October to the end of May. During the dry season the trees are leafless and produce no wood as they are in a state of cambial dormancy (Coster, 1928).

Sample preparation

Firstly, increment cores were cut into segments of 5 cm length and secondly, transverse or cross-sections of approximately 500 µm thickness for the teak sample, 350 µm for the oak sample and 1000 µm for the pine sample were cut with a high-precision diamond saw (ISOMED5000, ITW Test & Measurement GmbH, Düsseldorf, Germany) or a core microtome (Gärtner and Nievergelt, 2010), respectively. Extractives, such as resins and oils, were removed from the wood cross-sections by boiling them in de-ionized water and ethanol. For further treatment, the cross-sections of resin-extracted wood were fixed between two stainless metal frame slides (FIGURE 2.1A) for use with the Leica system and between two conventional microscope slides (26 x 76 mm, Thermo Scientific, Menzel GmbH, Braunschweig, Germany) for the Zeiss system. Three of these slides, each carrying up to three cross-sections of maximum 6 cm length can be mounted onto the slide holder of each microscopic dissection system. Hence, in total cross-sections from a wood core measuring c. 54 cm in length can be processed by a UV-laser-based dissection system in one operation.

Sample collection

Depending on the thickness of wood cross-sections, samples are viewed under the microscopes in transmitted- or reflected-light mode. Series of tissues of interest are first marked with mouse or screen-pen (FIGURES 2.2, 2.3). Every segment drawn was dissected

with the UV-laser beam and collected for the Leica system by gravity into single silver ($\delta^{18}O$) or tin ($\delta^{13}C$) capsules standing in a collection holder. For the Zeiss system tissue was taken up with a forceps and put into silver/tin capsules.
In the first experiment on an oak sample (*Q. robur*), resin-extracted wood and cellulose of ray parenchyma and xylem tissue from six (cellulose) and eight (wood) consecutive tree rings were cut, respectively (FIGURE 2.4A). Cellulose extraction was performed according to the standard method as described by Wieloch et al. (2011).
In the second and third experiment, tree-ring parts of interest were graphically subdivided on a pen-screen in radial direction into equidistant parts of 150 µm in width for the teak sample (FIGURE 2.3) and 20 µm in width for the pine sample. Cutting lines were drawn parallel to wood anatomical structures and tree-ring boundaries independent from their shape. The number of segments per year varied depending on the tree-ring width.

Stable isotope analyses

Oxygen isotope ratios were measured using a high temperature TC/EA pyrolysis oven (at 1400°C) coupled online to an Isotope Ratio Mass Spectrometer (IRMS; Delta V Advantage, Thermo Scientific, Bremen, Germany). The carbon isotope ratios were measured by combustion (at 1080°C) using an elemental analyser (Model NA 1500; Carlo Erba, Milan, Italy) coupled online to an IRMS (Isoprime Ltd. Cheadle Hulme, UK). Sample masses of 130-220 µg of resin-extracted wood or cellulose were used for IRMS analyses. Sample replication resulted in a reproducibility of better than ±0.1‰ for $\delta^{13}C$ values and up to ±0.3‰ for $\delta^{18}O$ values. The isotope ratios are given in the delta (δ) notation, relative to the standards VPDB for $\delta^{13}C$ and VSMOW for $\delta^{18}O$ (Craig, 1957).

Determination of wood density

Wood density of the intra-annually resolved pine sample was precisely calculated from the masses of equidistant subsections of equal volume (20 x 1000 x 4000 µm) that were weighed by a micro balance (AX26 DeltaRange, Mettler Toledo GmbH, Greifensee, Switzerland).

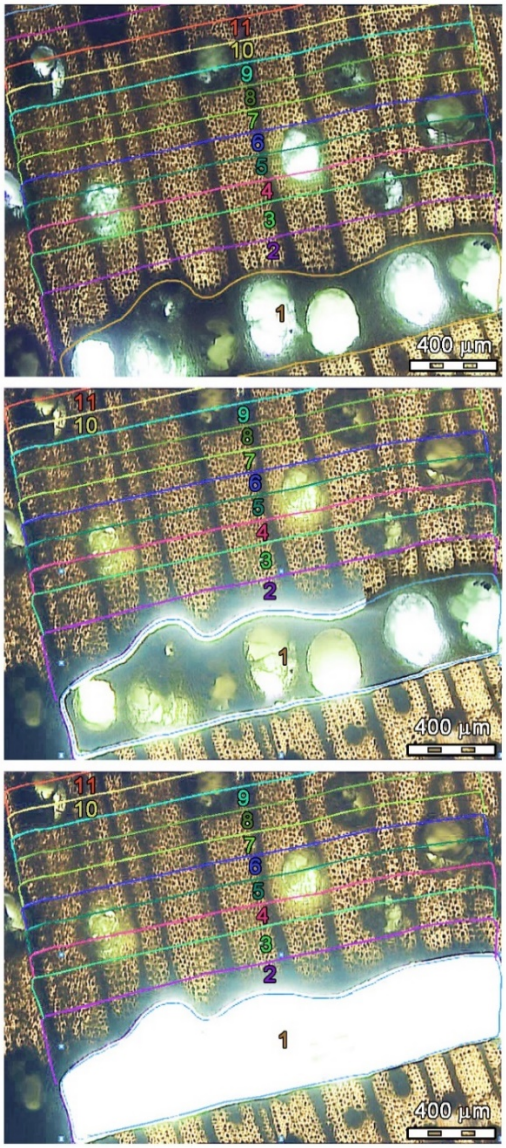

FIGURE 2.3 | Microscopic image of a teak (*Tectona grandis*) cross-section (500 µm thickness, magnification x5). Consecutive sections of intra-annual tree-ring parenchyma and xylem tissue marked with numbers for the cutting process with an UV-laser microdissection microscopt (LMD7000, Leica). Screen shots before, during and after UV-laser-based microscopic dissection of wood parenchyma band.

2.3. Results

Influence of ray parenchyma on the $\delta^{13}C$ signature in tree rings of oak (Quercus robur)

All $\delta^{13}C$ values from resin-extracted wood ($\delta^{13}C_{wd,}$ FIGURE 2.4B) of the ray parenchyma were found lower than those of the associated xylem tissue with a mean difference of 0.21‰. This is well above the analytical precision of ±0.08‰. Despite the significant

general offset, $\delta^{13}C$ signals of ray and xylem tissue follow the same year-to-year variability and trend as confirmed by a R^2 of 0.99. Likewise, cellulose $\delta^{13}C$ values ($\delta^{13}C_{cel}$, FIGURE 2.4C) from ray and xylem tissue show the same year-to-year variability. However, the $\delta^{13}C_{cel}$ values of ray parenchyma are slightly higher compared to the $\delta^{13}C_{cel}$ values of xylem tissue. The mean difference is 0.26‰ with R^2 of 0.96 and analytical precision of ±0.08‰.

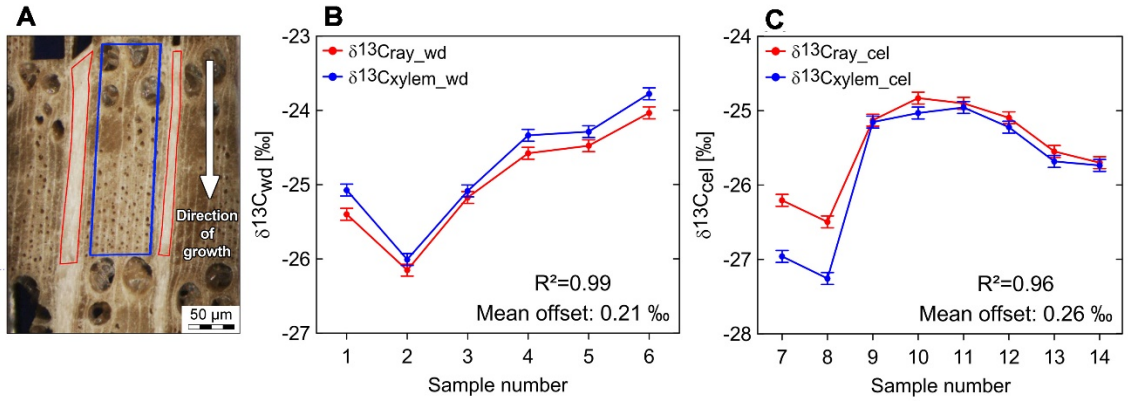

FIGURE 2.4 | Comparison between $\delta^{13}C$ values from resin-extracted wood ($\delta^{13}C_{wd}$) and cellulose ($\delta^{13}C_{cel}$) of ray parenchyma and xylem tissue in tree rings of an oak sample (Quercus robur). (A) Microscopic image of an oak cross-section (350 µm thickness) with schematic example of dissected tree-ring xylem and ray tissues for cutting process with the UV-laser-based microscopic dissection method. (B) Tree-ring $\delta^{13}C$ values ($\delta^{13}C_{wd}$) of ray parenchyma and xylem cells from six consecutive tree rings dissected with the UV-laser microscope. (C) Cellulose $\delta^{13}C$ values ($\delta^{13}C_{cel}$) of ray parenchyma and xylem cells from eight consecutive tree rings. The analytical precisions of ±0.08‰ are shown as error bars. The $\delta^{13}C$ signals of ray and xylem tissue follow the same year-to-year variability and trend, but reveal offsets that are opposite in sign depending on whether wholewood or cellulose is analysed.

High-resolution intra-annual $\delta^{18}O$ results from teak (*Tectona grandis*)

The intra-annual $\delta^{18}O$ profiles of a teak tree ($\delta^{18}O_{wd}$) from Indonesia show a clear annual cycle (FIGURE 2.5A). Annual wood formation starts with a parenchyma band showing $\delta^{18}O_{wd}$ values that are similar to the $\delta^{18}O_{wd}$ values at the end of the previous tree ring. Wood formed directly after the parenchyma band is characterized by rapidly rising $\delta^{18}O_{wd}$ values up to the seasonal maximum appearing early in the growing season. This $\delta^{18}O_{wd}$ maximum is followed by a decline to a seasonal minimum typically in the 2nd third of each tree ring before $\delta^{18}O_{wd}$ is marginally rising again in the last third of the growing season. The pattern described is rather consistent in spite of the different numbers of sub-sections per year and follows the annual cycle in rainfall amount and its corresponding isotope signature (FIGURE 2.5B). The high-resolution pattern of the year 1985 does not show

distinct high values at the beginning of the growing season and together with the year 1984 two minima during a growing season are revealed. Note, that for tree-ring dating, we followed the convention for the southern hemisphere, which assigns to each tree ring the year in which radial growth begins (Schulman, 1956).

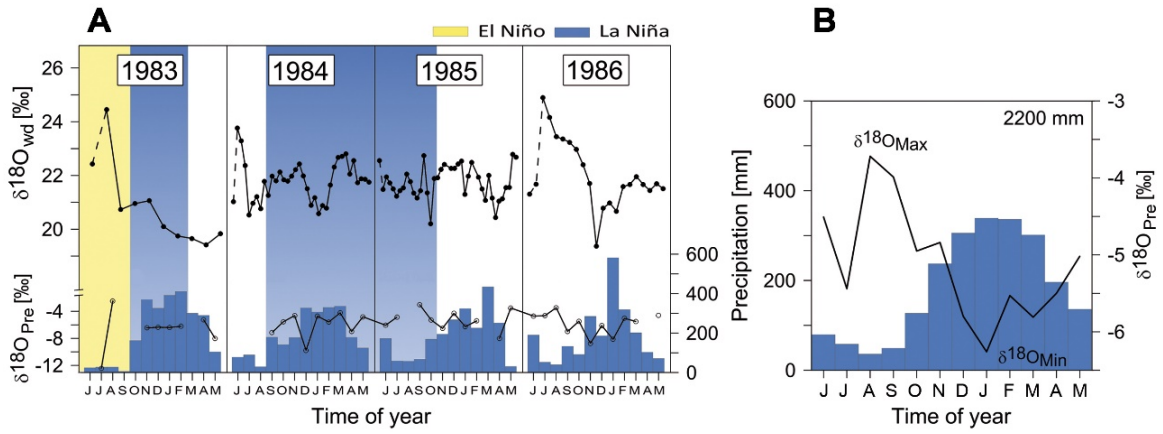

FIGURE 2.5 | Intra-annual $\delta^{18}O_{wd}$ variations from teak (*Tectona grandis*) collected in the eastern part of Central Java, Indonesia and corresponding precipitation data. (A) High-resolution isotope data are plotted vs monthly precipitation sums at the study site (GPCC V6, mean of 9 nearest grid-points, Schneider et al., 2011) and $\delta^{18}O$ values in precipitation ($\delta^{18}O_{Pre}$) of the corresponding year from Jakarta/ Indonesia (IAEA/WMO, 2006). Dissected part of parenchyma band is marked as a dashed line. El Niño and La Niña events are highlighted in yellow and blue, respectively (NOAA, 2013). (B) Average monthly precipitation sums (bars) for the eastern part of Central Java (GPCC V6, 1901-2010, mean of 9 nearest grid-points, Schneider et al., 2011) and mean $\delta^{18}O$ in precipitation (line) for Jakarta/ Indonesia (1962-1998) (IAEA/WMO, 2006) are shown. The seasonal $\delta^{18}O_{wd}$ pattern reflect the annual cycle of $\delta^{18}O$ in precipitation and corresponding seasonal changes in the amount of precipitation at the study site (Schollaen et al., 2013b). $\delta^{18}O_{wd}$ pattern is sensitive to rainfall extremes caused by ENSO events.

High-resolution intra-annual $\delta^{13}C$, $\delta^{18}O$ and wood density of white pine (Pinus strobus)

The $\delta^{13}C_{wd}$ profile begins with a downward trend of c. 1‰ during the first third of the tree ring (FIGURE 2.6B). $\delta^{13}C_{wd}$ values rise again in the middle part before they increase strongly by >2‰ to a seasonal maximum followed by a sharp and drastic decrease at the very end of the latewood. In contrast, the $\delta^{18}O_{wd}$ profile is characterized by a broad peak in the first third of the tree ring, reaching $\delta^{18}O_{wd}$ values of >30‰. A second increase, but less pronounced, is indicated for the last part of the ring, with a maximum that is synchronous to the peak in $\delta^{13}C_{wd}$. The wood density profile starts with low values and follows synchronously, although attenuated, the increase and decline of $\delta^{18}O_{wd}$ within the first half of the tree ring. Starting from a minimum in the middle of the tree ring, wood density increases towards the end of the tree ring. Beside the general increase in density, a few intra-annual density fluctuations (IADFs) are visible. Increasing $\delta^{13}C_{wd}$ values are related

to these short-term intra-ring density fluctuations with a short time lag. At the end of the growing season all parameters ($\delta^{13}C_{wd}$, $\delta^{18}O_{wd}$, wood density) reach their seasonal maxima.

The corresponding seasonal courses of temperature, precipitation and relative air humidity for the year 1977 do not deviate strongly from the long-term mean, except for a conspicuous dry period of 3 wk in May (FIGURE 2.6A). Only one strong rainfall event was recorded during this period and relative humidity was persistently below 60%.

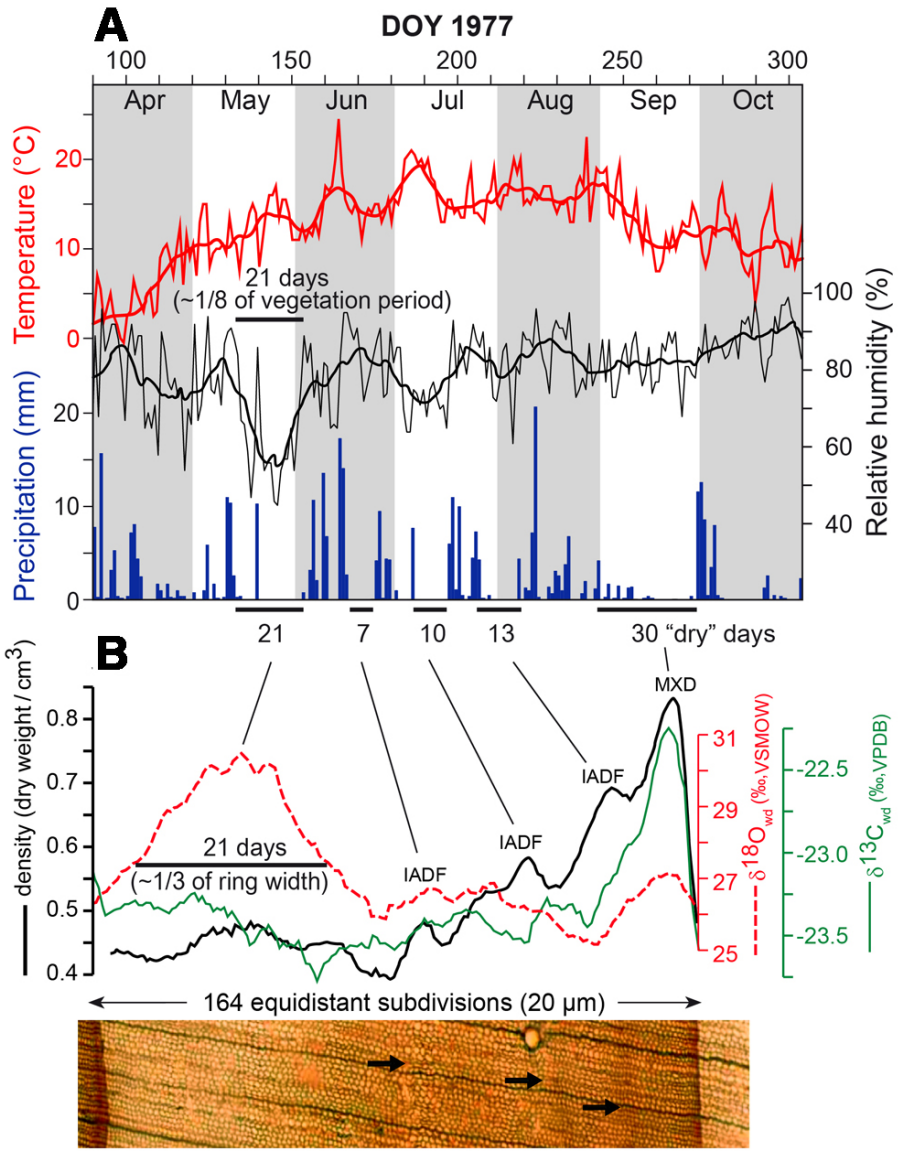

FIGURE 2.6 | Seasonal variations of wood density and stable isotope ratios ($\delta^{13}C_{wd}$, $\delta^{18}O_{wd}$) of a pine tree (*Pinus strobus*) from northwestern Germany for 1977 (B) and the corresponding daily temperature, precipitation and relative humidity data (A). Intra-annual density fluctuations (IADFs) are marked with arrows in the photomicrograph. Seasonal moisture signals in $\delta^{18}O_{wd}$ are weighted by non-linear intra-annual growth dynamics. DOY, day of year.

2.4. Discussion

Ray parenchyma and xylem tissue of deciduous trees show offsets in $\delta^{13}C$, but same year-to-year variability

Our results exhibit the same year-to-year variability between the $\delta^{13}C$ signals of ray parenchyma and xylem tissue over 6 and 8 yr, respectively (FIGURE 2.4). The similarity of data from the different woody tissues may indicate that they result from the same physiological and biochemical processes. Of course, during the vegetation period assimilates are used at the same time for vessel-, fibre- and ray parenchyma-formation. However, ray cells live longer, up to several years and thus their structure and chemical composition may change over longer time intervals. Furthermore, woody rays are the main storage organs for non-structural carbohydrates, for example sugars and starch. Accumulation and mobilization of non-structural carbohydrates may be accompanied by increased metabolic activity and respiration of parenchymatic tissue as compared to xylem tissue. Indeed, the offsets found between $\delta^{13}C$ of ray parenchyma and xylem tissue seem to reflect differences in chemical composition and metabolic activity. Ray parenchyma dissected from resin-extracted wood is depleted in ^{13}C as compared to xylem tissue (FIGURE 2.4B). Our finding confirms a study by Vaganov et al. (2009) using LA-C-GC-IRMS on wood tissue of four consecutive tree rings from a Norway spruce (*Picea abies*) sample. Data revealed a similar ^{13}C-depletion of ray parenchyma of up to 0.23‰ in comparison to tracheids. Vaganov et al. (2009) explain the lower $\delta^{13}C_{wd}$ values as a result of continuing incorporation of lignin into the long-lived parenchyma cells. Lignin is generally depleted in ^{13}C by up to 3‰ as compared to cellulose (e.g. Harlow et al., 2006; Loader et al., 2003; Wilson and Grinsted, 1977). Hence, a slightly higher content of lignin in ray cells may well cause the observed ^{13}C depletion over xylem tissue in coniferous wood (Vaganov et al., 2009) and in broad-leaf deciduous oak of this study. However, UV-laser-based microscopic tissue dissection allows chemical treatment, like cellulose extraction, prior to IRMS analysis. In contrast to a depletion in ^{13}C of resin-extracted wood we found cellulose of ray parenchyma ($\delta^{13}C_{cel}$) to be slightly enriched in ^{13}C when compared to cellulose from xylem tissue. This minor, but apparent enrichment of cellulose of woody rays may be promoted by slightly enhanced catabolic metabolism, i.e. enhanced respiration making ATP available for the biochemical processes of accumulation and mobilization of starch. Gleixner et al. (1993) showed that 'lighter' sugar molecules are preferentially used in catabolic, or respiratory reactions, whereas 'heavier' ones are involved in polymerization of cellulose, for example. Hence, an increased carbon isotope partitioning between anabolic and catabolic metabolism in ray parenchyma may result in the observed slight enrichment in $\delta^{13}C_{Cel}$ in comparison with xylem tissue. Note, that the differences in $\delta^{13}C$ between woody rays and xylem tissue may not be constant (Fig.6,

Vaganov et al., 2009). Varying cellulose to lignin ratios or respiration rates may cause the observed differences in the offsets in $\delta^{13}C$ and may also act on longer timescales.
A recent study on ray parenchyma from Spanish juniper (*Juniperus thurifera*) revealed that time series based on the abundance of ray cells reveal complementary climatic signals to those derived from tree-ring width chronologies (Olano et al., 2013). Our results demonstrate that the $\delta^{13}C$ values of ray parenchyma and xylem tissue contain the same year-to-year variability. Hence, we can assume from this pilot study that the $\delta^{13}C$ signals of ray cells may not provide additional information in dendroclimatic studies. However, the offsets in $\delta^{13}C$ between ray cells and xylem are dependent on whether wood or cellulose is analysed. This result indicates the crucial value of the new dissection method as it allows for new approaches towards a better understanding of the physiological processes controlling ray parenchyma and xylem cell formation.

High-resolution $\delta^{18}O$ values in tree rings of Indonesian teak are sensitive to rainfall extremes caused by ENSO

The seasonal tree-ring $\delta^{18}O_{wd}$ pattern in Indonesian teak is hypothesized to reflect the annual cycle of $\delta^{18}O$ in precipitation and corresponding seasonal changes in the amount of precipitation at the site (FIGURE 2.5). It could be shown, that high $\delta^{18}O_{wd}$ values during the start of the growing season represent the $\delta^{18}O_{Pre}$ signature of the prior dry season, while lowest tree-ring $\delta^{18}O$ values reveal the $\delta^{18}O_{Pre}$ signature of the main rainy season (Schollaen et al., 2013). Towards the end of the growing season tree-ring $\delta^{18}O$ values increase again following the $\delta^{18}O$-trend of precipitation. The described pattern fits nicely during the years of 1983 and 1986. The low rainfall amount during the dry season of 1983 is caused by an El Niño event (El Niño 1982-83). The two minima in tree-ring $\delta^{18}O$ values during the year 1984, as well as the missing upward trend at the beginning of the growing season in year 1985 can be explained by rather high rainfall amounts due to an ongoing La Niña phase (blue shaded periods). This demonstrates that sub-seasonal tree-ring $\delta^{18}O$ records of Indonesian teak are very sensitive to rainfall extremes caused by ENSO, with high $\delta^{18}O_{wd}$ values during El Niño events and low $\delta^{18}O_{wd}$ values during La Niña events.
Correlations between $\delta^{18}O_{wd}$ and rainfall amount were also found in several other studies on tropical or subtropical trees (e.g. Brienen et al., 2012; Managave et al., 2010b; Poussart et al., 2004; Sano et al., 2012). However, to our knowledge, this is the first time that intra-annual $\delta^{18}O_{wd}$ values in tropical trees are shown to reflect the rainfall pattern over an entire year with distinct rainy and dry season signals. This underlines the value of high-resolution intra-seasonal isotope measurements of tropical wood, especially in the light of extreme rainfall events often associated with El Niño and La Niña.

High-resolution stable isotope variations in white pine reflect seasonal changes of climatic conditions weighted by nonlinear growth dynamics

Tree rings are integrating environmental information over the vegetation period. The intra-annual variations in $\delta^{13}C_{wd}$, $\delta^{18}O_{wd}$ and wood density are mainly driven by interactions between seasonal variation in meteorological conditions, soil water availability and plant response. Specific weather events, such as dry periods are clearly recorded in the seasonal pattern of $\delta^{13}C$, $\delta^{18}O$ and wood density (e.g. Barbour et al., 2002; Eilmann et al., 2010; Sarris et al., 2013). In this study a detailed view of the weather conditions of the year 1977 at our site in northwestern Germany indicates several time periods with no or less rainfall, so called 'dry' days (FIGURE 2.6A). The corresponding intra-annual pattern of $\delta^{13}C_{wd}$ (FIGURE 2.6B) follows a typical course observed for coniferous species with a gradual increase in $\delta^{13}C_{wd}$ to a maximum in latewood followed by a sharp decline at the very end of the tree ring (Barbour et al., 2002; cf. Leavitt, 1993; Schulze et al., 2004; Walcroft et al., 1997). Short-term increases in $\delta^{13}C_{wd}$ values of the second half of the tree ring were observed after dry periods and are in agreement with the wood density pattern. In contrast, the first dry period in May is not well observed in the $\delta^{13}C_{wd}$ pattern. However, this dry period in late spring, characterized by low rainfall as well as low relative humidity, is well represented in the $\delta^{18}O_{wd}$ record by a conspicuous broad peak. It seems that $\delta^{18}O_{wd}$ is much more sensitive to changes in moisture conditions than $\delta^{13}C_{wd}$ and wood density at the beginning of the growing season. During the second half of the growing season it appears to be *vice versa*, i.e. $\delta^{13}C_{wd}$ and wood density reflect moisture deficits better than $\delta^{18}O_{wd}$ does.

Furthermore, environmental information seems to be integrated in the tree ring in a non-linear way. The 'dry' period of 21 d in May represents approximately only one eighth of the vegetation period, while the $\delta^{18}O_{wd}$ peak represents one third of the whole tree-ring width. The ability of a tree ring to integrate environmental information depends on the rate of wood cell formation and the longevity of cells. Within the vegetation period these two features are inversely related (FIGURE 2.7). While thin-walled earlywood cells are formed at a high rate, they may only live for days up to a few weeks. Thick-walled latewood cells are built at very slow rates, but may live up to several months and integrate environmental information over a much longer period of time (FIGURE 2.7A). Hence, environmental conditions reflected by intra-annual tree-ring parameters are weighted by seasonal dynamics of wood formation. Additionally, other seasonal changes related to tree physiological processes such as kind and size of carbohydrate pools (amount of C and O), partitioning between catabolic and anabolic metabolism, as well as metabolic flux rates in conjunction with corresponding isotope fractionations have to be considered (Fig. 2.7B and e.g. Gessler et al., 2009; Helle and Schleser, 2004a; Werner et al., 2012).

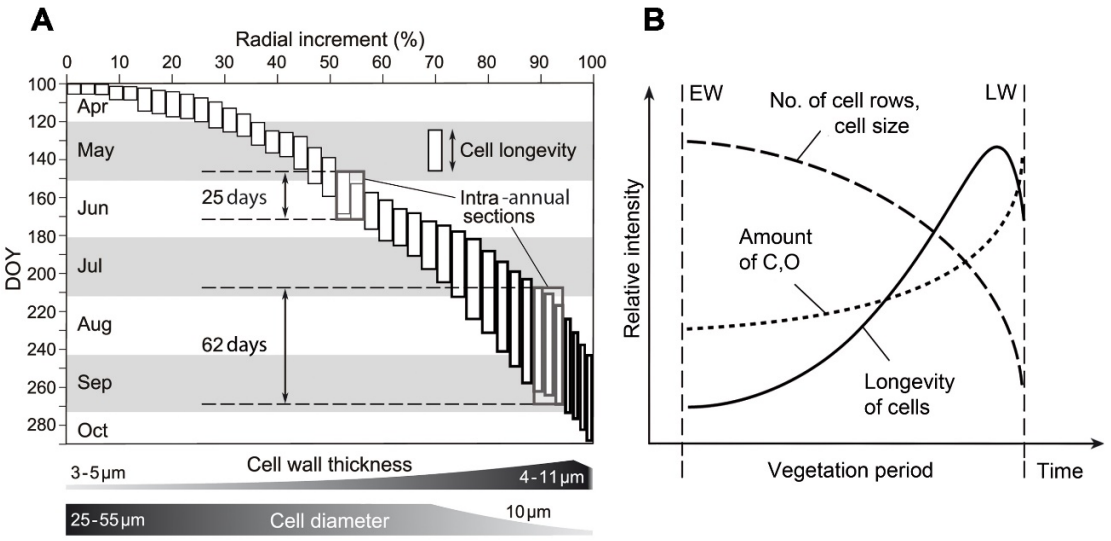

FIGURE 2.7 | Non-linear seasonal growth increments and longevity of cells during the vegetation period for conifers at temperate sites (A; DOY, day of year). (B) Seasonal dynamics of major factors influencing tree-ring stable isotope ratios of wood cell formation is characterized by increasing cell wall thickness, cell longevity and amount of C/O per cell row (elemental mass/wood density), while cell diameter is decreasing.

Evaluation and comparison of UV-laser-based microscopic dissection systems

The results presented suggest that UV-laser-based microscopic dissection is a very useful method for sampling woody tissue in stable isotope studies. It can be used likewise for dissecting whole tree rings and intra-annual sampling at very high spatial resolution. The two UV-laser microdissection microscopes of Leica (LMD7000, Software Version 6.7.1.3952, Leica Microsystems GmbH, Wetzlar, Germany) and Zeiss (PALM MicroBeam, Software Version 4.5.0.9, Carl Zeiss Microscopy GmbH, Jena, Germany), we tested in these studies, differ concerning their practical implementations and applications (TABLE 2.1). The laser from Leica is being moved via optics and the cross-section samples are mounted on a fixed stage. The Leica system uses high-precision optics to steer the laser beam by means of prisms along the desired cut lines on the tissue. As a side effect, the laser can only cut drawn lines or areas marked within the actual microscopic field of view. If larger areas, for example whole tree rings, need to be dissected additional shapes must be defined and additional dissections are required for gathering a single large sample. The dissected sample tissues principally fall down by gravity into collection vessels, e.g. tin or silver capsules. Thus, samples can be prepared directly for conventional autosampler systems coupled to isotope ratio mass spectrometers. An important limitation of the Leica system is the lack of an automatic z-focus adjustment that would allow repeated laser cutting of thicker cross-sections.

Compared to the Leica microscope, the objectives of the Zeiss microscope are installed inversely, which means underneath the sample holder. Hence, tissues of interests are

marked via mouse or screen pen on the lower sample side and can be selected beyond the visible screen. Thus, tissues of interests can be marked as big as necessary, since the laser stays fixed while the sample is moved by the high-precision stage during the dissection process. The UV-laser passes through the glass slide and the dissected sample tissues remain in position. After all marked tissue has been dissected specimens are being picked up manually with a forceps and transferred into tin or silver capsules for stable isotope measurements. Dissected sample tissues were too heavy for laser-induced sample transfer that comes with the Zeiss system. The Zeiss system has an automatic z-focus feature that allows for defining the number of automatic cutting iterations. For each cutting cycle the focus of the UV-laser beam will be adjusted by a pre-defined z-focus delta value. As the Zeiss laser is less powerful than the laser from Leica more cutting iterations are generally required. Together with the manual collection of dissected specimens, the overall sampling process with the Zeiss system requires more time than with the Leica system. On the other hand, the dissection process with the Zeiss can be operated automatically, for example over night. The Leica system requires fulltime presence of the user. Firstly, the adjustment of z-focus of the laser beam has to be done manually. Secondly dissected specimens sometimes tilt, stick and do not fall down into the collection vessels as the cutting line of the laser beam is much narrower than the thickness of the sample.

The use of the UV-laser microdissection microscopes is not necessarily faster than traditional methods for the dissection of wood tissue. In general, the cutting process of selected tissue lasts between 1 to 2 minutes, depending on the size of the selected area, the thickness of the cross section, density of the wood material and the UV-laser settings. If further cutting iterations are required, more time is needed. The average sample throughput per 8-hour day may vary between 20 to 120 samples. This includes the on-screen selection of area, the automatic UV-laser-based microscopic dissection and the collection of specimens, as well as considering unpredictable interferences (e.g. stuck specimens (Leica LMD7000)). With some modification of the current sample collection methods the UV-laser microdissection could also be run automatically over night, which would increase sample throughput drastically.

At this stage, the key advantage using the novel technique is on-screen selection of areas and ultra-high resolution sampling of plant tissue at an unprecedented precision. Furthermore, both systems provide electronic documentation of the dissection processes b photo or video sequences, as well as a report of labeled and dissected elements.

TABLE 2.1 | Comparison of the characteristics of the two UV-laser-based microscopic dissection systems tested.

Zeiss microdissection microscope (PALM MicroBeam /software v4.5.0.9)	Leica microdissection microscope (LMD7000 /software v6.7.1.3952)
General characteristics	
Laser specifications: Wavelength: 355 nm Max. pulse energy: 100 µJ Laser beam stays fixed, stage is moved	Laser specifications: Wavelength: 349 nm Max. pulse energy: 120 µJ Laser beam is moved, stage stays fixed
Cutting process with different magnifications (e.g. x2.5, x5 or x10)	Cutting process with different magnifications (e.g. x5, x10 or x20)
Best range of sample thickness: 100-1000 µm	Best range of sample thickness: 100-1000 µm
Advantages	
Selection of tissue/shape beyond the visible screen Automatic z-focus adjustment/ cutting iterations possible Better software handling and multifarious choice of drawing tools	Laser has more power and less cutting iteration needed Fast sample collection process by semi-automatic sample collection into tin or silver capsules by gravity Automatic image documentation before and after each dissection by image-database (IM500)
Limitations	
Nonautomatic collection of selected tissues of interests in tin/silver capsules (specimens are being picked up manually with a forceps and transferred into tin/silver capsules) Laser has less power and frequently cutting iteration needed Nonautomatic image documentation of the laser dissection process	Lack of automatic z-focus Drawing area of interests larger than the field of view is not possible Control check of dissected samples needed after every cutting process as samples may stick and do not fall down automatically

2.5. Conclusions

We presented a novel method for dissecting plant tissue in stable isotope studies by using UV-laser-based microscopic dissection. Using two commercially available UV-laser microdissection microscopes, we prepared high-resolution intra-annual wood samples from various tree species of different climate zones for carbon and oxygen isotope analyses with conventional IRMS systems.

The UV-laser-based microscopic dissection enables precise selection of relevant plant cells/tissues on video screen by pen. This procedure allowed us to detect that $\delta^{13}C$ of xylem cells and woody ray parenchyma of the deciduous species (*Q. robur*) have the same year-to-year variability, but reveal offsets that are opposite in sign depending on whether

wholewood or cellulose is analysed. Furthermore, we showed that UV-laser-based microscopic dissection facilitates electronically documented sub-seasonal sampling of tree rings with irregular shapes or narrow ring widths. This is a prerequisite for establishing long and continuous high-resolution isotope chronologies for high-quality climate reconstructions. Single cell rows can be sampled and thus short-term climatic events such as droughts or extensive rainfall events (e.g. caused by ENSO) may be related directly. The three applications demonstrate that the use of this new technique enables the user to sample plant tissue at ultra-high resolution and unprecedented precision.

This new technique opens new ways for studying environmental information in tree rings non-linearly integrated over the vegetation period. The combination of direct growth measurements, which provide exact growth rates of tree rings (e.g. punching method (Forster et al., 2000; Rossi et al., 2006), dendrometers) and precisely selected and dissected specimens may provide a better time-match between high-resolution stable isotope ratios and real-time climate data. Comprehensive eco-physiological process studies on stable isotope signal transfer in the arboreal system can be combined with qualitative and quantitative microscopic investigations on anatomical properties. As wood anatomical properties are climate sensitive (e.g. Fonti et al., 2010; Liang et al., 2013; Olano et al., 2013), more and more studies are attempting to combine quantitative wood anatomy and stable isotope analysis (e.g. Battipaglia et al., 2010; De Micco et al., 2012; Ponton et al., 2001; Rossi et al., 2013). Such investigations may explicitly profit from UV-laser-based microscopic dissection. For instance, detailed assessment of carbon and oxygen isotope variability in woody parts such as resin ducts, rays, fibres, vessels or parenchyma cells is possible, since they can now be precisely targeted on thin sections by UV the novel method.

The use of UV-laser-based microscopic dissection systems offers new possibilities in view of relating plant structure with plant functioning (derived from isotope ratios) in studies on vulnerability, resilience and adaption of plants to past and present global change. Multidisciplinary analyses (cell structure, wood density and wood chemistry analyses) on the same wood sample are now possible with a complete recovery of the sample due to the use of thin sections.

Acknowledgements

We are grateful to Heiko Baschek, David Göhring and Sophie Wendler for support in the laboratory, to Andreas Hendrich for help with the layout of figures, and to Sonia Simard, Wei Liang, Hagen Pieper and Uwe Schollän for fruitful discussions. Furthermore, we thank three anonymous reviewers and the editor for their valuable comments and suggestions. This study was funded by the ISOWOOD-Breeding (BMBF, 0315427B), INDOPAL (HE3089/1-1) and CADY (BMBF, 03G0813H) project.

Preface to Chapter 3

Wood is composed of several chemical components, with cellulose and lignin as major constituents and so-called accessory components (usually less than 1% mass) like resins and oils. All of them vary in their isotopic signatures because of individual pathways of formation (Wilson and Grinsted, 1977). Generally, primary plant products like sugars, starch or cellulose are characterized by higher carbon or oxygen isotope ratios. In contrast, plant constituents, like resins or lignin, deriving from a long chemical pathway of secondary metabolism always show low $\delta^{13}C$ or $\delta^{18}O$ values (Gleixner et al., 1993). Hence, varying parts of cellulose, lignin or resins may cause some isotope variability within tree-ring series that significantly reduce the climate signal of a record. Furthermore, it is well known that wood cells are lignified some time during the vegetation period after their cell walls are fully developed. This may not constrain inter-annual isotope studies, however, particularly resins, colourants and tannins can be quite mobile within a trunk of a tree and their relative content is highly variable. Therefore most studies analyzing stable isotopes of tree rings prefer to analyze a single component, usually cellulose because of its immobility and rather few and easy to handle chemicals that are needed for extraction.

Despite, cellulose is isolated from wholewood through a repetition of chemical treatments, which are at present very time and labour intensive, being often the limiting factor for the exploitation of long-term high-resolution tree-ring isotope time series. Thus, several studies tested whether wholewood or cellulose isotope chronologies better reflect climate variations with contradictory results. On the one hand, studies suggest that cellulose extraction may not be necessary since there is no significant differences between the stable carbon and oxygen isotope data of wholewood and cellulose (Barbour et al., 2001; Borella et al., 1998; Harlow et al., 2006; Loader et al., 2003; Saurer et al., 2000; Taylor et al., 2008; Verheyden et al., 2005). On the other hand, researchers report that cellulose provide a more temporally stable proxy of past climate and suggest that cellulose extraction is a necessary step in studies seeking to investigate climate signals in stable isotope chronologies (Battipaglia et al., 2008; Cullen and Grierson, 2006; Ferrio and Voltas, 2005; Szymczak et al., 2011). According to Loader et al. (2003), cellulose extraction may provide little additional information when the main focus lies on long-term climate trends, while it can be more critical if information on extreme events such as droughts or high-rainfall years is required.

In the following chapter an improved methodology for high-throughput isotope analysis of tree rings is presented, using cellulose cross-sections. It shortens drastically the whole process of sample preparation (cellulose extraction, homogenization, tree-ring dissection) in time, allowing to increase in the number and length of individual tree-ring series.

Chapter 3

Tree-ring dissection from cellulose thin sections – an improved procedure of sample preparation for stable isotope analysis of tree rings

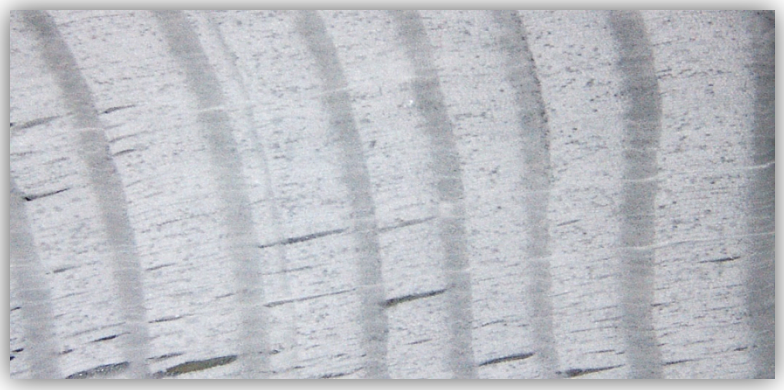

cellulose cross-section of Larch (*Larix decidua*)
(Author´s picture: photograph taking after cellulose extraction)

This chapter is in preparation for publication:

Authored by Karina Schollaen, Heiko Baschek and Gerhard Helle

GFZ - German Research Centre for Geosciences, Section 5.2 Climate Dynamics and Landscape Evolution, Telegrafenberg, 14473 Potsdam, Germany

Abstract

Stable isotopes in tree rings have become widely used archives in environmental and palaeoclimatological studies. However, the dissection of tree rings and the extraction of cellulose and homogenization for stable isotope analysis of tree rings are still labour intensive and the time limiting steps of the procedure of sample preparation. We provide a guideline for a modified method of cellulose extraction from wholewood cross-sections and subsequent dissection of tree rings or parts thereof that requires no additional homogenization. The methodology comprises three major steps from wood cores or segments to cellulose samples readily packed for isotope ratio mass spectrometry. In a first step whole wood thin sections of 1 mm or less in thickness need to be cut with a microtome or a high precision saw. Secondly, a high-throughput cellulose extraction method is applied, that allows cellulose to be extracted directly from wholewood cross-sections utilizing a special device for holding several perforated teflon sheets with individual cross-sections in between. Finally, defined tree ring samples are being dissected from derived cellulose cross sections using a razor blade/scalpel and a binocular in a way that sample homogenization is no longer necessary. Likewise, UV-laser microdissection or UV-laser ablation-IRMS can be utilized for precise high-resolution stable isotope analyses. This methodology was applied to several different coniferous and deciduous tree species with a broad range of wood anatomical characteristics and wood chemical properties. The efficiency of the cellulose extraction procedure was tested by Fourier Transform Infrared spectrometry and compared with standard extraction methods by analyzing the isotopic signal of stable carbon and oxygen isotopes. The approach facilitates the possibility to extract numerous tree rings per sample at one step, while the cell structure remains mostly intact. After some practicing tree ring samples can be dissected from the cellulose laths with the size of the specimen adjusted so that the definite mass needed for an IRMS measurement. The new cellulose extraction and tree-ring dissection technique is an important step to optimize the stable isotope analysis process in two ways: faster and costumer friendly cellulose extraction and the possibility for more precise tree-ring separation at annual to high-resolution scale.

Keywords: c*ellulose extraction, stable isotope analyses, tree rings, wood anatomy, high-precision sampling, conifers, deciduous wood*

3.1. Introduction

Stable isotope records from tree rings are emerging as powerful proxies in paleoclimatic and plant physiological studies (e.g. Grießinger et al., 2011; Heinrich et al., 2013; Helle and Schleser, 2004a; Schollaen et al., 2013; Treydte et al., 2006). For stable isotope analyses (hydrogen (H), carbon (C) or oxygen (O)) different wood components (wholewood, lignin or cellulose) can be analysed, where cellulose is often the preferred sample material because of its singular composition and its immobility (e.g. McCarroll and Loader, 2004).

There are rapid advancements in analytical methodology for stable isotope measurement (Boettger et al., 2007; Saurer et al., 1998). However, the chemical preparation of cellulose from wood tissue is still a time-consuming process. A variety of tree-ring α-cellulose or holocellulose extraction methods is available for isotopic analysis (Brendel et al., 2000; Cullen and MacFarlane, 2005; Gaudinski et al., 2005; Green and Whistler, 1963; Laumer et al., 2009; Leavitt and Danzer, 1993; Loader et al., 1997; Rinne et al., 2005; Wieloch et al., 2011). In all of these methods, now called "standard" methods, tree rings were first subdivided manually by knife/scalpel or microtome before putting through cellulose extraction process. Despite novel techniques for batch-wise isolation of cellulose (Wieloch et al., 2011) allowing simultaneous treatment of up to several hundred micro samples, individual grinding and chemical treatment of every single sample is required. In order to reduce the peeling-grinding-chemical processing for each individual tree ring Loader et al. (2002) made a first attempt to extract cellulose directly from standard increment cores. Li et al. (2011) first reported about a technique to extract α-cellulose directly from wholewood cross-sections. They conducted a high-resolution intra-annual $\delta^{13}C$ and $\delta^{18}O$ analysis on a 3 mm wide annual ring from a 3.5 to 4 mm thick α-cellulose cross-section revealing no discrepancies from the standard methods. A breakthrough in terms of high sample throughput was introduced by Nakatsuka et al. (2011), Kagawa et al. (2012) and Kagawa and Nakatsuka (2014) where a container made of teflon punching sheet was designed to prevent disintegration of cellulose laths (see also Xu et al., 2011). The basic principle allows cellulose extraction from wood laths in one single batch providing exactly the same chemical conditions for all samples by using an extractor made of polytetrafluoroethylene material (PTFE, commonly known as teflon). This method significantly reduces the time needed for cellulose preparation while retaining the wood cell fabric mostly intact.

Based on the state-of-the-art presented by Kagawa et al. (2012), we modified the technique of cellulose extraction from wholewood cross-sections and developed a special device for holding several perforated teflon sheets with individual cross-sections in between. It allows cellulose extraction of thinner wholewood cross-sections than previously published. We

evaluate the performance of the high-throughput cellulose extraction method in conjunction with a precise dissection of tree ring samples for IRMS. The method, here called “cross-section extraction and dissection (CED) method” was tested and verified on different tree species. To validate the chemical purity of the cellulose obtained by extraction on cross-sections we used FTIR spectrometry and compared stable isotope measurements of the new cross-section method with results from the standard cellulose extraction method. We give a practical guideline for using this method and discuss advantages and constraints.

3.2. Experimental design

We follow a preparation scheme that is containing 9 steps, including modified steps of cellulose extraction from wood laths as presented by Nakatsuka et al. (2011) and Kagawa et al. (2012). The procedure finally provides specimens that are ready for IRMS analysis, but also allows other dendrochronological methods to be applied as large parts of the original samples (wood cores/segments) remain intact due to the use of thin sections:

(1) preparation of a plane wood surface by sanding or with a WSL core-microtome (Gärtner and Nievergelt, 2010),
optional: Scanning of the wood core for tree-ring widths measurement
(2) preparation of thin wholewood cross-sections (0.6 - 1.6 mm thickness and up to 30 cm in length) with a high-precision diamond saw or a core microtome,
(3) cleaning in an ultrasonic bath to remove wood swarf (if wood surface was polished or when using the high-precision diamond saw instead of the preparation with a microtome),
(4) subdivision of wood cores into 5 to 10 cm long segments,
optional: Cell structure measurements applying confocal laser scanning microscopy (CLSM) (Liang et al., 2013),
(5) enclosing of wholewood cross-sections in customized teflon punching and positioned in a special teflon extraction unit (FIGURE 3.1),
(6) chemical treatment of cellulose extraction as described by Green and Whistler (1963),
(7) freeze-drying of cellulose cross-sections within their extraction units,
(8) manual separation of tree rings under a binocular microscope or with an UV-laser microdissection microscope (Schollaen et al., 2014), and specimen collection in tin or silver capsules and
(9) stable carbon (C) and oxygen (O) isotope analysis via conventional Isotope Ratio Mass Spectrometry (IRMS) coupled online to a combustion or pyrolysis furnace.

The experimental design is explained in detail in the following subsections.

Preparation of cross-sections

To evaluate the applicability of the most critical process of cellulose extraction on tree-ring cross-sections we tested extraction on wholewood cross-sections from several coniferous and deciduous trees. Sample material was chosen to represent different wood growth rates and differently shaped tree ring boundaries, as well as a broad range of various cell structure features. After wood surface preparation and analysis of ring widths accurate cross-sections with varying thicknesses, ranging from 0.6 mm to 1.6 mm were produced. This was done by using a special high-precision, water cooled, diamond saw (ISOMED5000, ITW Test & Measurement GmbH, Düsseldorf, Germany), that was at the GFZ modified for handling samples of up to 30 cm in length. Alternatively a microtome (e.g. advanced core- microtome of the Swiss Federal Insitute for Forest, Snow and Lanscape Research) or any other appropriate saw (e.g. a double bladed saw, Dendrocut from Walesch Electronics GmbH, Switzerland) can be used.
Very soft woods, like baobab, with a high water content were frozen with liquid nitrogen and kept in dry ice. This provides sufficient hardiness for the cutting process ensuring accurate cross-sections.
The resulting cross-sections were then cut into segments of approx. 5 cm in length because shorter wood samples are easier to handle before and after the cellulose extraction process, as well as for manual tree-ring dissection using a binocular. Furthermore, for UV-laser-based microdissection as well as confocal laser scanning microscopy samples with a length of 5 cm are preferred according to the size of the respective object holders.
Additional remove from swarf by mean of an ultrasonic bath are necessary when the wood surface was polished or by using the high-precision diamond saw.

Cellulose extraction from wholewood cross-sections

The basic principle of this cellulose extraction method has been described by Nakatsuka et al. (2011) and Kagawa et al. (2012). In the following we describe a modified method using a special extraction device that has been established at the Dendrolaboratory of the GFZ in Potsdam.
In principle the novel extraction device is made of 2 main components (FIGURE 3.1):

Punching sheet sample holders (size: 70 x 30 mm) with spacer slides (2 mm thick) that keep samples of various thickness and width (e.g. from 5 or 10 mm cores) in position during the extraction process.

A teflon casing with: A lower mount (250 mm x 110 mm, 10 mm thick) with six rectangular wells (71 x 31 mm, 4 mm deep) for holding the punching sheet sample holders. Chemical solutions can percolate through the punching sheet holder by a rectangular hole (60 x 20 mm). An upper mount of the same dimensions as the lower mount, but with the wells being 2 mm deep, only. Both mounts are fitted together and fixed with teflon screws.

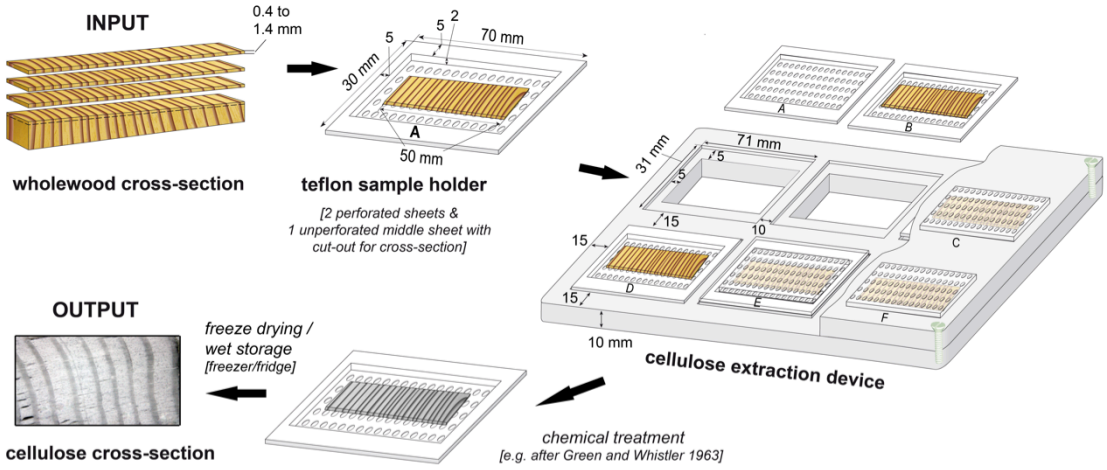

FIGURE 3.1 | Scheme of the cellulose extraction from wholewood cross-sections using 6 individual sample holders (70 x 30 mm) made of teflon punching sheets to be placed in a teflon mount (250 x 110 mm). Up to 5 cellulose extraction devices can be placed in a special glass container for chemical treatment. The glass container is put into a shaking water bath for applying a constant temperature of 60°C during the extraction process. Permanent labels (e.g. A..F) engraved on the individual sample holders and each teflon mount (e.g. M1, M2) provide unambiguous sample assignment.

These main components (6 teflon punching sheet holders placed in a teflon casing) built up one extraction unit. Several of these extraction units can be placed on top of each other with spacers in between ensuring appropriate circulation of chemical solutions at constant temperature (FIGURE 3.1). The cellulose extraction units are placed into a glass container that is positioned in a heated shaking water bath (Julabo, SW-21C). The glass container, made out of single borosilicate glass plates, is glued together with aquarium glue. The glue is chemical resistant against the used chemicals.

The shaking water bath allows cellulose extraction at a constant temperature (60°C) as described by Green and Whistler (1963). We are following a protocol that is outlined in detail by Wieloch et al. (2011). This study was focused on holocellulose, because isotopic differences between holo- and alpha-cellulose were found rather constant with time and of being small of higher order (e.g. Boettger et al., 2007).

For changing chemical solutions or washing of samples during the extraction procedure the extraction units are removed from the glass container with exhausted chemical solution and put into another glass container with new chemicals or de-ionized water. This

procedure saves time and causes minimum strain to fragile thin sections, hence avoiding damages to the cellulose cross-sections. After bleaching the resulting holocellulose samples are repeatedly rinsed with deionized water and stored in a freezer by -20°C. Thereafter the frozen cellulose cross-sections were freeze-dried for 2 days and then carefully taken out of the teflon sheets with a forceps. Dry cellulose cross-sections are kept between two labeled conventional microscope slides (26 x 76 mm, Thermo Fisher Scientific; Menzel GmbH, Braunschweig, Germany) fixed with a clamp or adhesive tape. Furthermore, very fragile samples are protected from any deformation with well fitted teflon sheets as spacers between the microscope slides.
After extraction process the water bath must be cleaned, dried and treated with teflon spray to protect the metal components against corrosion.

Tree-ring dissection from cellulose cross-sections

For stable isotope analysis tree-rings or parts thereof can be dissected from cellulose cross-sections by UV-laser microscopic dissection, in particular when ring widths are very narrow and/or growth ring boundaries are curved or asymmetric (Schollaen et al., 2014). In this study tree rings were separated manually using a scalpel under a binocular microscope with transmitted light. Tree-ring samples were cut along the tree-ring boundaries with great caution ensuring that the entire ring width is represented by the isotope sample (FIGURE 3.2).

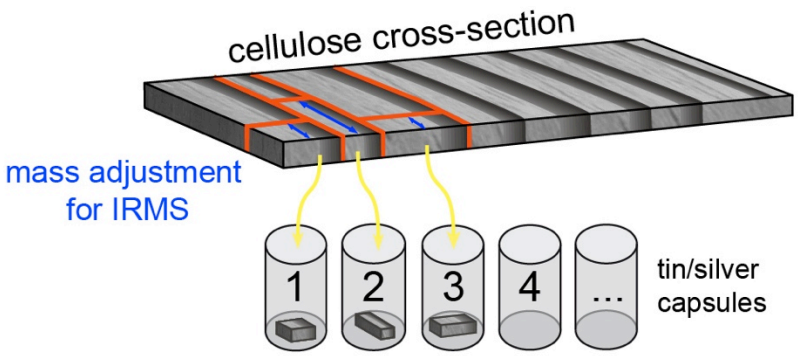

FIGURE 3.2 | Tree-ring dissection technique using cellulose cross-sections.Cellulose is separated perpendicular to the tree-ring boundaries and loaded into tin or silver capsules for IRMS analysis. Sample mass is adjusted and no sample homogenization is required. The sampling method allows precise tree-ring separation at annual to high-resolution scale.

The sample mass was adjusted for IRMS analysis by radial cuttings. Sample weight was controlled with a microbalance (AX26 DeltaRange; Mettler Toledo GmbH, Greifensee, Switzerland) and by adding or subtracting cellulose pieces resulting from the radial separation (perpendicular to the tree-ring boundaries) of tree-ring cellulose. In doing so, homogenization is no longer required and cellulose can be directly loaded into tin or silver

capsules for carbon and oxygen isotope analysis, respectively. Furthermore, provided that the IRMS has got an excellent linearity and the person who is performing the tree-ring cellulose dissection is well experienced, weighing may no longer be necessary for each sample when following this procedure.

Stable isotope analysis

Measurements of oxygen isotope ratios were carried out by high temperature TC/EA pyrolysis (at 1400°C) coupled online via Conflo IV to an IRMS Delta V Advantage (Thermo Fisher Scientific, Bremen, Germany). The TC/EA unit has been fitted with a reversed He carrier gas feed from the bottom (Gehre et al., 2004). The orginal autosampler is replaced by an autosampler from a Carlo-Erba NA 1500 (Milan, Italy) that is enclosed in a vacuum tight hood that is continuously being flushed with Argon. This is to avoid any uptake of moisture from air by the samples while waiting for the analysis.
The gas chromatograph for separating CO from H_2 and N_2 is equipped with a molecular sieve 5-A zeolite column, maintained at 75°C during normal operation. To protect the GC-column against fine graphitic dust particles during operation and against water while cleaning the pyrolysis tube (reactor) a chemical trap filled with magnesium perchlorate between the GC-column and the reactor was installed.
Measurement of stable carbon isotopes has been undertaken by combustion using an elemental analyser (Model NA 1500; Carlo Erba, Milan, Italy) coupled online via open split to an Isoprime IRMS (Isoprime Ltd, Cheadle Hulme, UK. The operating temperature of the combustion oven and the GC column were set to 1080°C and 80°C, respectively.
Masses of cellulose sample and reference materials weighed for stable oxygen and carbon isotope analyses were between 130-160 µg and 180–220 µg, respectively. Reproducibility of replicated measurements of reference material was better than ± 0.1‰ for $\delta^{13}C$ and ± 0.3‰ for $\delta^{18}O$, respectively. For all analyses we used Helium 5.0 as carrier gas. The isotope ratios are given in the delta (δ) notation, relative to the standards VPDB for $\delta^{13}C$ and VSMOW for $\delta^{18}O$ (Craig, 1957).

Chemical purity test

Nakatsuka et al. (2011) and Kagawa et al. (2012) tested and proved the chemical purity of their cellulose extraction from wholewood laths. Likewise, we evaluated the chemical purity of the cellulose gained from wholewood cross-section samples by applying FTIR (Fourier transform infrared) spectrometry identifying the functional groups for resin, lignin, cellulose and hemicellulose. The FTIR spectra were measured by direct absorbance using the KBr pellet technique. 1 mg of different cellulose cross-sections from one tree species (teak, *Tectona grandis*) and reference samples of α-cellulose powder (Fluka and Merck- α-cellulose) were milled, mixed with 450 mg of KBr-powder and pressed under

high pressure to thin pellets. The resultant pellets were vacuum dried by 50°C for 24h before placing them on a Vertex 80v FTIR-spectrometer (Bruker Optics, Germany). Each spectrum was measured at a spectral resolution of 0.25 cm^{-1} and 128 scans were taken per sample.

Furthermore, we compared exemplarily the stable isotope values of two different trees from teak wood, obtained by the new cross-section method and the standard method. With this comparison we wanted to test for discrepancies in the stable isotope ratios of carbon and oxygen between both cellulose extraction techniques.

3.3. Results

Fourier Transform Infrared (FTIR) spectrum analysis

The FTIR method is a well-known method to show the wood components composed of cellulose, holocellulose, lignin and extractives. The most characteristic changes in the FTIR spectra during the extraction of holocellulose occur on the wavelengths marked in (FIGURE 3.3). Here we compared the spectra of hemicellulose cross-sections from teak wood samples with the corresponding wholewood samples (completely untreated and resin extracted) and laboratory cellulose standards. There are many well-defined peaks (FIGURE 3.3 grey shaded bars) in the wholewood sample caused by functional groups of lignin (Harrington et al., 1964; Pandey and Theagarajan, 1997; Pandey and Pitman, 2003): 1598cm^{-1}/ 1511cm^{-1} for aromatic skeleton in lignin, 1460cm^{-1} C-H resulting from deformation and benzene vibration in lignin and 1270cm^{-1}/ 1226cm^{-1} from C–O stretching vibration in lignin. The particular absorption of hemicellulose components is around 1732cm^{-1}. The spectra of cellulose cross-sections from wood shows none of these peaks and the position of bands are approximately the same as for the standard samples of Fluka and Merck α-cellulose.

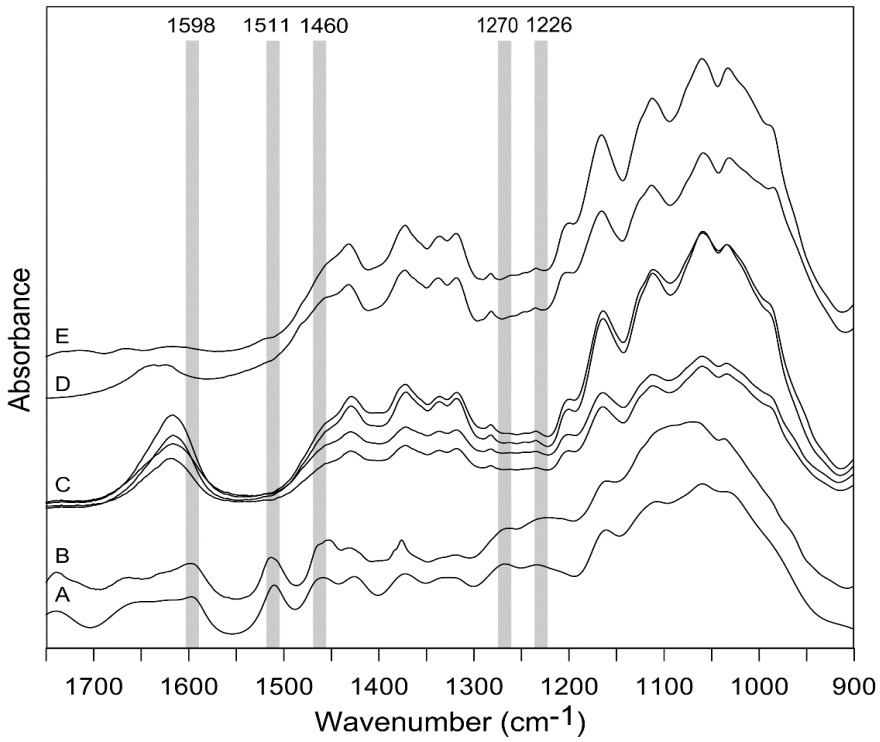

FIGURE 3.3 | FTIR Spectra of (A) untreated wholewood, (B) resin extracted wholewood, (C) holocellulose of wood samples, (D) α-cellulose standards (Merck) and (E) α-cellulose standards (Fluka). The wood samples are all from *Tectona grandis*. Grey shaded bars mark lignin-specific bands (Pandey and Theagarajan, 1997; Pandey, 1999). FTIR spectra of the cellulose cross-sections show no sign of residual lignin.

Comparison of cellulose preparation techniques

To further evaluated the suitability of the cellulose obtained by the cross-section extraction method we compared the measured stable isotope ratios with those obtained from cellulose extracted with the standard method. Therefore we measured the carbon and oxygen stable isotope values of two different teak trees by analyzing a time period at the beginning of tree growths and a time period from most recent tree rings (FIGURE 3.4). This was done to obtain stable isotope values from the heart- and sapwood part of the tree. We found high statistically significant correlation between the stable isotope datasets, especially for carbon isotope data which are nearly identical. This comparison shows that the extracted cellulose by cross-sections has similar chemical compositions as cellulose obtained by standard methods.

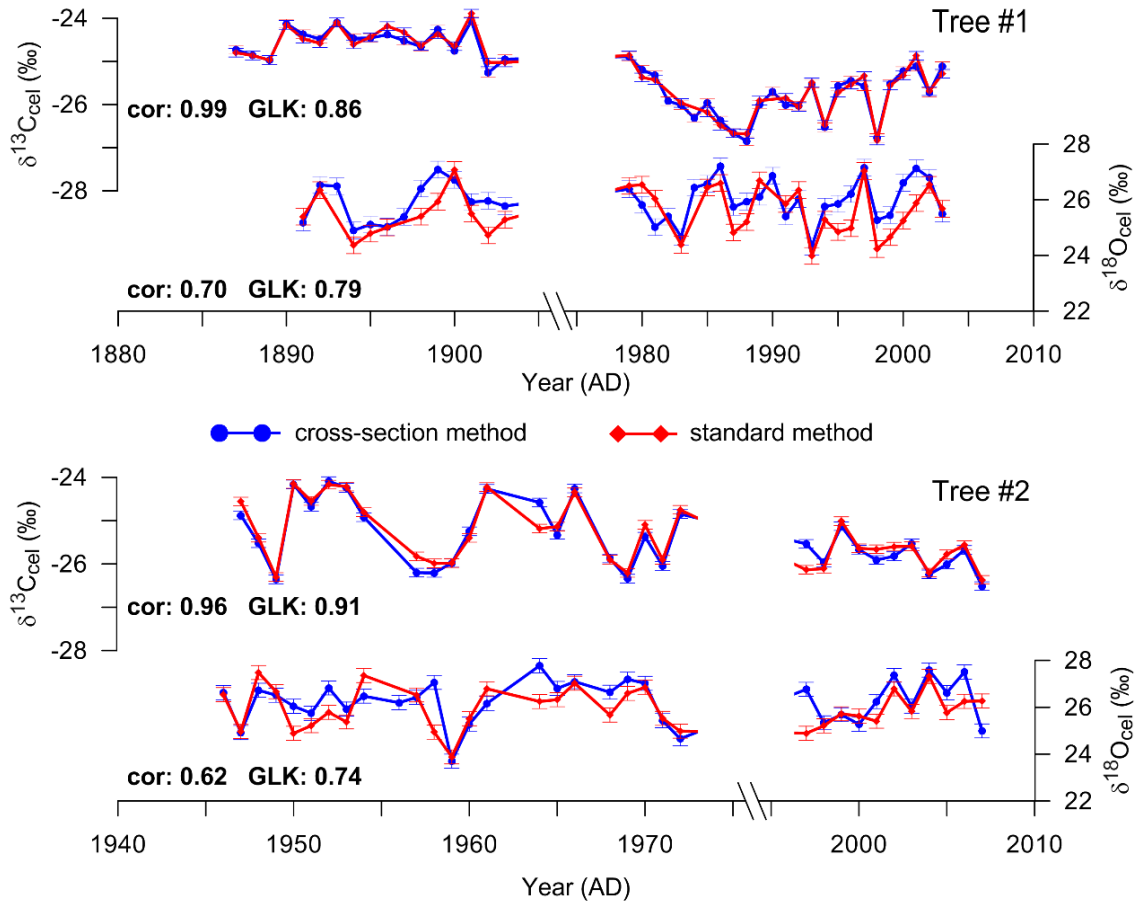

FIGURE 3.4 | Comparison between $\delta^{13}C$ and $\delta^{18}O$ values from cellulose of two teak trees using the standard method of cellulose extraction (red lines) and the cross-section method (blue lines). The analytical precision is shown as error bars. GLK: Gleichläufigkeit (Cropper, 1979; Esper et al., 2001); cor: Pearson correlation coefficient. The stable isotope records of the 2 different methods are well correlated and show a high degree of synchronization suggesting that the cellulose extraction directly from tree-ring cross-sections is working properly.

Example data

To evaluate the practical application of the cellulose cross-section method we tested the cross-section extraction and dissection procedure on several tree species with different cell structure types. In general the new extraction method works properly for coniferous as well as for deciduous wood. FIGURE 3.5 shows images of the selected coniferous and deciduous tree species before and after cross-section extraction. The tree-ring structures largely remained well identifiable. Characteristic features as tracheid fabrics (see coniferous wood samples), vessels (see deciduous wood samples), parenchyma bands (e.g. teak and baobab sample) or woody rays (e.g. oak sample) are equally visible in the wood and cellulose cross-sections. Even rings that are very narrow or with irregular shapes remain visible, as shown for larch and juniper, respectively.

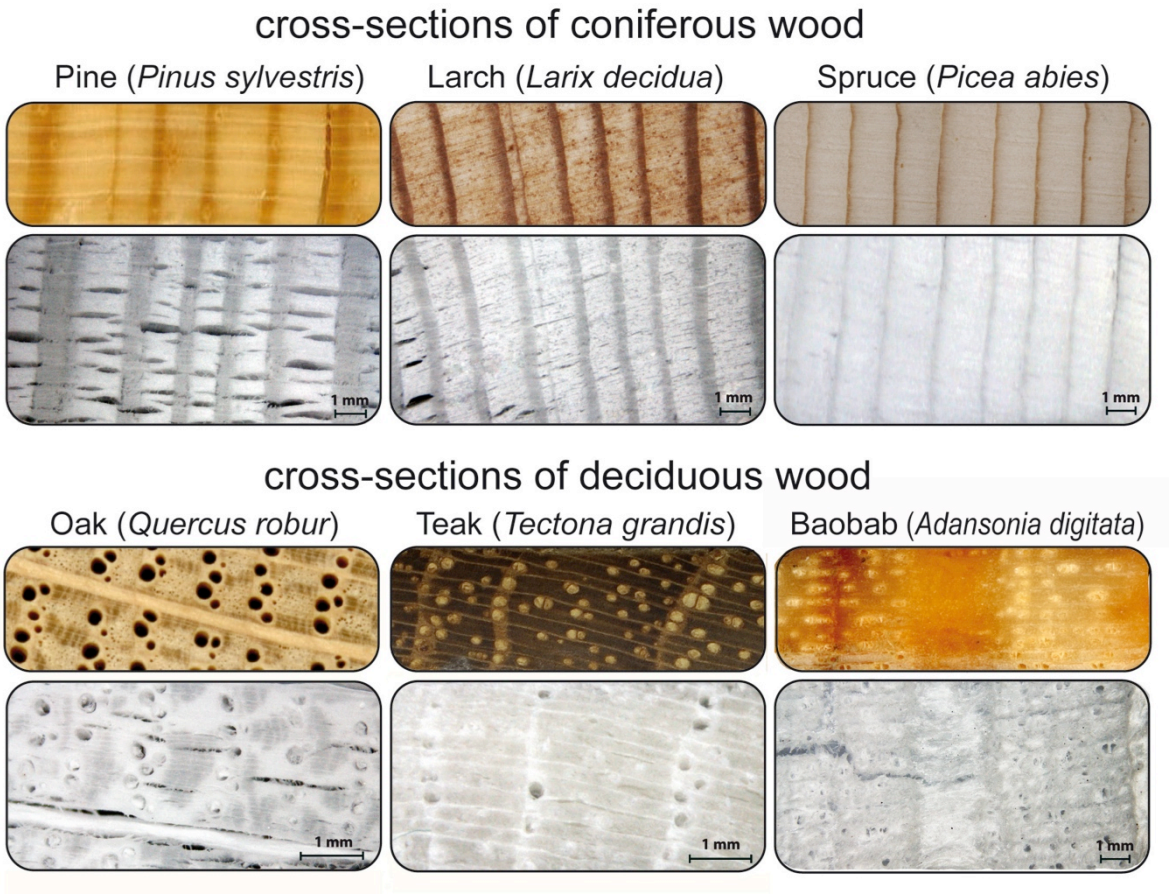

FIGURE 3.5 | Tree species that have been tested for cellulose extraction on wholewood cross-sections. Upper pictures of each species show wholewood cross-sections, lower pictures display the cellulose cross-section obtained.Note: fo r pine, oak and teak the pictures shown are from the same sample, but not exactly the identical cross-section for wholewood and cellulose. Tree-ring structures remained clearly visible after the cellulose extraction process, although freeze drying has frequently caused shrinkage cracks. These can be avoided by keeping the samples wet until tree-ring dissection.

3.4. Discussion

We present a guideline for a modified method of cellulose extraction from wholewood cross sections and subsequent dissection of tree-rings or parts thereof that requires no additional homogenization. The procedure was applied to different tree species with a broad range of various cell structures, wood growth rates as well as potentially different amounts of lignin and resin.

Evaluation of the cellulose extraction method on cross-sections

The chemical purity tests of the holocellulose obtained from the cross-section extraction method confirm that the cellulose extraction procedure is working properly as the FTIR

spectra of the cellulose show no lignin and resin peaks. In addition, the comparison with isotope data obtained from standard extraction methods show significant high synchronization. Despite the expected FTIR peak around 1732 cm^{-1} that is supposed to be significant for hemicellulose components such as mannose and xylose, we found no significant peaks in this area (FIGURE 3.3). Cellulose is hygroscopic by nature and water adsorbs very fast to oven-dry cellulose. This might explain the relative intense peak around 1616 cm^{-1} deriving from the cellulose cross-section samples.

The CED- method has several benefits compared to the standard extraction methods. Due to the use of cross-sections wood from numerous tree rings can be extracted at one step. Cross-sections of in total 180 cm in length (correspond to 6 wood cores of 30 cm length) can be extracted at a time. The chemical treatment is consistent for all samples and renewal of NaOH- or $NaClO_2$- solutions is easy and fast. Less space for the extraction aperture is needed in the laboratory, i.e. the fume hood. Another benefit is that the cell structures largely remain visible and can be still distinguished under a binocular with transmitted light. Thus tree-ring dissection and collection into tin or silver capsules can be made in a single step without homogenization and by minimizing the efforts for weighing. The new method also facilitates dissection of very narrow tree-rings and furthermore offers potential for applying UV-laser-based microscopic dissection for highly resolved and very precise intra-annual tree-ring stable isotope analysis. Finally, due to the use of cross-sections multidisciplinary analyses (tree-ring width, stable isotope, quantitative wood anatomy, wood density) are possible on the same wood samples, since the isotope analyses no longer sacrifice a whole wood core.

This method can be applied to wood samples from a large number of different coniferous and deciduous tree species. However, caution should be taken if the cross-sections are too thin or too thick. Cellulose cross-sections thinner than 0.6 mm are very fragile and difficult to handle. On the other hand, cross-sections thicker than 1.6 mm may need a longer extraction procedure and, more important, shrinkage during cellulose extraction or drying may cause distortions in vertical direction (parallel to wood fibres or vessels) that prevent from precise and unambiguous dissection of defined tree rings.

The flexible usage of custom designed teflon sheets within teflon casings allows cellulose extraction from wholewood cross-sections of different size and thickness. However, with respect to convenient handling we recommend the use of wood samples with max. 10 cm length, min. 2 mm width and max. 1.6 mm thickness. Generally cellulose cross-sections are more difficult to handle and more sensitive to breakage than wholewood cross-sections, thus gentle handling during the extraction process and especially during the tree-ring dissection is required as decribed above.

Tree-ring dissection and preparation for IRMS without homogenization

Modern online IRMS systems allow the measurement of very small samples with well reproducible results from sample masses with carbon or oxygen contents of less than 25 µg (ca. 50 µg of cellulose). Large numbers of tree-ring samples cannot be weighed without huge efforts in time and manpower. As a compromise sample masses ranging between 130–160 µg ($\delta^{18}O$) and 180-220 µg ($\delta^{13}C$) are used for IRMS analysis at the Dendrochronology Laboratory of the GFZ. Nonetheless, these amounts are still small and evoke additional challenges to conventional methods of cellulose extraction and sample homogenization before or after extraction. Laumer et al. (2009) tested different homogenization approaches grinding the wood sample before extraction, homogenization of cellulose by freeze milling or ultrasonic treatment and came to the conclusion that all methods are applicable for stable isotopes analysis. The enormous sample lost and time intensive cleaning procedure by grinding or freeze milling makes these approaches unsuitable. The loss of sample material by means of ultrasonic homogenization is rather small. However, oxygen isotopic exchange between sample and water in consequence of increased temperatures resulting from too long ultrasonic treatment is a known but frequently underestimated threat. Some laboratories do use higher amounts of sample material (>1mg) in order to reduce inhomogeneity effects. However, many tree-ring records from long-lived trees at timberline sites rarely do provide enough wood material from their narrow and frequently wedging rings. The cross-section dissection method described here (FIGURE 3.2) may make (ultrasonic) homogenization obsolete providing a good linearity of the IRMS. Furthermore, it takes advantage of modern online IRMS systems that are capable of analyzing very small samples amounts.

A special focus on the tree species presented here, lies on tropical tree species, where the isotope dendroclimatology is still very much in development. However, in the last decades, the potential of stable isotope records from tropical tree species, such as cedar (e.g. Brienen et al., 2012) or teak (e.g. Schollaen et al., 2013), have been developed largely to improve the palaeoclimate picture of tropical climate. The examples shown in FIGURE 3.5 demonstrate that the cross-section extraction and dissection method can be applied very well for tropical tree species. This opens new possibilities for studies on tropical species with more complicated wood anatomical structures, like baobab (*Adansonia digitata*), a species with high potential for providing millennial stable isotope records for climate reconstructions (Robertson et al., 2006; Slotta et al., 2014).

3.5. Conclusion

We conclude that this method of extracting cellulose and dissecting tree rings directly from cross-sections is an important approach to optimize stable isotope analysis in two ways: faster and costumer friendly extraction and precise tree-ring dissection and collection of homogenous samples at annual to high-resolution scale. The question of whether or not cellulose extraction is required for stable (oxygen) isotope analysis on tree-ring chronologies may become superfluous, as cellulose extraction and homogenization are no longer a time limiting step.

Acknowledgements

We thank Akira Kagawa & Takeshi Nakatsuka for introducing the new method of cellulose extraction from wood laths and their helpful comments during its establishment at the GFZ, Potsdam. We are grateful to Carmen Bürger and David Göhring for support in the laboratory, and to Kirstin Jansen, Franziska Slotta, Bastian Ullrich and Jessica Baker for testing successfully the introduced method and providing sample images. We thank Monika Koch-Müller and Hans-Peter Nabein who enabled the FTIR spectrometry and gave valuable help with data interpretation. Furthermore we thank Ingo Heinrich and Julia Kaplick for fruitful discussions. This study was funded by the Joint DFG/FAPESP Research Grant Proposal (HE3089/5-1), the HIMPAC (HE 3089/4-1), as well as by the CADY (BMBF, 03G0813H) project. This study is a contribution to the Virtual Institute of Integrated Climate and Landscape Evolution Analysis –ICLEA– of the Helmholtz Association.

Preface to Chapter 4

After introducing novel approaches for precise and efficient stable isotope analysis from tree rings, the following two chapters will focus on the investigation of stable isotope records from tropical trees and their use as climate proxies.

Tropical dendrochronology was long considered impractical because the occurrence of annual growth rings in the humid tropics has been denied for a long time as a consequence of lacking clear seasonality. However, Coster (1927) and Berlage (1931) described already early in the 20th century the existence of annual growth rings in teak trees from tropical Indonesia. Within the last decade, research on tropical dendrochronology has advanced rapidly, nevertheless the number of studies is still very limited.

Annual growth rings are formed when the tree experiences cambial dormancy for a annually recurring distinct period of the year. This is usually the winter time in mid- or boreal latitudes, whereas in tropical regions such a period is mostly a dry season or a short dry period as shown by tree-ring studies from tropical Asia and Australia (e.g. Baker et al., 2008; Buckley et al., 2010; Buckley et al., 1995; Buckley et al., 2007; D'Arrigo et al., 1994; D'Arrigo and Smerdon, 2008; D'Arrigo et al., 2006; Heinrich et al., 2008; Pumijumnong and Eckstein, 2011; Pumijumnong et al., 1995; Sano et al., 2009), from tropical Africa (e.g. Fichtler et al., 2003; Krepkowski et al., 2011; Stahle, 1999; Therrell et al., 2006; Trouet et al., 2010) and from the American tropics (e.g. Biondi, 2001; Biondi et al., 2005; Bräuning et al., 2009; Brienen and Zuidema, 2005; Schöngart et al., 2004; Volland-Voigt et al., 2011; Worbes, 1999). Furthermore a period revealing cambial dormancy could be an annually recurring flooding period as in Amazonian floodplain forests (e.g. Schöngart et al., 2002) or regular salinity fluctuations in mangrove forests (e.g. Robert et al., 2011; Verheyden et al., 2004b).

More and more studies on tropical trees apply stable isotope measurements to evaluate the climatic growth response (e.g. Ballantyne et al., 2010; Fichtler et al., 2010; Gebrekirstos et al., 2009; Krepkowski et al., 2013; Poussart et al., 2004; Sano et al., 2012; Verheyden et al., 2005; Worbes et al., 2013; Xu et al., 2013), and to demonstrate the possibility of using even ‘ringless’ species for dendroclimatic studies (e.g. Anchukaitis et al., 2008; Evans and Schrag, 2004; Loader et al., 2011; Poussart and Schrag, 2005).

As teak is one of the tree species in tropical and subtropical Asia that shows high potential for climate investigations (Pumijumnong, 2013) revealing multi-centennial ring-width chronologies (e.g. Buckley et al., 2007; D'Arrigo et al., 1994), the following chapter presents the first well replicated stable isotope chronologies of Indonesia and revealing climate signals. This new palaeoclimatic study adds another piece to the puzzle, yielding a better understanding of the global climate system.

Chapter 4

Multiple tree-ring chronologies (ring width, $\delta^{13}C$ and $\delta^{18}O$) reveal dry and rainy season signals of rainfall in Indonesia

Teak (*Tectona grandis*) trees in Indonesia
(Author´s picture: photograph taking during field campaign 2008)

This chapter was published in:

Quaternary Science Reviews, 2013, V. 73, p. 170-181

Authored by Karina Schollaen[a], Ingo Heinrich[a], Burkhard Neuwirth[b], Paul J. Krusic[c], Rosanne D. D´Arrigo[d], Oka Karyanto[e] and Gerhard Helle[a]

[a]*GFZ - German Research Centre for Geosciences, Section 5.2 Climate Dynamics and Landscape Evolution, Telegrafenberg, 14473 Potsdam, Germany*
[b]*DeLaWi Tree-Ring Analyses, Preschlinallee 2, D-51570 Windeck, Germany*
[c]*Bert Bolin Centre for Climate Research, Department of Physical Geography and Quaternary Geology, Stockholm University, SE-106 91 Stockholm, Sweden*
[d]*Tree-Ring Laboratory, Lamont-Doherty Earth Observatory, P.O. Box 1000, Route 9W, Palisades, NY 10964, USA*
[e]*Faculty of Forestry, Gadjah Mada University, Yogyakarta, Indonesia*

Abstract

Climatic hazards, such as severe droughts and floods, affect extensive areas across monsoon Asia and can have profound impacts on the populations of that region. The area surrounding Indonesia, including large portions of the eastern Indian Ocean and Java Sea, plays a key role in the global climate system because of the enormous heat and moisture exchange that occurs between the ocean and atmosphere there. Here, we evaluate the influence of rainfall variability on multiple tree-ring parameters of teak (*Tectona grandis*) trees growing in a lowland rain forest in Central Java (Indonesia). We assess the potential of, annually resolved, tree-ring width, stable carbon ($\delta^{13}C$) and oxygen ($\delta^{18}O$) isotope records to improve our understanding of the Asian monsoon variability. Climate response analysis with regional, monthly rainfall data reveals that all three tree-ring parameters are significantly correlated to rainfall, albeit during different monsoon seasons. Precipitation in the beginning of the rainy season (Sep-Nov) is important for tree-ring width, confirming previous studies. Compared to ring width, the stable isotope records possess a higher degree of common signal, especially during portions of the peak rainy season ($\delta^{13}C$: Dec-May; $\delta^{18}O$: Nov-Feb) and are negatively correlated to rainfall. In addition, tree-ring $\delta^{18}O$ also responds positively to peak dry season rainfall, although the $\delta^{18}O$ rainy season signal is stronger and more time-stable. The correlations of opposite sign reflect the distinct seasonal contrast of the $\delta^{18}O$ signatures in rainfall ($^{18}O_{Pre}$) during the dry (^{18}O-enriched rain) and rainy (^{18}O-depleted rain) seasons. This difference in $^{18}O_{Pre}$ signal reflects the combination of two signals in the annual tree-ring $\delta^{18}O$ record. Highly resolved intra-annual $\delta^{18}O$ isotope analyses suggest that the signals of dry and rainy season can be distinguished clearly. Thereby reconstructions can improve our understanding of variations and trends of the hydrological cycle over the Indonesian archipelago.

Keywords: *oxygen and carbon stable isotopes, tree rings, tropics, dendroclimatology, monsoon, multiparameter approach, tectona grandis, seasonal rainfall variability*

Highlights

- First well replicated, centennial, multi-parameter TRW, $\delta^{13}C/\delta^{18}O$ record from teak.
- $\delta^{13}C$ and $\delta^{18}O$ records reveal significant higher rainfall signals than tree-ring widths.
- Tree-ring $\delta^{18}O$ responds to peak dry and rainy season rainfall.
- High-resolution $\delta^{18}O_{TR}$ values can distinguish seasonal rainfall variability.
- Reconstruction of seasonal rainfall variability over Indonesia is possible with $\delta^{18}O_{TR}$.

4.1. Introduction

The climate of Indonesia is governed by an equatorial monsoon system with distinct rainy and dry seasons (e.g. Aldrian and Susanto, 2003; Hastenrath, 1991). Monsoon variations can cause extreme droughts and related wildfires as well as severe flooding, hence, the monsoon has an enormous affect on the livelihood of millions of people (e.g. Boer, 2005). The island of Java, one of the most densely-populated places on the globe, is particularly vulnerable to extremes in rainfall. Understanding long-term, tropical, monsoon variability is crucial since the tropics appear to impact climate worldwide (e.g. Evans et al., 2001; Sarachik and Cane, 2010; Ummenhofer et al., 2013). However, instrumental climate data in this area are spatially and temporally limited. High-resolution proxy records would improve considerably our understanding of past monsoon variations.

Tree rings are one of the most important archives in palaeoclimate research because of their precisely dated, annually resolved information, and the broad geographical distribution of trees (Hughes, 2011). Previous studies in Asia have revealed relationships between tree-ring width and climate parameters such as rainfall (e.g. Berlage, 1931; Pumijumnong et al., 1995; Ram et al., 2008), sea surface temperature (e.g. D'Arrigo et al., 2006) or monsoon related parameters like drought frequency and intensity (e.g. Borgaonkar et al., 2010; Buckley et al., 2007). However, no land rainfall reconstruction from tree-ring width indices exists for the Indonesian Archipelago.

Tree rings not only record growth rates as measured in ring widths, but also provide stable isotope ratios that are directly controlled by a range of external and internal factors that are reasonably well understood (Barbour, 2007; Farquhar et al., 1982; Helle and Schleser, 2004b; McCarroll and Loader, 2004; Roden et al., 2000). Therefore, it is reasonable to expect tree-ring stable isotope records could provide climate information beyond that contained in ring widths.

The carbon and oxygen isotope composition in tropical tree rings contains information about hydrological changes in the arboreal system. $\delta^{13}C$ has mainly been used to study changes in intrinsic water-use efficiency of trees, as well as physiological responses to climatic changes (e.g. Brienen et al., 2011; Cernusak et al., 2007; Fichtler et al., 2010; Gebrekirstos et al., 2009; Hietz et al., 2005; Nock et al., 2011). $\delta^{18}O$ in tropical timber has been proven to primarily represent the isotopic composition of rain, i.e. the source-water (e.g. Brienen et al., 2012; Evans and Schrag, 2004). Plant physiological effects like leaf water enrichment due to transpiration (Barbour, 2007; Helle and Schleser, 2004b; McCarroll and Loader, 2004; Roden et al., 2000) do not seem to be particularly pronounced in $\delta^{18}O$ records from tropical tree rings (e.g. Brienen et al., 2012). Variation of $\delta^{18}O$ in rainfall is determined by several factors where the amount of rain (Araguás-Araguás et al., 1998; Dansgaard, 1964) plays a key role in producing a strong inverse

correlation (FIGURE 4.2A).

The majority of tree-ring oxygen isotope studies from lowland tropics undertaken so far, relies on just a few replicated samples (1-3), and mostly reveals the expected significant negative correlation with rainfall amounts (Ballantyne et al., 2010; Evans, 2007; Evans and Schrag, 2004; Managave et al., 2011; Poussart et al., 2004), although in one instance a positive correlation with rainfall amount was found (Managave et al., 2010b). From tropical or sub-tropical Asia centennial, or even longer, stable isotope records are scarce (e.g. Managave et al., 2011; Sano et al., 2012; Zhu et al., 2012). To date no well replicated, long-term, stable isotope record exists from lowland teak trees.

In this study, we present the first well-replicated centennial stable isotope records ($\delta^{13}C_{TR}$ and $\delta^{18}O_{TR}$) for Indonesia derived from teak. We selected a site for isotope analyses previously reported to have a rather weak ring width climate signal (D'Arrigo et al., 2006). The aim was to test if tree-ring stable isotopes reveal a better relationship to rainfall than ring widths. Hence, we compared carbon and oxygen isotopes ($\delta^{13}C_{TR}$, $\delta^{18}O_{TR}$), as well as tree-ring width (TRW) chronologies from the same material to regional monthly rainfall data and seasonal sums of monthly rainfall in order to assess isotopic variability on inter-annual scales. Finally, we use highly resolved intra-annual $\delta^{18}O_{TR}$ data to explain the transfer of the $\delta^{18}O$ rainfall signal ($\delta^{18}O_{Pre}$) of dry and rainy season into the tree rings of teak to prove potential additional value of isotope analyses for climate investigations.

4.2. Material and Methods

Regional setting

Teak samples were collected from a lowland rain forest at an elevation of 380 m a.s.l. The study site, named Donoloyo, is located 90 km east of the city of Yogyakarta in the eastern part of Central Java, Indonesia (07°52’S, 111°11’E) (FIGURE 4.1). The same site was part of an earlier investigation on teak tree-ring width described in D'Arrigo et al. (2006). This study site is a very old forest and for the last few decades, a protected area. In former times only selected timber were taken from this forest for the construction of palaces and mosques.

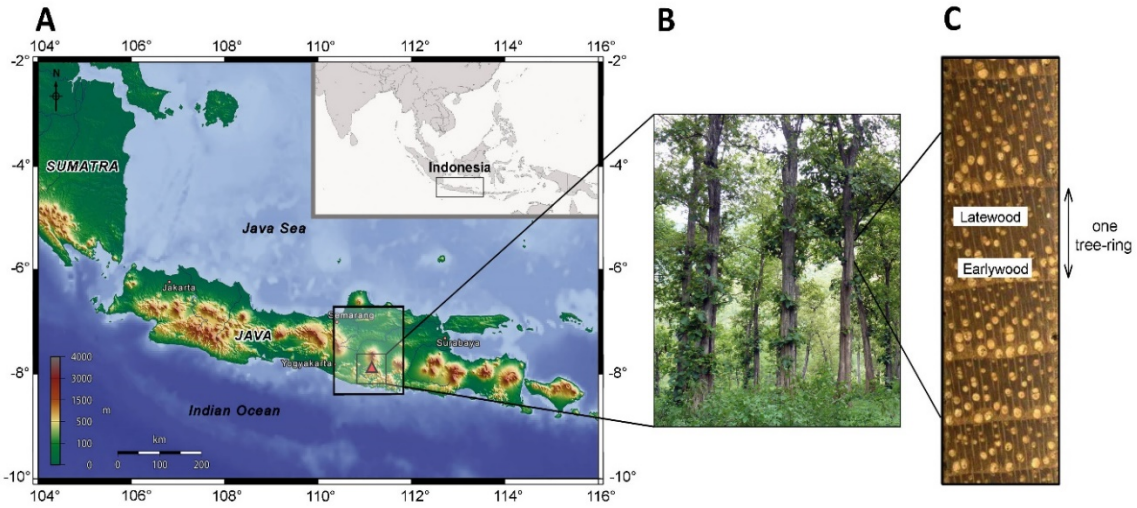

FIGURE 4.1 | Map showing the location of the study site (A) in a lowland rain forest (380 m a.s.l.) in the eastern part of Central Java (07°52'S, 111°11'E). (B) Photograph shows the study site (Donoloyo) with teak (Tectona grandis) trees. (C) Microscopic image showing wood anatomical structure of a teak cross section from the study site.

Most of the Indonesian archipelago receives rainfall throughout the year and encompasses a variety of rainfall regimes (Braak, 1921-29). However, Central and Eastern Java are influenced by the equatorial monsoon climate, characterized by distinct rainy and dry seasons (FIGURE 4.2A). The rainy season begins with the arrival of the north-west monsoon in October and normally persists till May of the following year. The dry season follows the south-east monsoon from June to September. The peak of the rainy season is centred between December and February, when a quasi-permanent low-pressure centre over the region develops and lower-tropospheric convergence is pronounced. More detailed information about the meteorology of Indonesia can be found in Sukanto (1969), Hackert and Hastenrath (1986) and McBride (1999).

The isotopic composition of rainfall over Java shows distinct seasonal changes linked to rainfall amount. Rainfall during the dry season (~200 mm on average (Jun-Sep), 1900-2002) is generally enriched in ^{18}O (less negative $\delta^{18}O_{Pre}$ values). This is a consequence of reduced condensation processes that leads to a "heavy" isotope composition in rainfall. Relative to the dry season, rain during the rainy season (~1700 mm on average (Oct-May), 1900-2002) is generally much more depleted in ^{18}O (more negative $\delta^{18}O_{Pre}$ values) due to extended, cumulative, rainout processes (Araguás-Araguás et al., 2000; Dansgaard, 1964; Gat, 1996). Data on the $\delta^{18}O$ of rain water is available from the Global Network of Isotopes in Precipitation (GNIP) maintained by the International Atomic Energy Agency (IAEA), Vienna. The closest GNIP station to our study site is ca 500 km away, near Jakarta. It provides data from 1962 to 1998. The seasonal rainfall pattern and amount recorded at this station are similar to that at Donoloyo (FIGURE 4.2A, grey line).

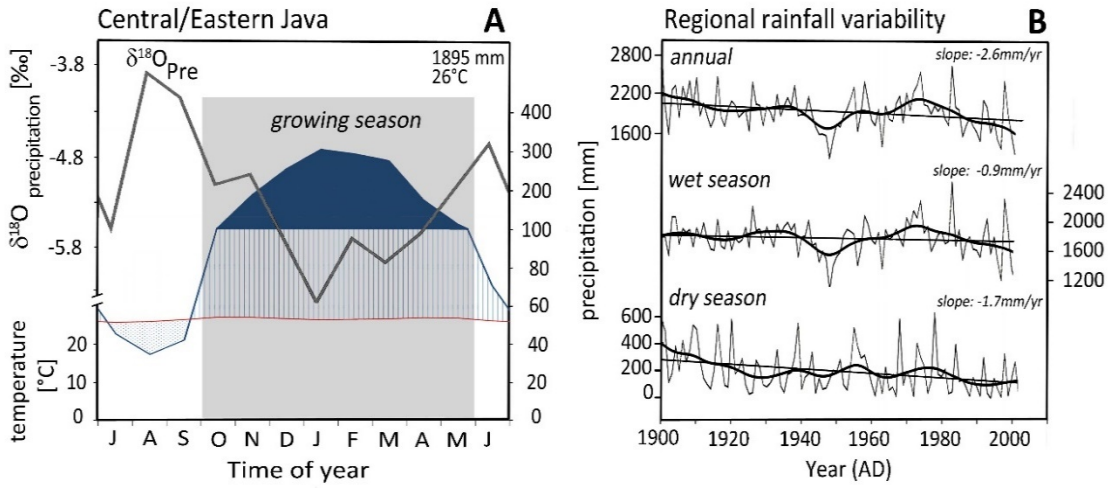

FIGURE 4.2 | (A) Mean monthly rainfall and temperature at the study site derived from a regional mean (REG) of different stations for rainfall (1900-2002; see Supplementary TABLE S4.1, FIG. S4.1) and gridded climate data for temperature (CRU3.0 1901-2002; Mitchell and Jones, 2005). Grey line indicates the monthly mean $\delta^{18}O$ values in rainfall ($\delta\,^{18}O_{Pre}$) for Jakarta/Indonesia (1962-1998; GNIP: http://www-naweb.iaea.org). The growing season (grey shadow) of teak extends approximately from October to May. At rainfall levels above 100 mm the axis scale is shortened (Walter and Breckle, 1991). (B) Regional rainfall for rainy (October to May) and dry (June to September) season and annual sum (REG, 1900-2002). 20-year cubic-smoothing splines (thick black lines) and linear trend lines (black lines) show long-term fluctuations and trends.

The amount of rainfall in the region of our study site shows a declining long-term trend (1900-2002) in the annual rainfall sum (-2.7 mm per year), with the dry season showing a very high and almost linear decrease (-1.7 mm per year) over the 20th century (FIGURE 4.2B). The rainy season is characterized by rather stable rainfall conditions from 1900 to 1940, a drastic decline during the 1940s, followed by increasing rainfall from 1950 to 1974. Since the late 1970s, total annual rainfall has decreased with higher year-to-year variability then previously recorded. The severe decline from 1945 to 1950 may be due to the drastic decrease in the number of reporting meteorological stations during the Indonesian National Revolution that occurred at the same time (see Supplementary FIGURE S4.2). Overall, since 1900, there has been a general trend towards drier conditions in Central/Eastern Java.

The vegetation period (growing season) for teak in Central and Eastern Java generally lasts from the beginning of October to the end of May (Coster, 1927, 1928; Geiger, 1915). From about mid-June to September (dry season) the trees are leafless and produce no wood as they are in a state of cambial dormancy (Coster, 1927, 1928). Bud burst and cambial activity start with the onset of the monsoon rains and flowering occurs towards the end of the rainy season. Thus teak is showing distinct annual growth rings, mainly due to the seasonality of rainfall in their habitat.

Ring-width chronology

The ring-width (TRW) chronology for this study site was developed from 32 wood cores of 16 teak trees (2 cores per tree, 5 mm diameter). Eight of the 16 trees were collected during a field campaign in November 2008 and another eight drawn from a collection used in a previous study by D'Arrigo and co-workers (D'Arrigo et al., 2006). All pre-treatment of the collected samples was carried out in the laboratory following standard procedures outlined in Stokes and Smiley (1968) and Schweingruber (1983). To improve the visibility of the tree-ring structure the surface of the core samples was cut with a microtome (WSL core microtome, Switzerland) and fine chalk was rubbed into the pores to increase ring contrast. For dating purposes, we followed the convention for the southern hemisphere, which assigns to each tree ring the year in which radial growth begins (Schulman, 1956). Subsequently, ring widths were measured and synchronized with the programme TSAPWin (Rinn, 2005) using statistical tests (Gleichläufigkeit, t-test). Visual crossdating (Fritts, 1976) was performed by skeleton plots (Douglass, 1935) and verified using COFECHA software (Holmes, 1983). We used the programme ARSTAN (Cook et al., 2012) for standardization and chronology construction. The individual raw ring-width series were standardized by fitting a cubic smoothing spline (Cook and Peters, 1981) with a 50% frequency response cut-off at 67% of the series length to each TRW series to remove age trends. Indices were calculated as ratios between the measured ring-widths and spline values. The resulting standardized index values were prewhitened using an autoregressive model, then averaged across all series using a be-weight robust mean to reduce the influence of outliers (Cook and Kairiukstis, 1990).

$\delta^{13}C_{TR}$ and $\delta^{18}O_{TR}$ chronologies

For dendroclimatic isotope studies four to six trees are considered sufficient (e.g. Leavitt, 2010). In this experiment we used seven different trees chosen according to the following criteria: (i) correct dating and highly correlated measurements with the master reference curve developed from all trees in the study (indicated by statistical parameters such as Gleichläufigkeit-values) (Cropper, 1979; Riemer, 1994; Schweingruber et al., 1990) and Pearson's correlation coefficient (Briffa and Jones, 1990; Wigley et al., 1984), (ii) distinct and straight tree-ring borders and (iii) fewest number of problematic zones containing such features as false, narrow or missing rings. We analyzed 108 years (1900-2007), a period long enough to provide sufficient calibration and verification with instrumental climate data, and reveal potential trends over the 20th century. The tree rings from all cores were separated individually with a scalpel and ground to assure homogeneity. Extractives, such as wood resins and oils, but also glue, pencil and chalk remains were removed from the wood with boiling de-ionized water and ethanol in a multiple sample isolation system for solids (Wieloch et al., 2011). Recent research has shown that the cellulose extraction is

not as crucial as previously thought 30-40 years ago (Borella et al., 1998; McCarroll and Loader, 2004; Taylor et al., 2008; Verheyden et al., 2005). Hence, resin extracted wood material was used instead of cellulose due to some very narrow rings which would not have provided sufficient amounts of cellulose for conventional online Isotope Ratio Mass Spectrometer (IRMS) determination of $\delta^{13}C$ and $\delta^{18}O$. Carbon isotope ratios were measured by combustion (at 1080°C) using an elemental analyser (Model NA 1500; Carlo Erba, Milan, Italy) coupled online to an IRMS (Isoprime Ltd. Cheadle Hulme, United Kingdom). Oxygen isotope ratios were measured using a high temperature TC/EA pyrolysis furnace (at 1400°C) coupled online to an IRMS (Delta V Advantage, Thermo Scientific, Bremen, Germany). Sample replication resulted in a reproducibility of better than ±0.1‰ for $\delta^{13}C_{TR}$ values and ±0.25‰ for $\delta^{18}O_{TR}$ values. The isotope ratios are given in the conventional delta (δ) notation, relative to the standards VPDB for $\delta^{13}C$ and VSMOW for $\delta^{18}O$ (Craig, 1957).

The carbon isotope record was corrected for anthropogenic changes in atmospheric CO_2 induced by fossil fuel burning and deforestation since industrialization (1850). A decline in the atmospheric $\delta^{13}C$ source was removed from the raw $\delta^{13}C_{TR}$ series by subtracting for each tree-ring stable isotope value the annual changes in $\delta^{13}C$ of atmospheric CO_2 obtained from ice cores and direct measurements (Leuenberger, 2007) resulting in a corrected $\delta^{13}C$ record ($\delta^{13}C_{cor1}$). To take account of changes in plant response potentially from increasing atmospheric CO_2 concentrations (pCO_2), a further correction was applied. Since this plant physiological effect is under debate, we show a range of published pCO_2 effects on $\delta^{13}C_{TR}$ (Feng and Epstein, 1995; Kürschner et al., 1996; Schubert and Jahren, 2012). For further data analysis we chose a moderate correction for pCO_2 effects on carbon isotope discrimination of 0.73‰ per 100 ppm ($\delta^{13}C_{Cor2}$; Kürschner et al., 1996; Schubert and Jahren, 2012). No corrections are required for the oxygen isotope data.

High-resolution intra-annual sampling of tree rings

High-resolution intra-annual sampling was performed by using an UV-Laser microdissection microscope (LMD7000, LEICA Microsystems, Wetzlar, Germany). First, cross-sections from the wood cores (5 mm diameter) were cut with a core microtome (Gärtner and Nievergelt, 2010). Second, the cross-sections (approximately 500 µm thickness) were fixed in special metal frame slides and mounted on the object holder of the microdissection microscope. The annual rings were graphically subdivided into several sub-sections in a radial direction with a pen screen. The number of sub-sections per ring varied depending on the tree-ring width and the size of dissected wood tissue. Every sub-section defined on the pen screen was dissected with the UV-laser beam and collected in a single silver capsule standing in a collection holder. The capsules were sealed and put onto an autosampler of a high temperature pyrolysis furnace coupled online to an IRMS.

Climate data and data treatment

The study site has a typical equatorial climate with rather stable temperature but notably variable rainfall (dry/rainy season) (FIGURE 4.2A). Hence, climate calibration was performed using rainfall data. We screened monthly rainfall data for more than 40 meteorological stations and selected 17 stations for calibration purposes based on the distance to the study site, number of missing values and length of measurements (Supplementary TABLE S4.1). All the selected meteorological stations (KNMI Climate Explorer: http://climexp.knmi.nl/) show the characteristic monsoonal rainfall pattern for Central and Eastern Java (FIGURE 4.2A) and a regional mean of rainfall series (REG; Supplementary FIGURE S4.2) was calculated (Jones and Hulme, 1996). The period 1900–2002 (103 years) was used for the climate versus tree-ring correlation analyses. In order to investigate the climate-proxy relationships we calculated Pearson's correlation coefficients between tree-ring parameters (TRW, $\delta^{13}C_{TR}$, $\delta^{18}O_{TR}$) and climate data on a monthly basis. For time scale units we followed the vegetation period as opposed to a calendar perspective. Thus a year lasts from October (start of growing season) to September of the following calendar year.

To test the temporal stability of rainfall on the tree-ring parameters, running correlations between the monthly climate records and the tree-ring series, over a 31 year time window, were calculated.

4.3. Results

Site chronologies

The TRW series from 16 trees agree reasonably well (expressed population signal (EPS) of 0.94, GLK=63%, TABLE 4.1). The year-to-year variability changes over time with low values at the beginning of the chronology (18th century) and greater variability over the 19th and 20th century (FIGURE 4.3A/B). The carbon isotope series show a low year-to-year variability (FIGURE 4.3C/D). The mean inter-series correlation after correcting for changing atmospheric $\delta^{13}CO_2$ values is relatively low (r=0.27), as well as the EPS value (EPS=0.72). However, the inter-series correlation and EPS increase after correction for the pCO_2 effect ($\delta^{13}C_{cor2}$: r=0.36, EPS=0.80, TABLE 4.1). In contrast to $\delta^{13}C$, the oxygen isotopes ($\delta^{18}O$) from the same seven individuals are well correlated (FIGURE 4.3E) and show a high degree of synchronization (r=0.55, GLK=70%, EPS=0.90, TABLE 4.1). Furthermore, the $\delta^{18}O_{TR}$ variance is stable throughout the entire 20th century and the mean year-to-year variability of $\delta^{18}O_{TR}$ is higher than of the $\delta^{13}C_{TR}$ record.

Interestingly, the chronologies of all three parameters show more or less the same multi-decadal long-term changes beginning with a declining trend during 1910-1930 followed by increasing values (1930-1960) and an obvious rising trend towards the end of each record (1990-2007).

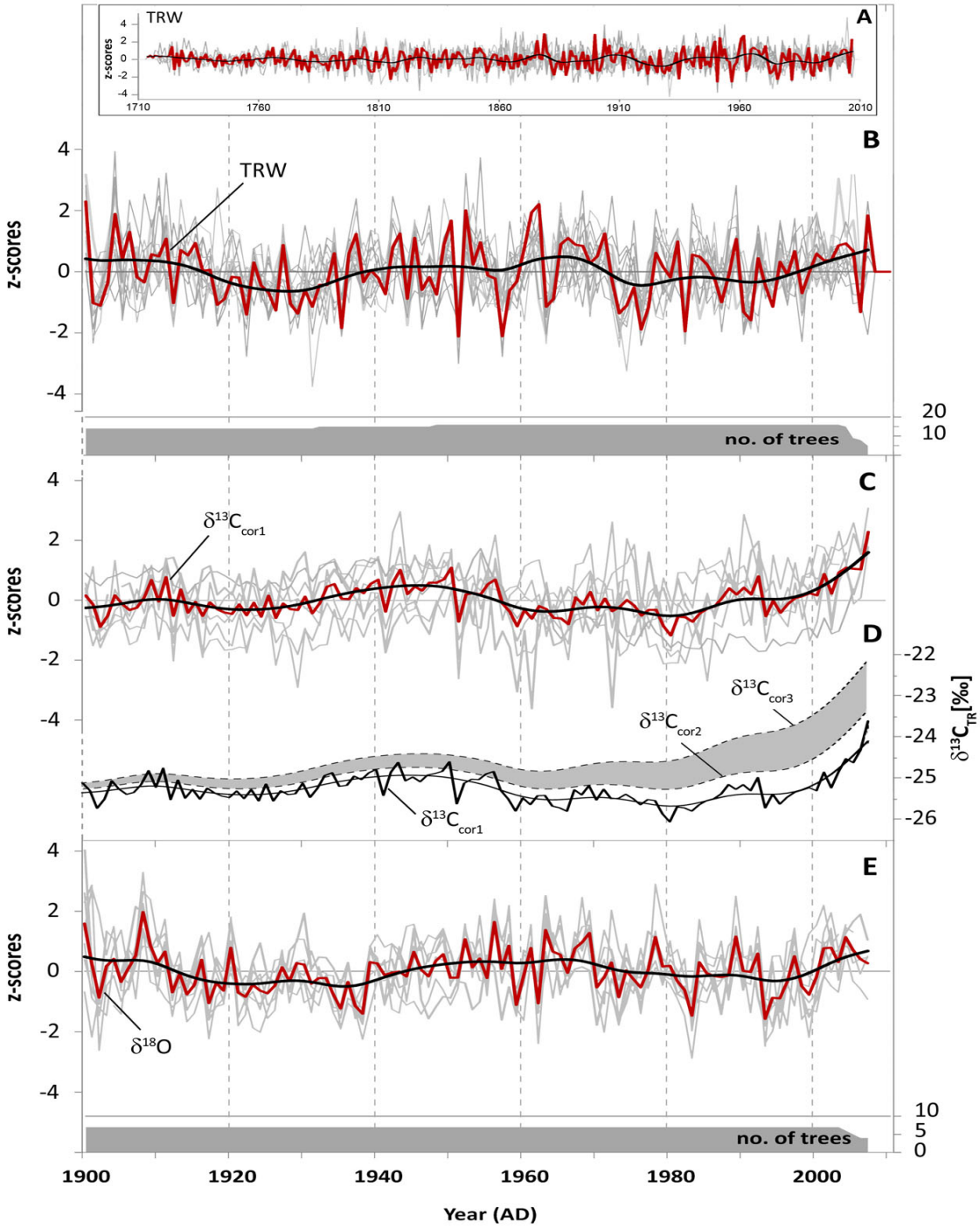

FIGURE 4.3 | Tree-ring series of ring width, $\delta^{13}C$ and $\delta^{18}O$ (red lines represent the mean chronology of each parameter). (A/B) Detrended tree-ring width series; (C/D) Corrected carbon isotope series: (C) Raw data corrected for changing $\delta^{13}C$ of atmospheric CO2 ($\delta^{13}C_{Cor1}$, thick red line), data after (Leuenberger, 2007), (D) Carbon isotopic data ($\delta^{13}C_{Cor1}$, thick black line) corrected for potential plant isotopic response to increasing atmospheric CO_2 concentration ($\delta^{13}C_{cor2}/_{cor3}$, grey shaded

area). Grey shaded area envelopes the minimum/maximum range of pCO2 correction according to literature ($\delta^{13}C_{cor2}$: Kürschner et al., 1996; $\delta^{13}C_{cor3}$: Feng and Epstein, 1995); (E) Oxygen isotope series. 20-year cubic-smoothing splines (thick black lines) fitted on the chronologies are depicted to show long-term fluctuations. Sample depths are shown as grey areas at the bottom of each graph (right axis).

TABLE 4.1 | Descriptive statistics for the tree-ring width (TRW), $\delta^{13}C_{TR}$ and $\delta^{18}O_{TR}$ chronologies. $\delta^{13}C_{TR}$ series include correction for changing atmospheric $\delta^{13}CO_2$ ($\delta^{13}C_{cor1}$:Leuenberger, 2007) and for changing plant response to increasing atmospheric CO_2 concentration ($\delta^{13}C_{cor2}$: Kürschner et al., 1996; $\delta^{13}C_{cor3}$: Feng and Epstein, 1995). CL: length of chronology; SD: standard deviation; GLK: Gleichläufigkeit (Cropper, 1979; Esper et al., 2001); Corr: series intercorrelation; EPS: expressed population signal (Wigley et al. 1984); AC1: autocorrelation first order; Inter-series corr: mean inter-series correlation.

	Time-span	CL	Nr. of trees	mean	SD	GLK [%]	corr	EPS	AC1	Inter-series corr
TRW	1714-2007	294	16	1.01	±0.24	63	0.48	0.94	0.31[a]	0.26 ($\delta^{13}C_{cor2}$)
$\delta^{13}C_{TR}$										
$\delta^{13}C_{cor1}$	1900-2007	108	7	-25.22	±0.34	61	0.27	0.72	0.62	
$\delta^{13}C_{cor2}$	1900-2007	108	7	-24.94	±0.41	61	0.36	0.80	0.72	0.25 ($\delta^{18}O_{TR}$)
$\delta^{13}C_{cor3}$	1900-2007	108	7	-24.46	±0.61	62	0.59	0.91	0.88	
$\delta^{18}O_{TR}$	1900-2007	108	7	21.17	±0.62	70	0.55	0.90	0.22	0.28 (TRW)

[a] Autocorrelation of Arstan standard chronology

Inter–annual tree response to rainfall

Simple linear correlation coefficients between the tree-ring series and monthly mean rainfall totals are shown from, the start of growing season, October, to September of the following year (FIGURE 4.4 and TABLE 4.2). The climate response between rainfall and tree-ring width (FIGURE 4.4A) shows significant positive correlations with the previous transitional month of May (pMay, r=0.26) and the previous dry season (pJun to pSep), as well as with the beginning of the rainy season, where the sum of September to November rainfall shows the highest correlation (r=0.27, p<0.01, TABLE 4.2). However, the strength and sign of the September to November correlation is not stable for the observed time period. The relationship falls below the significance level from 1920 to 25 and 1960 to 75, and changes sign during the latter (right plot in FIGURE 4.4A, TABLE 4.2).

The $\delta^{13}C_{TR}$ chronology (FIGURE 4.4B) shows a highly significant negative relation to the current rainy season, with December to May rainfall exhibiting the highest influence (Dec-May r=-0.41, p<0.001, TABLE 4.2). The negative signal is stable from 1935 to 1970 (right plot in FIGURE 4.4B, TABLE 4.2).

$\delta^{18}O_{TR}$ generally shows significant positive and negative correlations with rainfall of the prior dry season (pJun-pSep) and with the current rainy season (growing period),

respectively (FIGURE 4.4C, TABLE 4.2). In the dry season only the month of August, which is the driest month of the year, showed a highly significant correlation (r=0.40, p<0.001, TABLE 4.2) with the $\delta^{18}O_{TR}$ record. During the rainy season it is the rainfall during the peak of rainy season (November to February) that shows the highest significant correlation (r=-0.40, p<0.001, TABLE 4.2). This rainy season signal is stable for the entire time period after 1920, whereas the positive signal of the peak of the dry season (August) is significant only before 1940 and after 1975 (right plot in FIGURE 4.4C). Seasonality, as reflected by the difference in rainfall between August and January, as well as between the most significant months of the prior dry season (pJun-pSep) and the peak rainy season months (Nov-Feb) reveals highly significant correlations (r=0.4 and r=0.53, p<0.001) and are stable over the whole 20th century. Correlations between the tree-ring $\delta^{18}O$ and the annual $\delta^{18}O_{Pre}$ values from the GNIP station in Jakarta (1962-1998, FIGURE 4.2A) show significant positive values (mean r=0.45, p<0.05), where 2 out of 7 tree-ring $\delta^{18}O$ series indicate highly significant correlations (r=0.63, p<0.01).

TABLE 4.2 | Pearson correlation coefficients between tree-ring parameters (TRW, $\delta^{13}C_{TR}$, $\delta^{18}O_{TR}$) and rainfall data for different time periods (*p<0.05, **p<0.01, ***p<0.001).

Tree-ring parameter	Time period	Annual[a]	Dry season[b]	Wet season[c]	Period of strongest relationship
TRW	1900-2002	0.10	0.22	-0.02	0.27** (pSep-Nov)
	1900-1924	0.44	0.50*	0.14	0.58*** (pMay-pSep)
	1925-1949	-0.02	0.41*	-0.12	0.41* (dry season)
	1950-1974	-0.17	-0.35	-0.03	-0.35 (dry season)
	1975-2002	0.03	0.38*	-0.11	0.44* (pJul-Nov)
$\delta^{13}C_{TR}$	1900-2002	-0.29**	-0.03	-0.32***	-0.41*** (Dec-May)
	1900-1924	0.11	0.30	-0.06	0.40* (pMay-pJun)
	1925-1949	-0.34	0.30	-0.45*	-0.61** (Dec)
	1950-1974	0.02	0.23	-0.21	-0.49* (Jan)
	1975-2002	-0.41*	-0.08	-0.35	-0.44* (Dec-Jan)
$\delta^{18}O_{TR}$	1900-2002	-0.04	0.35***	-0.27**	-0.40*** (Nov-Feb); 0.40*** (pAug) 0.53*** (Diff. dry-wet season)
	1900-1924	0.70***	0.71***	0.28	0.76*** (pJul-pAug)
	1925-1949	-0.51**	0.13	-0.54**	-0.54** (wet season)
	1950-1974	-0.37	-0.12	-0.43*	-0.73*** (Nov-Feb)
	1975-2002	-0.33	0.47*	-0.50**	-0.52** (Nov-Feb)

[a] Annual= July to June next year.

[b] Dry season= pJune to pSeptember.

[c] Wet season= October to May.

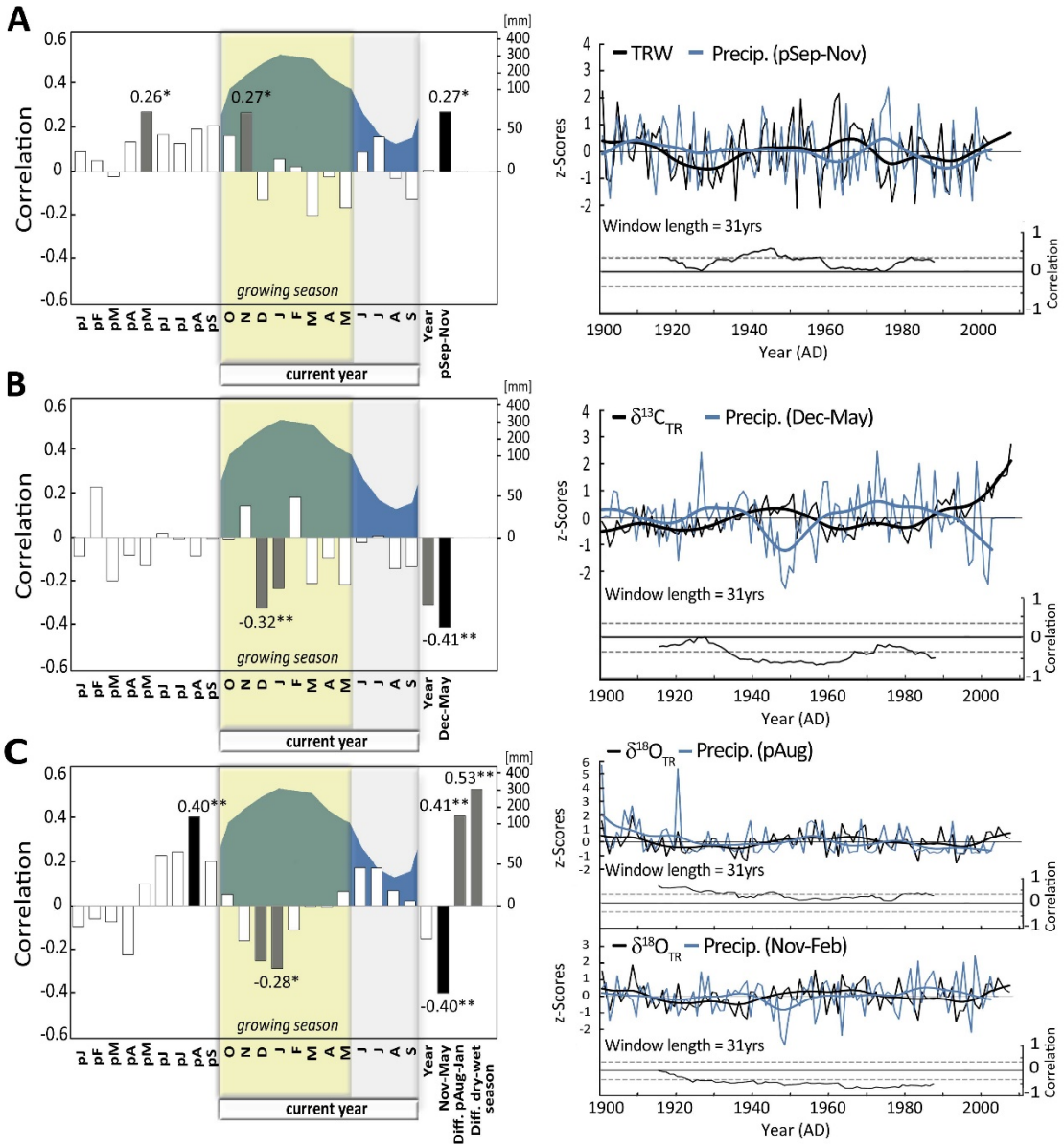

FIGURE 4.4 | Left: Correlations of (A) TRW, (B) $\delta^{13}C_{TR}$ and (C) $\delta^{18}O_{TR}$ chronologies with monthly and seasonal rainfall (1900-2002). The climate response plots are separated into three parts by vertical lines. The left part covers months of the previous year (previous year January to September) followed by the current year (October to following year September). The right part depicts seasonal means. Long-term seasonal average of rainfall is shown as blue shaded area in the background. Most significant correlations are indicated with grey bars, where highest correlations are highlighted in black (**p<0.001,* p<0.01). Right: Time series of tree-ring parameters and corresponding rainfall of periods with highest influence. Moving correlations for overlapping 31-year periods (95% confidence levels are indicated) and 20-year cubic smoothing spline (thick blue and black lines) are shown.

Intra-annual cyclicity in high-resolution $\delta^{18}O_{TR}$ records

The opposite correlations found for the tree-ring $\delta^{18}O$ and monsoonal rainfall amount of dry and rainy season, respectively, are conspicuous. Highly resolved intra-annual $\delta^{18}O_{TR}$

data may help to understand the observed relations. FIGURE 4.5B shows growing season $\delta^{18}O_{TR}$ profiles at various numbers of sub-sections per year from one teak tree. Consecutive $\delta^{18}O_{TR}$ values are plotted relative to their positions within the rings formed in 1983, ’84 and ‘86. The $\delta^{18}O_{TR}$ profiles reveal a clear annual cycle. Annual wood formation starts with a parenchyma band having $\delta^{18}O_{TR}$ values that are similar to the $\delta^{18}O_{TR}$ values at the end of the previous tree ring. Wood being formed shortly after the parenchyma band is characterized by rapidly rising $\delta^{18}O_{TR}$ values up to the ring maximum early in the growing season. After the maximum is reached, $\delta^{18}O_{TR}$ values decline to a seasonal minimum typically in the 2nd third of each tree ring before $\delta^{18}O_{TR}$ slightly rises again in the last third of the growing season. The pattern described here was found rather consistent in spite of the different numbers of intra-annual data points, i.e. sub-sections per year. However, this shows that the number of intra-ring data points can affect the variance of intra-annual $\delta^{18}O_{TR}$ and complicates the climatic interpretation of such data.

4.4. Discussion

Tree-ring parameters and their rainfall signals

Climate correlation tests showed that all three tree-ring parameters are significantly influenced by seasonal rainfall amounts. The correlations of stable isotope records with rainfall were mostly significant and constant over time. The 300-year long TRW chronology produced similar correlation patterns with rainfall as found in previous Javanese teak studies (Berlage, 1931; D'Arrigo et al., 1994; DeBoer, 1951; Jacoby and D'Arrigo, 1990; Murphy et al., 1989). However, the TRW chronology did not reveal stable correlations with regional rainfall data sets. Previous authors concluded that teak growth is positively correlated with rainfall in the prior dry season (around May to September), but mainly controlled by the transitional months of the corresponding monsoons, May/June and October/November. Teak studies from Thailand (Buckley et al., 2007; Pumijumnong et al., 1995) likewise note that rainfall at the beginning of the wet monsoon is the most significant climate factor controlling tree-ring growth, whereas Indian studies reveal significant positive relationships with rainfall over the whole Indian Summer Monsoon season (Borgaonkar et al., 2010; Shah et al., 2007) and annual total rainfall (Ram et al., 2008).

The negative relationship found between $\delta^{13}C_{TR}$ and the main rainy season (Dec-May) is well in line with the theories of carbon isotope discrimination during photosynthesis and seasonal changes in post-photosynthetic signal transfer from the leaf level into the developing wood tissue (e.g. McCarroll and Loader, 2004). Contrary to the TRW data,

$\delta^{13}C_{TR}$ reveals no significant correlation with the very early growing season. Why? At the very beginning of the growing season, i.e. rainy season, early wood formation relies on assimilates from previous years, accumulated as starch reserves. Previous year's starch is not necessarily isotopically labelled by the climate signal of its formation period. It rather exhibits a general enrichment of ^{13}C as compared to less polymerized assimilates. Consequently, the incorporation of starch derived ^{13}C masks a potential early growing season climate signal of tree-ring $\delta^{13}C$ (e.g. Helle and Schleser, 2004a) and could not be found in this study. With the progressing growing season, developing leaves subsequently provide new assimilates for wood growth, which carries the signal of the current growing season in their $\delta^{13}C_{TR}$. As the temperatures at our study site are quite stable over the entire year it is likely that stomatal conductance driven by varying stomatal aperture in response to moisture supply is controlling the c_i/c_a ratio and finally resulting in the observed significant negative correlation between tree-ring $\delta^{13}C$ and the rainfall of the Dec-May period (main rainy season). However, too much rain during this period of the year may weaken the relationship as revealed by decreased correlations during wet phases around 1920-30 and 1970-80 (FIGURE 4.4B, FIGURE 4.2B).

The $\delta^{18}O_{TR}$ record shows stable inverse relation with the November to February interval of the rainy season, i.e. the wettest period of the year, and a notable significant positive correlation with the rainfall of prior driest month August. Interestingly, the correlation of tree-ring $\delta^{18}O$ with rainfall is significant during those months of the year that are generally characterized by both the highest and the lowest $\delta^{18}O$ values in rainfall (FIGURE 4.2A). This is because the source water signal of the soil is dominated by the seasonally changing $\delta^{18}O$ signature in rainfall that is highest during the peak of the dry season (August) and lowest during the peak of the rainy season (January). Any influence of groundwater due to uptake from deeper soil reservoirs during the vegetation period seems unlikely since the volcanic soil substrate at the site is well-drained and teak has a shallow root system. Thus, tree-ring $\delta^{18}O$ in teak provides rainy and dry season signal of $\delta^{18}O$ in rainfall. This is emphasized by the significant positive correlation found between the tree-ring $\delta^{18}O$ and the annual $\delta^{18}O_{Pre}$ values from the GNIP station in Jakarta. The finding suggests that the $\delta^{18}O_{TR}$ signal may be coherent over larger areas. During the first 25 years of the 20th century our $\delta^{18}O_{TR}$ has the highest (positive) correlation with dry season rainfall in contrast to the high negative correlation with the main rainy season (Nov-Feb) during the remaining part of the 20th century (FIGURE 4.4C, TABLE 4.2). This may result from the wetter conditions particularly prevailing during the dry seasons of the first 25 years of the 20th century (FIGURE 4.2B), which strengthens the dry season signal in the tree-ring $\delta^{18}O$. Such shifts in intra-annual tree-ring proxy response to changing rainfall conditions cannot be detected or confirmed without independent proxy or instrumental data sets. However,

intra-annual stable isotope data from tree rings can help to disentangle contrasting isotopic effects of dry and rainy season rainfall amount.

Rainfall signals in tree-ring $\delta^{18}O$ as a function of the hydrological seasonal cycle

High-resolution intra-ring $\delta^{18}O$-records (FIGURE 4.5B) give more detailed insight into the seasonal hydrological cycle and its effects on tree-ring $\delta^{18}O$. Our observations largely corroborate those outlined by Evans and Schrag (2004) for evergreen tropical species without distinct tree rings. Lower intra-annual $\delta^{18}O_{TR}$ values correspond to periods of higher rainfall with lower evapotranspiration and vice versa. However, how can a dry season influence the tree-ring $\delta^{18}O$ of a deciduous species that is leafless and does not grow at all during this period of the year? To explain this we adapted in FIGURE 4.5A a conceptual oxygen isotope model to the hydrological conditions at our study site for comparison. During the dry season no leaf transpiration and photosynthesis occurs, and no wood is formed. Consequently, no direct impact of the prevailing hydrological conditions can be expected. However, the rain water that is potentially seeping into the soil is enriched in ^{18}O due to reduced condensation processes (Jun–Sep, long-term mean 1900-2002: 200 mm, range: 0-628 mm, $\delta^{18}O_{Pre}$= -3.8‰) and possibly high soil water evaporation rates promoted by direct insolation. This leads to ^{18}O-enrichment in soil water that culminates shortly before the beginning of the growing period.

With the beginning of the rainy season increasing rainfall amounts with subsequently lower $\delta^{18}O$ values begin to dilute and lower the initially high $\delta^{18}O$ signal of the soil water (FIGURE 4.5A (2)). At the same time, trees` cambial activity and leaf photosynthesis start (October/November). Altogether, at the beginning of the growing season the uptake of ^{18}O-enriched soil water, in conjunction with enhanced ^{18}O-enrichment of leaf water (driven by transpiration), result in high $\delta^{18}O_{TR}$ values for the first third of each tree ring (FIGURE 4.5B (Max)). However, for a short time at the very beginning of the growing season ^{18}O-enrichment of leaf water may not be a contributing factor as long as young leaves are not fully developed and their stomata are not fully operational. Hence, the initial parenchyma band of teak tree rings is probably not affected by dry season rainfall conditions but from a physiological connection to the previous year growth. If the parenchyma is formed prior to bud burst then its formation relies on stored assimilates carrying the $\delta^{18}O_{TR}$ signature of the previous growing season. Towards the maximum of rainy season (January-March), enhanced condensation processes lead to a progressive depletion in heavy ^{18}O isotopes of rain water, which results in an ^{18}O-depleted soil water signal reaching its lowest $\delta^{18}O$ signature during the peak of the rainy season (Jan-Feb) (FIGURE 4.5A (3)). Soil water evaporation and its related ^{18}O-enrichment are strongly reduced as the soil is shaded from direct insolation by the canopy of the trees. Likewise, the impact of leaf water ^{18}O-enrichment is decreased to a minimum at this time of lowest vapour pressure deficit and

highest relative air humidity conditions. This combination of conditions coincides with the low $\delta^{18}O_{TR}$ values found in the middle section of each tree ring (FIGURE 4.5B (Min)). At the end of the rainy season, i.e. growing period, intra-annual tree-ring $\delta^{18}O$ tends to increase again following mainly the isotope trend of the rain water with some modification by ^{18}O-enrichment in leaf water due to evapotranspiration rates that vary with vapour pressure deficit.

The high resolution intra-annual tree-ring $\delta^{18}O$ data indicate that high $\delta^{18}O_{Pre}$ values in dry season are well reflected in the high $\delta^{18}O_{TR}$ values found in the first third of each tree ring (FIGURE 4.5A (2), FIGURE 4.5B (Max)), whereas minimum $\delta^{18}O_{Pre}$ values of the major rainy season are reflected by low $\delta^{18}O_{TR}$ values for the middle part of a tree ring (FIGURE 4.5A (3), FIGURE 4.5B (Min)).

Rainfall amount during the rainy season normally is several times higher than during the dry season and the rainfall signal of rainy season is largely imprinted in the $\delta^{18}O_{TR}$ of two thirds of a tree ring. Thus, the signal of the rainy season should be stronger than the signal of the dry season. However, respective correlations are opposite in sign but of similar magnitude (FIGURE 4.4C). Hence, rainfall conditions persisting during the dry season seem to imply stronger isotopic effects in the tree rings. To verify this hypothesis we analysed the influence of seasonal extremes in rainfall on the annual $\delta^{18}O_{TR}$ values.

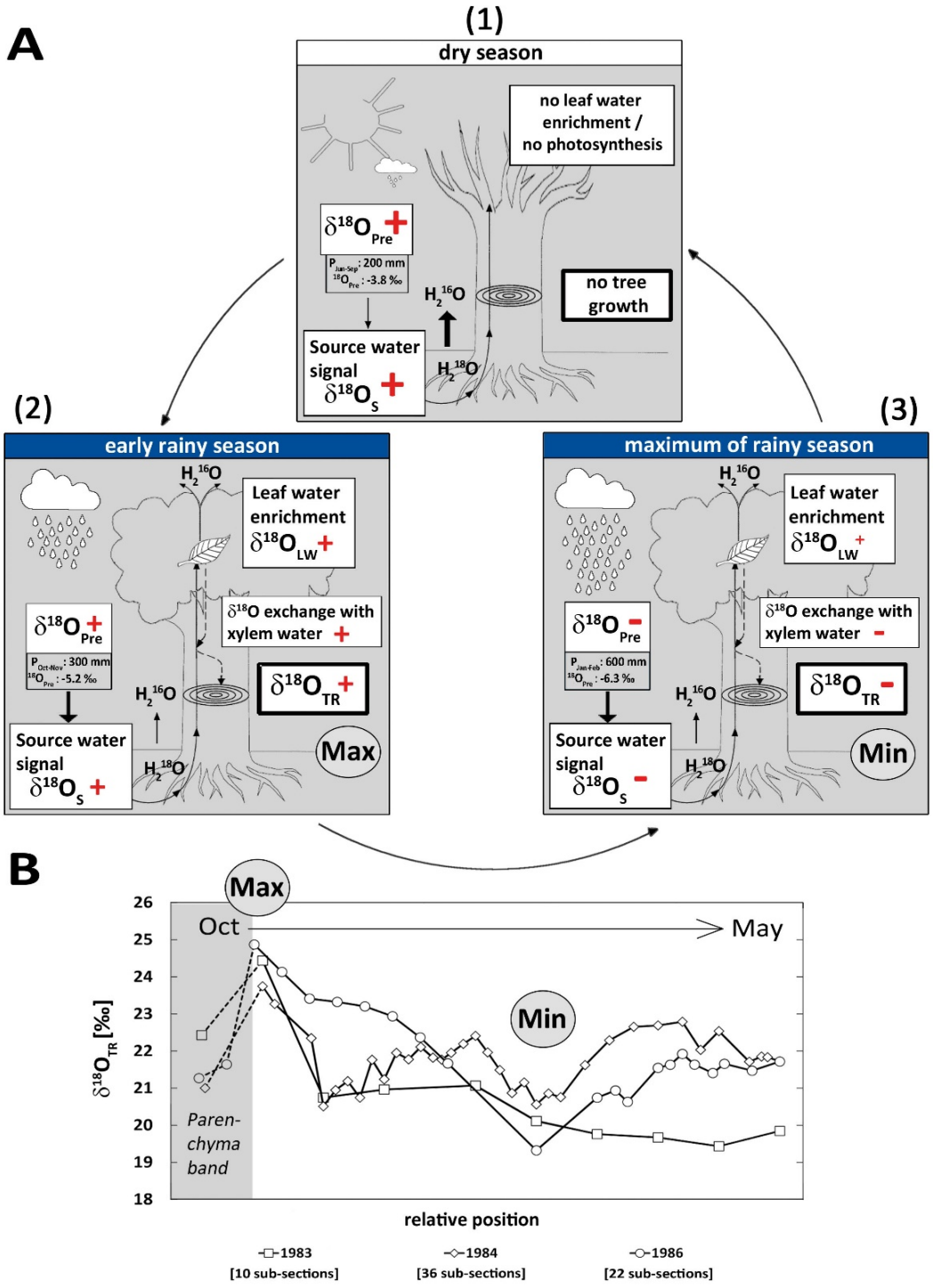

FIGURE 4.5 | (A) A conceptional model of oxygen isotope fractionation and the seasonal cycle of rainfall in the tropics. The values given for the meteoric water source ($\delta^{18}O_{Pre}$) and the amount of rainfall are taken from the isotopic composition of GNIP-station Jakarta and regional climate data sets. "+" and "-" indicate the relative strength and direction of isotopic shifts for relevant processes. (B) Intra-annual $\delta^{18}O$ variations from a teak tree as a function of time of the growing season (Oct-May). The number of sub-sections per ring varied depending on the tree-ring width and the size of dissected wood tissue.

Seasonal extremes in rainfall and their isotopic footprint on $\delta^{18}O_{TR}$ data

A dry season with above average rainfall has a particularly strong influence on tree-ring $\delta^{18}O$ when the following rainy season is rather dry (R^2=0.64, FIGURE 4.6A). Even when followed by a rainy season with rainfall above average the signal of a rather moist dry season is not completely diminished in the annual tree-ring $\delta^{18}O$ (R^2=0.07, FIGURE 4.6B). On the other hand, dry season rainfall variability below average is not reflected in tree-ring $\delta^{18}O$, no matter if the following rainy season is likewise "dry" (FIGURE 4.6C) or "wet" (FIGURE 4.6D). Consequently, the signal of the rainy season is well expressed when the preceding dry season was rather dry (FIGURE 4.6E). Interestingly, a dry season with above average rainfall apparently strengthens the signal of a rainy season with below average rainfall in tree-ring $\delta^{18}O$ (R^2=0.63, FIGURE 4.6F). In general, a dry season with enhanced ^{18}O-enriched rainfall sets a high initial $\delta^{18}O$-source level. Hence, a following rainy period with reduced rain, and a less than normal ^{18}O-depleted signature, is only partly diluting the ^{18}O-enrichment signal of dry season`s rain. The extent to which a "wet" dry season signal is overwritten depends on the rainfall amount during the rainy season. This leads us to the conclusion that the annual $\delta^{18}O_{TR}$ record cannot give unambiguous information about rainfall conditions during individual seasons (dry and rainy season). However, the seasonality, the difference between dry and rainy season rainfall amount, does show a high correlation (r=0.53; FIGURE 4.4C). The rainfall signal from dry or rainy season is damped in the tree-ring $\delta^{18}O$ values due to seasonally alternating isotope signatures in $\delta^{18}O_{Pre}$. Only high-resolution $\delta^{18}O_{TR}$ records seem to provide detailed information about both, the dry and rainy season rainfall variability.

Previous $\delta^{18}O$ teak studies from Indonesia on two cores showed a common climate influence on inter-annual scale for time period 1950-1980 (Poussart et al., 2004). Poussart et al.´s intra-annual $\delta^{18}O$ analyses for the same time span showed a similar pattern as we found with a maximum early in the growing season, followed by a gradual decrease and often a sharp increase towards the end of the growing season. However, in their study a correlation with local or regional rainfall pattern was not tested in detail. $\delta^{18}O$ studies on teak from India (Managave et al., 2010a; Managave et al., 2011) found both negative and positive correlations with the amount of rainy season rainfall at inter- and intra-annual scale. Studies in tropical regions of South-America have likewise reported negative correlation with the rainfall amount during rainy season (Ballantyne et al., 2010; Brienen et al., 2012), as have isotope studies in Southeast Asia (Sano et al., 2012; Xu et al., 2011; Zhu et al., 2012). However, none reported correlations with dry and rainy season rainfall as revealed here for Indonesian teak.

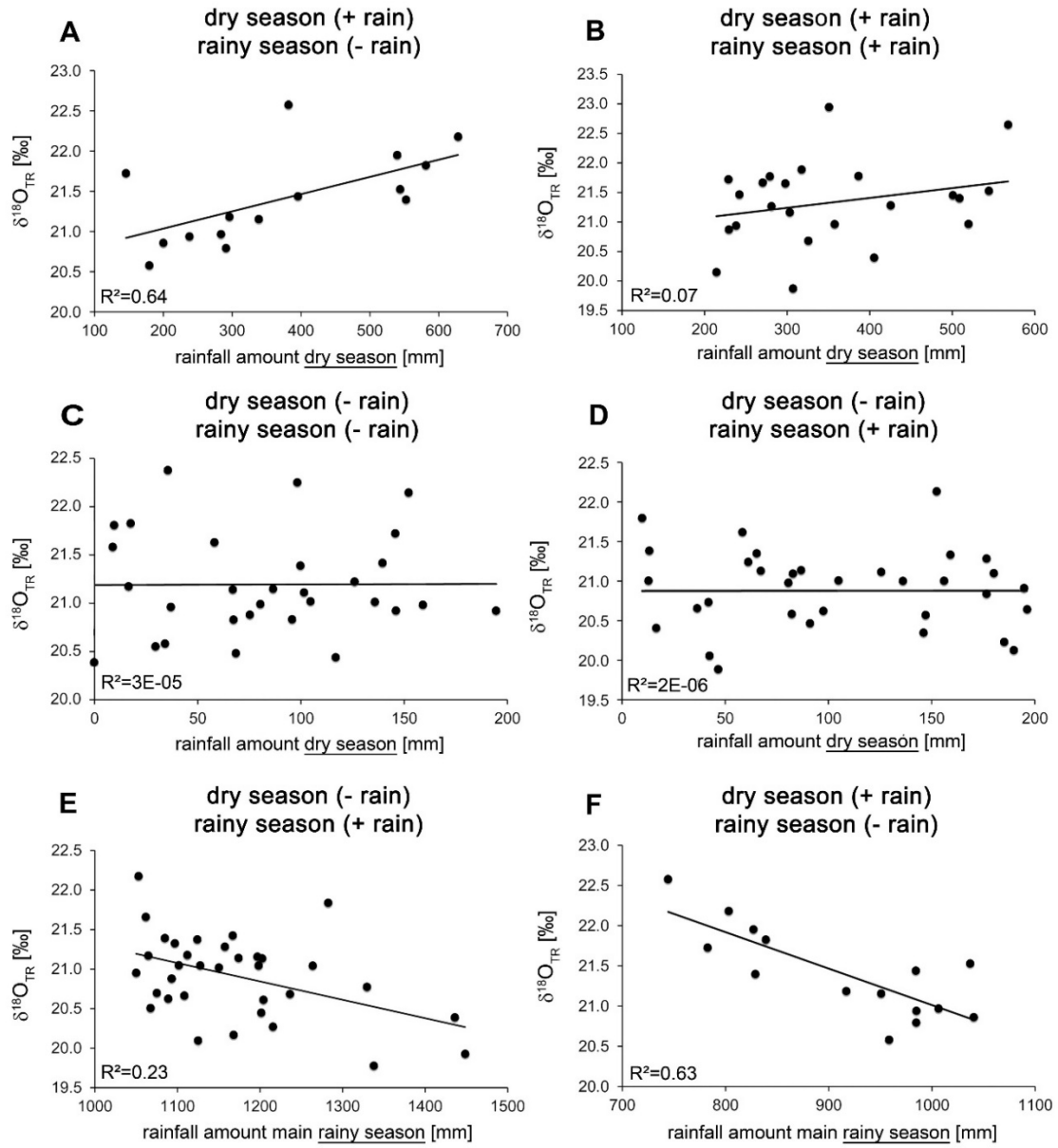

FIGURE 4.6 | Comparison of the influence of different rainfall conditions during dry and rainy season on the tree-ring $\delta^{18}O$ values. ''+'' and ''-'' represent below or above average rainfall amount for corresponding season. A dry season with above average rainfall has a strong influence on $\delta^{18}O_{TR}$ when the following rainy season is rather dry (A), but is weakly reflected when the following rainy season has above average rainfall (B). A dry season with below average rainfall is not reflected in $\delta^{18}O_{TR}$, no matter if the following rainy season is likewise drier (C) or wetter (D) than average. The signal of the rainy season is well expressed when the preceding dry season was rather dry (E). Interestingly, a dry season with above average rainfall apparently strengthens the signal of a rainy with below average rainfall $\delta^{18}O_{TR}$ (F). See text for further details.

4.5. Conclusions and perspectives

We tested the dendroclimatological potential of multiple, centennial, tree-ring records (ring width, $\delta^{13}C_{TR}$ and $\delta^{18}O_{TR}$) of *Tectona grandis* in Central Java. All three tree-ring records revealed a seasonal rainfall signal, but for different time intervals and with different stability in time. As shown in previous studies tree-ring widths correlate positively with transitional months of the monsoon (e.g. D'Arrigo et al., 1994). Newly developed stable isotope records show a higher degree of common forcing and display a significant negative correlation with rainy season precipitation. In addition, our $\delta^{18}O_{TR}$ revealed a positive correlation with dry season rainfall. These relationships of opposite signs reflect a distinct seasonal contrast of the $\delta^{18}O_{Pre}$ signature of Central Java rainfall variability. Thus the formation of tree-ring $\delta^{18}O$ is related to dry and rainy season pattern, whereas the main rainy season signal is dominant and stable in time. However, the dry season has a weakening effect on the main rainy season $\delta^{18}O_{Pre}$ signal depending on the respective seasonal rainfall conditions. High-resolution $\delta^{18}O_{TR}$ records permit to disentangle the seasonal cycle of $\delta^{18}O$ in rainfall.

We have shown that stable isotope records from Indonesian teak offer additional information to climate investigations. However, to distinguish seasonal rainfall variability across the tropical Indo-Pacific region further studies need to focus on high-resolution stable isotope studies. Long-term reconstruction of annual rainfall variability (rainy and dry season rainfall), including unusual rainfall anomalies such as during ENSO events, may be possible with tree-ring $\delta^{18}O$ and could improve our understanding of the Asian monsoon system. Such studies will be promoted by novel methods like UV-Laser micro-dissection sampling that enable sample preparation with the highest precision able to accommodate tree-ring samples with large variations in ring-width and irregular shape of tree-ring boundaries.

Acknowledgements

This study was supported by the CADY (BMBF, 03G0813H), the HIMPAC (DFG, HE 3089/4-1) and the INDOPAL (HE3089/1-1) projects. We thank Tomy Listyanto and Navis Rofii for their assistance in the field work. Heiko Baschek, Carmen Bürger and David Göhring are thanked for support in the laboratory and Isabel Dorado and Katja Fregien for fruitful discussions. Furthermore, we are also grateful to two anonymous reviewers for their constructive and helpful comments.

Supplementary data

FIGURE S4.1 | Map of Central/Eastern Java indicating the study site (red triangle) and climate stations with rainfall data (black dots).

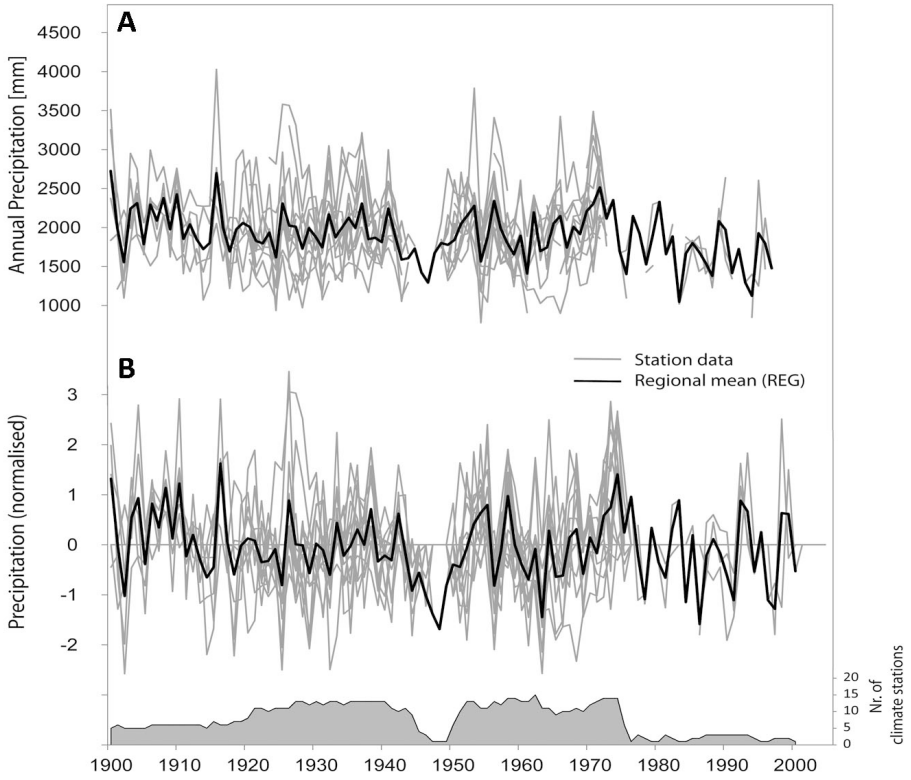

FIGURE S4.2 | Annual (July to June) rainfall data from climate stations (Table S1). (A) rainfall means; (B) data normalized over individual series lengths, mean of this series (REG) and number of series contributing to the mean.

TABLE S4.1 | Climate stations with rainfall data used for calculating of regional rainfall mean (REG).

Climate station	Nr.	Coordinates	Altitude (m)	Time period	Distance to study site (km)
Purwantoro	1	-7.85N, 111.27E	500	1905-1975	10
Sungkur	2	-7.85N, 111.38E	95	1920-1975	20
Batuwarno	3	-7.98N, 110.01E	380	1944-1996	20
Wuryantoro	4	-7.90N, 110.87E	180	1920-1975	35
Giritontro	5	-8.08N, 110.86E	280	1944-2002	40
Pracimantoro	6	-8.05N, 110.81E	450	1944-2002	45
Mojo	7	-7.43N, 110.05E	85	1926-1975	50
Bendo	8	-8.15N, 111.68E	120	1900-1975	60
Delanggu	9	-7.62N, 110.70E	130	1900-1975	60
Tumpakmergo	10	-8.23N, 111.82E	88	1926-1975	70
Ngranti	11	-8.15N, 110.63E	300	1920-1971	70
Tanjungtirto	12	-7.80N, 110.47E	115	1900-1975	80
Randublatung	13	-7.20N, 111.38E	55	1915-1975	80
Nglangon	14	-7.15N, 111.15E	80	1900-1975	85
Karangasem	15	-7.00N, 111.10E	158	1900-1975	100
Kerek	16	-6.90N, 111.88E	110	1900-1975	130
Semarang	17	-7.00N, 110.40E	3	1957-2003	130

Preface to Chapter 5

The study of Chapter 4 demonstrates that stable isotope records of Indonesian teak trees reveal significant correlation with the rainfall peaks of dry and rainy season. Indonesian rainfall is strongly linked to large-scale Indo-Pacific Ocean variability, such as ENSO variations (Aldrian et al., 2007; Aldrian and Susanto, 2003; Allan, 2000; Haylock and McBride, 2001; Jourdain et al., 2013). The El Niño–Southern Oscillation cycle, recurring every 2 to 7 years, is a fluctuation between unusually warm (El Niño) and cold (La Niña) conditions in the tropical Pacific and the most prominent year-to-year climate variation on Earth. ENSO originates in the tropical Pacific through interactions between the ocean and it is unique among climate phenomena in its strength, predictability and global impact (e.g. McPhaden et al., 2006). Over the Indonesian Archipelago El Niño events can result in extreme droughts and La Niña events in extensive floods causing much hardship for the populations of that regions.

In its Fifth Assessment Report, Working Group 1 of the Intergovernmental Panel on Climate Change (IPCC, 2013) concluded that ENSO will remain the dominant mode of inter-annual variability in the tropical Pacific. It is furthermore stated that, due to increased moisture availability, ENSO-related precipitation variability will likely intensify on regional scales. However, it is still uncertain whether the decadal-scale modulation of ENSO properties (amplitude and spatial pattern) of recent decades is due to anthropogenic effects or natural variability since the confidence of projected changes in ENSO for the 21st century remains low. Good observations of the coupled air-sea feedbacks controlling the ENSO behaviour are available only since the late 1970s, making observed historical ENSO variations uncertain. Therefore, more reliable high-resolution proxy data are needed which can provide more detailed information on past ENSO pattern.

In the following chapter, the tree-ring $\delta^{18}O$ record, introduced in Chapter 4, is tested as a potential ENSO proxy. Thereby, we distinguished between different ENSO flavors taking into account that since the late 1990s, the maximum SST warming during El Niño events has been frequently observed in the central equatorial Pacific (Warm Pool El Niño) and not as for 'standard' El Niños over the eastern equatorial Pacific (Cold Tongue El Niño) (IPCC, 2013).

Chapter 5

ENSO flavors in a tree-ring $\delta^{18}O$ record of *Tectona grandis* from Indonesia

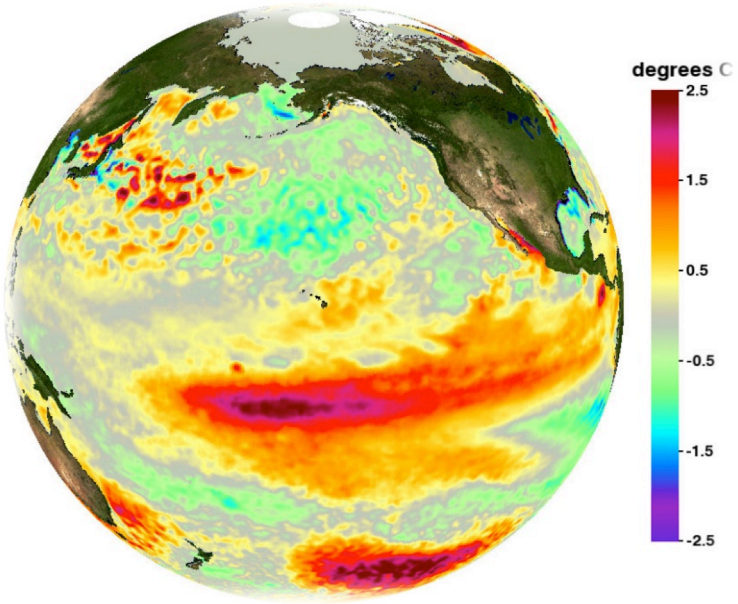

SST anomaly during the peak of the 2009-10 El Niño, the strongest Warm Pool El Niño observed to date.
(Image produced by Physical Oceanography Distributed Active Archive Centre (PO.DAAC) of NASA JPL.)

This chapter was published in:

Clim. Past Discuss., 2014, Vol. 10, p. 3965-3987

Authored by Karina Schollaen[a], Christina Karamperidou[b], Paul J. Krusic[c], Edward R. Cook[d] and Gerhard Helle[a]

[a]*GFZ - German Research Centre for Geosciences, Section 5.2 Climate Dynamics and Landscape Evolution, Telegrafenberg, 14473 Potsdam, Germany*
[b]*Department of Meteorology, University of Hawai'i at Manoa, Honolulu, Hawai'i, USA*
[c]*Bolin Centre for Climate Research, Department of Physical Geography and Quaternary Geology, Stockholm University, Stockholm, Swedend; Navarino Environmental Obs. Messinia, Greece*
[d]*Tree Ring Laboratory, Lamont-Doherty Earth Observatory, Columbia University, USA*

Abstract

Indonesia's climate is dominated by the equatorial monsoon system, and has been linked to El Niño-Southern Oscillation (ENSO) events that often result in extensive droughts and floods over the Indonesian archipelago. In this study we investigate ENSO-related signals in a tree-ring $\delta^{18}O$ record (1900-2007) of Javanese teak. Our results reveal a clear influence of Warm Pool (central Pacific) El Niño events on Javanese tree-ring $\delta^{18}O$, and no clear signal of Cold Tongue (eastern Pacific) El Niño events. These results are consistent with the distinct impacts of the two ENSO flavors on Javanese precipitation, and illustrate the importance of considering ENSO flavors when interpreting palaeoclimate proxy records in the tropics.

Keywords: *El Niño, ENSO flavors, precipitation teleconnections, oxygen isotopes, tree rings, dendroclimatology*

Highlights

- The Javanese $\delta^{18}O_{TR}$ record correlates significantly with WP El Niños and La Niñas.
- The tree-ring proxy illustrate the importance of considering ENSO flavors.
- Indonesia is a key location for finding land-based precipitation proxies.

5.1. Introduction

The tropical warm pool waters surrounding the Indonesian maritime continent (IMC) are the region of the highest convective activity in the world (D'Arrigo et al., 2006). The IMC is known for its exceptionally high rainfall throughout the year and is a center of heat flux essential to the global climate system (Yulihastin et al., 2010). Indonesia's regional climate is governed by the Australian-Indonesian Monsoon (Wheeler and McBride, 2005) and the associated seasonal movement of the Inter Tropical Convergence Zone (ITCZ). Variations of the equatorial monsoon system significantly impact the livelihood of over 230 million people living in the world's fourth most populated country.

The El Niño-Southern Oscillation (ENSO) phenomenon contributes to the rainfall pattern of the IMC and has been thought to interact with the monsoons (e.g. Hendon, 2003; Lau and Nath, 2000). Recent studies have drawn attention to the existence of more than one variant or '*flavors*' of El Niño (Ashok et al., 2007; Kug et al., 2009; Larkin and Harrison, 2005; Ren and Jin, 2011; Takahashi et al., 2011). The canonical ENSO (Sarachik and Cane, 2010), also referred to as eastern Pacific (EP) El Niño (Kao and Yu, 2009) or Cold Tongue El Niño (Kug et al., 2009; Ren and Jin, 2011), exhibits SST anomalies localized in the eastern equatorial Pacific. The El Niño variant with maximum SST anomalies located in the central equatorial Pacific is referred to as the central Pacific (CP) El Niño (Kao and Yu, 2009), Warm Pool (WP) El Niño (Kug et al., 2009; Ren and Jin, 2011), date line El Niño (Larkin and Harrison, 2005) or El Niño Modoki (Ashok et al., 2007; Takahashi et al., 2011). In this study we use the terms Cold Tongue (CT), and Warm Pool (WP) El Niño (Ren and Jin, 2011) to describe these two ENSO flavors.

Identifying the mechanisms responsible for the CT and WP ENSO flavors is an active field of research. At present, there is no consensus on whether the increased frequency of WP ENSO events in recent decades (Ashok et al., 2007; Kao and Yu, 2009; Kug et al., 2009; Lee and McPhaden, 2010) are a result of anthropogenic greenhouse gas (GHG) forcing (Yeh et al., 2009), or natural variability (McPhaden et al., 2011; Newman et al., 2011). In addition, the simulation of ENSO flavors in Global Climate Models (GCMs) is still subject to limitations in our understanding of the phenomenon. Consequently, there is much uncertainty in whether ENSO activity will be enhanced or damped in the future, or if the relative frequency of ENSO flavors will change (Collins et al., 2010). Long records of ENSO activity are essential for identifying trends and multidecadal changes in the patterns of sea surface temperature associated with ENSO, making palaeoclimate reconstructions particularly attractive for shedding light onto the past and future of ENSO flavors.

Recent research on ENSO-proxy teleconnections recommends, that when interpreting proxy data, details in the differences between ENSO flavors, with regards to SST's, precipitation and salinity, should be taken into account *(Karamperidou et al., submitted)*. Certain regions like Java lie in key locations where interannual precipitation variability is

significantly correlated to one ENSO flavor but not the other (see FIGURE 5.1). Thus, long-term rainfall proxies from Java can be useful for distinguishing between ENSO flavors, and for studying their relation to monsoon variability.

Over the last decade there have been several attempts to reconstruct continuous time series of ENSO variability using different proxy archives such as corals (e.g. Abram et al., 2008; Charles et al., 2003; Cobb et al., 2013; Evans et al., 2002; Linsley et al., 2004; Pfeiffer et al., 2009; Quinn et al., 2006; Wilson et al., 2006), tree-ring widths (e.g. D'Arrigo et al., 2005; Fowler et al., 2012; Stahle et al., 1998) or tree-ring stable isotopes (Sano et al., 2012). Furthermore, several multi-proxy reconstructions of ENSO variability are available (e.g. Braganza et al., 2009; D'Arrigo et al., 2006; Emile-Geay et al., 2013; Mann et al., 2000; Wilson et al., 2010). However, many of these reconstructions are based on extratropical proxy records, particularly from tree-ring widths, and thus do not represent ENSO activity directly.

Tree-ring stable isotopes often provide additional climate information where the more commonly used tree-ring proxies (e.g., ring width and maximum latewood density) do not, or where the teleconnection signal is weak. In tropical regions, oxygen isotope data from tree rings ($\delta^{18}O_{TR}$) are often more sensitive to precipitation than ring width (e.g. Brienen et al., 2012; Schollaen et al., 2013). $\delta^{18}O_{TR}$ data are primarily controlled by the isotopic composition of precipitation, i.e. the source water, and relative humidity (e.g. Barbour, 2007; McCarroll and Loader, 2004). The isotopic composition of precipitation ($\delta^{18}O_{Pre}$) depends on a number of factors, the so-called 'kinetic isotope effects' (Araguás-Araguás et al., 2000). One of these effects, 'the amount effect', is the inverse correlation between rainfall amount and $\delta^{18}O_{Pre}$ values, and a crucial driver in determining $\delta^{18}O_{Pre}$ values in the tropics (e.g. Brienen et al., 2012; Zhu et al., 2012). Thus $\delta^{18}O_{TR}$ records offer a promising approach to examine monsoon activity, and large-scale climate variations such as ENSO.

In previous studies we investigated relationships between seasonal rainfall variability and tree-ring stable isotope records from Javanese teak trees on inter- to intra-annual time scales (Schollaen et al., 2014; Schollaen et al., 2013). In this study we explore the signal strength of ENSO flavors in our annually resolved $\delta^{18}O_{TR}$ record from Java, the only well replicated, centennial $\delta^{18}O$ record from Javanese teak in existence. We place particular emphasis on the time stability of the teleconnected $\delta^{18}O$/ENSO relationship. To the best of our knowledge this is the first time the relationship between tree-ring proxies and the two ENSO flavors is tested. We find a unique WP El Niño signal in the $\delta^{18}O_{TR}$ record from Java, supporting the notion that proxies from carefully selected regions are valuable for answering questions of past and present ENSO variability, and for constructing reliable ENSO reconstructions.

5.2. Data and Methods

Proxy data and site description

We use a tree-ring $\delta^{18}O$ chronology from a lowland rainforest in the eastern part of Central Java, Indonesia (07°52'S, 111°11'E; 380 m a.s.l.), spanning the period 1900-2007. The $\delta^{18}O_{TR}$ record is built from 7 teak (*Tectona grandis*) trees, collected from the Donoloyo Cagar Alam (site DNLY in D'Arrigo et al., 2006) shown as green lines in FIGURE 5.2. This $\delta^{18}O_{TR}$ chronology and its dendroclimatological potential as a rainfall indicator has been described in detail in (Schollaen et al., 2013). Indonesia receives significant rainfall year-round but experiences a distinct wet and dry season. The wet season (approx. October/November to April/May) coincides with movement of the Inter-Tropical Convergence Zone to the Southern Hemisphere, while the dry season (June to September) corresponds with a predominance of dry southeasterly winds from Australia (Aldrian et al., 2007). The isotopic composition of precipitation ($\delta^{18}O_{Pre}$) over Java shows that distinct seasonal changes are linked to rainfall amount resulting in high $\delta^{18}O_{Pre}$ values during the dry season, and low $\delta^{18}O_{Pre}$ values during the rainy season (Fig. 5b, Schollaen et al., 2014). Instrumental records (e.g. Aldrian and Susanto, 2003; Allan, 2000; Haylock and McBride, 2001) and reanalysis products (Aldrian et al., 2007; Jourdain et al., 2013) show rainfall anomalies in Indonesia are affected by ENSO: During a warm ENSO phase (El Niño events) the tropospheric air flow (Walker Circulation) weakens and the Indonesian Low pressure system migrates eastward into the tropical Pacific, resulting in drought over much of the country. Conversely, a cold ENSO phase (La Niña events) brings excess rain to the region (Sarachik and Cane, 2010). In this study, we further show that precipitation anomalies in Java are sensitive to ENSO flavors. FIGURE 5.1 shows the relationship between precipitation data and the WP and CT El Niño indices (see Sect. 2.2 for definition of the indices) for the IMC and Pacific region. WP El Niños are associated with drought over Java (FIGURE 5.1, upper panel), and have a strong influence on the Australian-Indonesian monsoon system (e.g. Kumar et al., 2006; Taschetto and England, 2009). On the other hand, Java lies on the nodal line of influence of CT El Niños (FIGURE 5.1, lower panel), which makes it a key location for obtaining records able to distinguish between the two ENSO flavors.

The growing season for teak in Central and Eastern Java occurs mostly during the wet season, from October to May (Coster, 1927, 1928; Geiger, 1915; Schollaen et al., 2013). In all subsequent analysis, we use the southern hemisphere convention, which assigns to each tree ring the year in which radial growth begins (Schulman, 1956). Thus lag-0 refers to the year n where tree growth starts: Oct_n-Sep_{n+1}. Lag-1 refers to Oct_{n-1}-Sep_n. ENSO-flavor indices are averaged over $Jan_{n+1}Feb_{n+1}$.

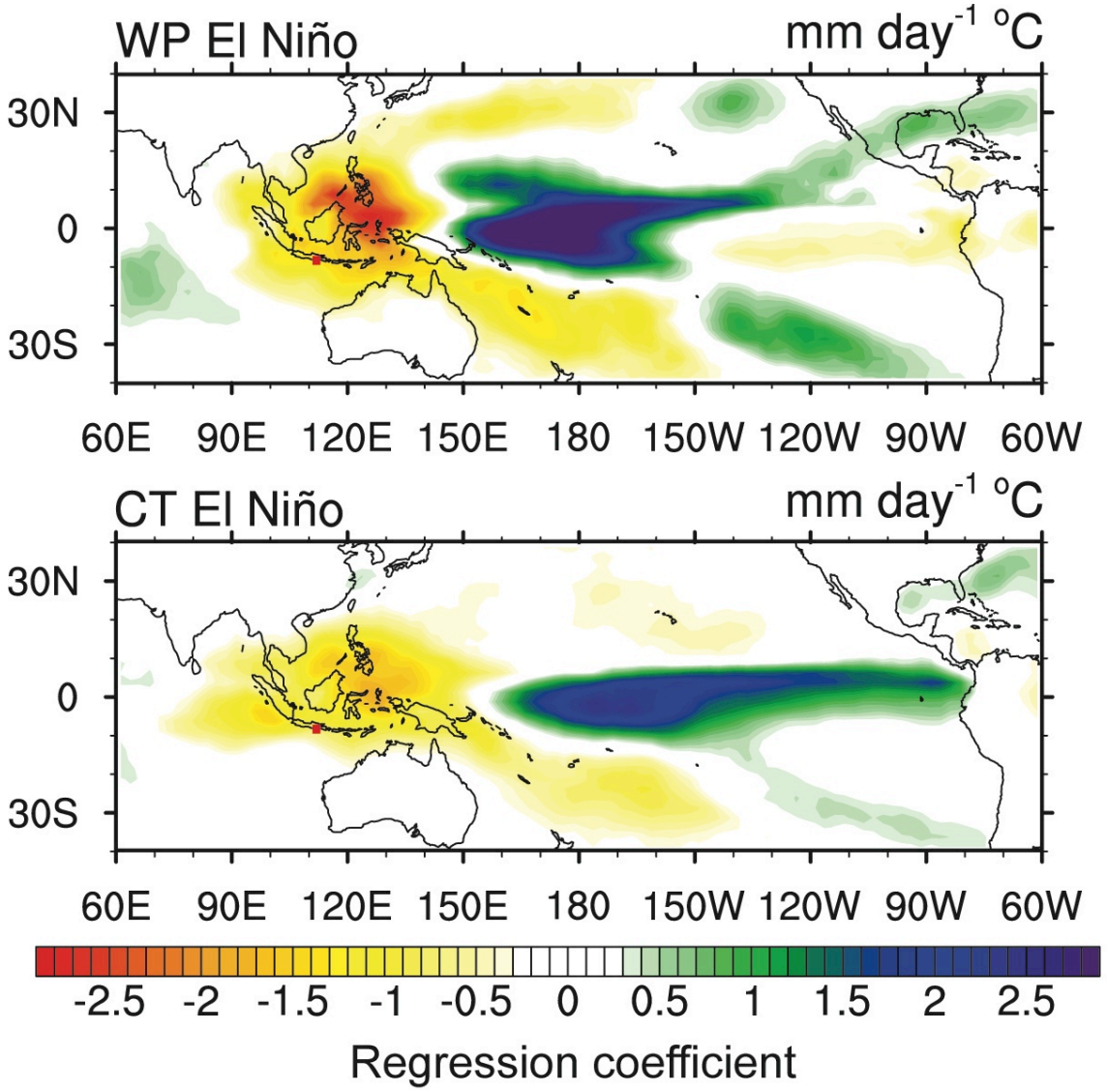

FIGURE 5.1 | Regression coefficients (mm day-1 °C) of precipitation on the Warm Pool (WP) and the Cold Tongue (CT) El Niño index. The two indices are computed as per Ren and Jin (2011) (1). Precipitation data are from the GPCP (Huffman et al., 2009), for the period 1987-2010. The tree-ring site is marked with a red squared.

Definition of ENSO flavors

We use the global SST dataset of Kaplan et al. (1998) to calculate ENSO indices, and the coordinate transform of the NINO3-NINO4 phase space by Ren and Jin (2011) to define the two ENSO flavors (Equation 1). No significant differences were found when using alternative indices for calculating ENSO flavors (not shown here) since the NINO3-NINO4 SST anomalies are so closely associated with rainfall anomalies in the Java region.

$$\begin{matrix} N_{CT} = N_3 - \alpha N_4 \\ N_{WP} = N_4 - \alpha N_3, \end{matrix} \quad \alpha = \begin{cases} 2/5 \ if \ N_3 N_4 > 0 \\ 0 \ otherwise \end{cases} \qquad (1)$$

For subsequent analyses we use the Jan-Feb ($Jan_{n+1}Feb_{n+1}$) time-averaged indices for years 1900-2007. We focus on the $Jan_{n+1}Feb_{n+1}$ period which represents the maximum rainy season in Java, when our $\delta^{18}O_{TR}$ record correlates the best with regional rainfall data (Schollaen et al., 2013). We classify each year as CT, or WP when N_{CT}, or N_{WP} are greater than one standard deviation of the respective monthly index. We classify a year as La Niña (LN) when NINO4 is negative by less than one standard deviation of the monthly NINO4 index. TABLE 5.1 shows the list of years classified as CT, WP, and LN according to the above criteria.

Distinguishing between the two corresponding types of La Niña events, as advocated by Kao and Yu (2009) and Ashok and Yamagata (2009), may not be necessary because the SST and precipitation patterns of the two La Niña types are not very distinctive (Kug and Ham, 2011).

TABLE 5.1 | Classification into ENSO flavors and phase based on JF values (see section "*Definition of ENSO flavors*"). Note the use of the southern hemisphere convention (Schulman, 1956), i.e. year n refers to $Jan_{n+1}Feb_{n+1}$.

ENSO classification	Years										
WP	1900	1902	1904	1907	1913	1927	1929	1939	1941	1957	1958
	1968	1978	1979	1987	1990	1994	2001	2002	2003	2004	
CT	1905	1911	1914	1918	1919	1923	1925	1930	1940	1965	1972
	1976	1982	1986	1991	1997						
LN	1909	1916	1917	1920	1924	1933	1938	1942	1949	1955	1970
	1973	1975	1983	1988	1998	1999	2000	2005	2007		

ENSO signal assessment

To assess the long-term temporal stability of the ENSO signal, running 31-year correlations were calculated between the $\delta^{18}O_{TR}$ record and the varying ENSO flavors. A Kalman filter analysis was also used as a time-dependent regression-modelling tool to test the temporal stability of the relationship between the $\delta^{18}O_{TR}$ record and the two ENSO flavors. In contrast to the running correlation procedure, the Kalman filter method uses maximum likelihood estimation to objectively test for the identification of time-dependence between predictor and predicted variables (see Visser and Molenaar (1988) for details, and Cook et al. (2002), Cook et al. (2013) or Wilson et al. (2013) for examples).

Furthermore, probability density functions of the correlation between $\delta^{18}O_{TR}$ variability and the different ENSO phases (WP, CT and LN), as well as during neutral conditions, were calculated. Finally, the spectral properties of the $\delta^{18}O_{TR}$ proxy time series were analyzed (Schulz and Mudelsee, 2002) and wavelet coherency analysis performed (Grinsted et al., 2004; Torrence and Compo, 1998).

5.3. Results

Monthly and seasonal correlations between the Javanese $\delta^{18}O_{TR}$ record (FIGURE 5.2, green line in all plots) and ENSO flavors (see section "Definition of ENSO flavors") were computed for both the concurrent year (lag-0) and the year prior to tree growth (lag-1) (TABLE 5.2). Statistically significant (95% level or higher) positive correlations were found between WP El Niño and the concurrent rainy season (Oct_n-May_{n+1}, r=0.26). Correlations are strongest when averaged over $Jan_{n+1}Feb_{n+1}$ (r=0.33), the period of maximum rainy season precipitation. Furthermore, there is a significant correlation with lag-1 January precipitation (Jan_n, r=0.22), indicating a WP El Niño influence on tree growth in the following year. Statistically significant negative correlations were found for La Niña events in January and February ($Jan_{n+1}Feb_{n+1}$, r=-0.24) (TABLE 5.2). No positive correlation was found between the tree-ring proxy and the CT El Niño flavor (TABLE 5.2). As noted, this El Niño flavor has a weaker influence over Java (FIGURE 5.1), therefore we expected the lag-0 correlation to be insignificant.

TABLE 5.2 | Correlation values between the annually resolved $\delta^{18}O_{TR}$ record and climate months of different ENSO flavors for the period from the year prior to growth (lag-1) to the current year (lag-0) and seasonal means (calculated over the 1900-2007 period). (**:p<0.001, *:p<0.01, bold: p<0.05).

Climate months *lag-1 lag-0*	WP El Niño	CT El Niño	La Niña
Oct_{n-1} | Oct_n	0.12 | **0.21**	-0.18 | -0.03	0.00 | -0.14
Nov_{n-1} | Nov_n	0.17 | 0.17	**-0.23** | -0.01	0.00 | -0.12
Dec_{n-1} | Dec_n	0.18 | 0.18	**-0.20** | 0.04	-0.01 | -0.15
Jan_n | Jan_{n+1}	0.**22** | **0.35****	-0.19 | -0.01	-0.06 | **-0.25***
Feb_n | Feb_{n+1}	0.15 | **0.29***	-0.15 |-0.06	-0.05 | **-0.21**
Mar_n | Mar_{n+1}	0.05 | **0.21**	-0.17 |-0.12	0.03 | -0.12
Apr_n | Apr_{n+1}	0.14 | **0.21**	**-0.21** | -0.09	-0.02 | -0.15
May_n | May_{n+1}	0.12 | **0.20**	-0.14 | -0.11	-0.03 | -0.12
Jun_n | Jun_{n+1}	0.14 | 0.08	-0.07 | -0.06	-0.08 | -0.03
Jul_n | Jul_{n+1}	0.12 | 0.16	-0.02 | -0.08	-0.09 | -0.10
Aug_n | Aug_{n+1}	0.11 | 0.10	-0.02 | -0.07	-0.10 | -0.05
Sep_n | Sep_{n+1}	0.17 | 0.01	-0.05 | -0.05	-0.11 | 0.02
peak wet season ($Jan_{n+1}Feb_{n+1}$)	**0.33****		**-0.24**
wet season (Oct_n-May_{n+1})	**0.26***		

Although the $\delta^{18}O_{TR}$ record correlates significantly (p<0.05) with ENSO flavors, the response is not stationary. FIGURE 5.2 presents the running 31-year correlation and Kalman filter analysis between the varying ENSO flavors and the tree-ring proxy for the period of highest correlation (see TABLE 5.2). The teleconnection with JF WP El Niño is strong and

significantly positive from the 1950s till present, with running correlations reaching 0.6, and an overall r of 0.43 ($p<0.001$) (FIGURE 5.2A). However, before 1950 the correlation falls to zero, and even becomes negative. The Kalman filter time-varying regression coefficients (beta weights) follow the same trend as the correlation values and reinforce the time dependency of the teleconnection. From 1950 onwards, the lower limits do not cross zero, which means that the beta weights are considered statistically significant. However, the correlation weakens slightly again in the beginning of the 21th century. The teleconnection with JF La Niña index (FIGURE 5.2C) is also time dependent with weak correlations before 1950 and after 2000, but a significant negative relationship in the second half of the century with $r=-0.38$ ($p<0.01$).

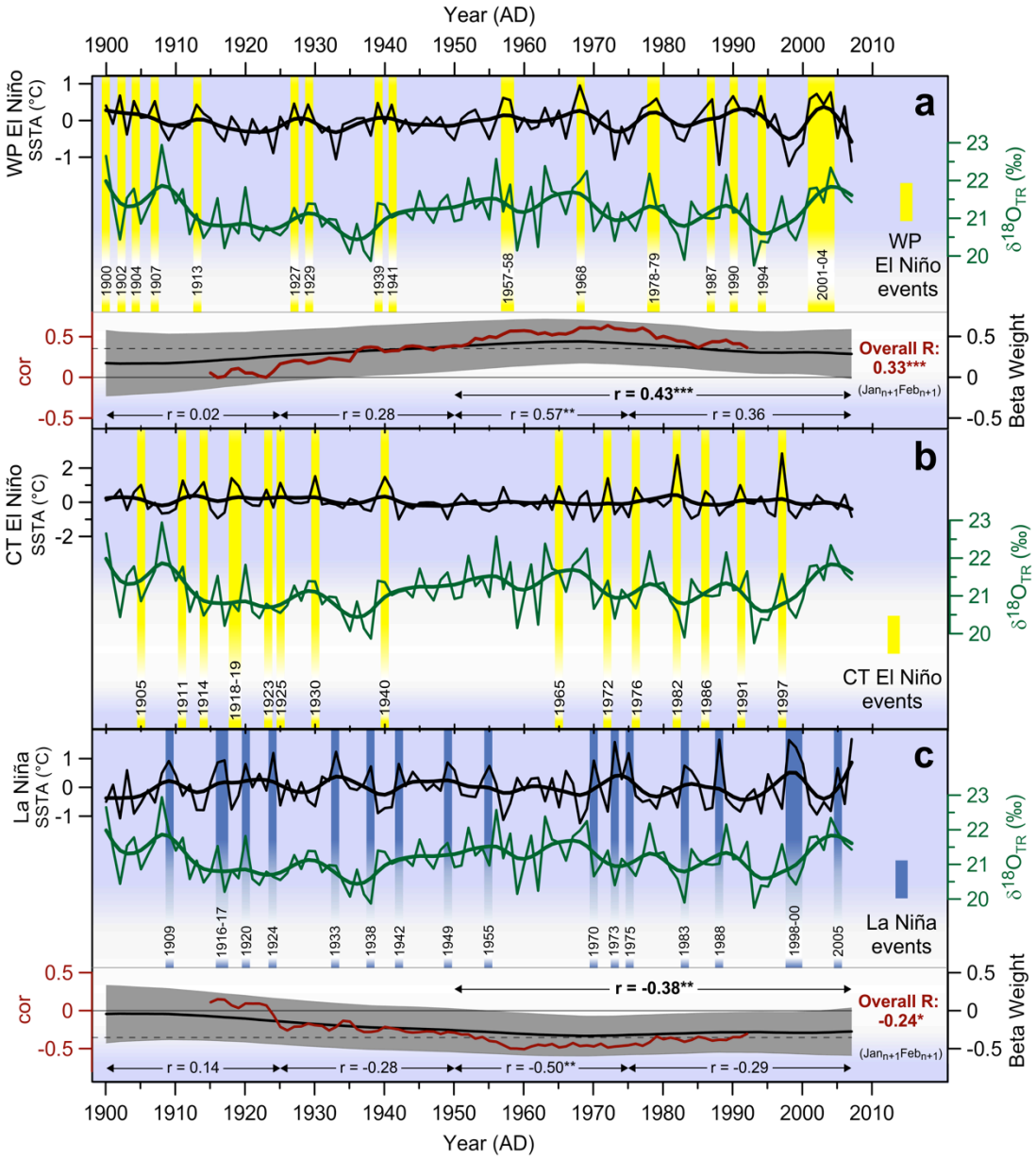

FIGURE 5.2 | Time series of the tree-ring $\delta^{18}O$ chronology (green) and the January to February ($Jan_{n+1}Feb_{n+1}$) time-averaged indices of (a) Warm Pool (WP) El Niño (black), (b) Cold Tongue (CT) El Niño and (c) La Niña (black). The WP and CT El Niño indices are computed as per Ren and Jin [2011] (1). Thick lines denote 10-year cubic smoothing spline. In the lower part of each figure the running 31-year correlation (red) is shown.. Dashed horizontal line indicates the 75% confidence level. Also shown are the results from a Kalman filter anaylsis (black line) used as a dynamic regression modeling tool. Grey shading denotes ± 2 standard error limits of the beta weights. Where the limits do not cross zero, the regression relationship are considered statistically significant (p=95%). ENSO events based on classification of TABLE 5.1 are highlighted in yellow (El Niño) and blue (La Niña), respectively. (***p < 0.001, **p < 0.01, *p<0.05).

The fingerprints of the ENSO flavors in the $\delta^{18}O_{TR}$ record can be seen in the probability density function (PDF) of $\delta^{18}O_{TR}$ anomalies (FIGURE 5.3). The WP probability mass is skewed towards positive anomalies associated with dry conditions. By contrast, the PDF for CT El Niño events exhibits bimodality with peaks in both positive and negative $\delta^{18}O_{TR}$ anomalies, suggesting this record is not a good proxy for CT El Niño variability. The PDF for the previous (lag-1) rainy season CT El Niño (dashed line) is also skewed towards negative $\delta^{18}O_{TR}$ anomalies, similar to that of lag-0 La Niña events (blue line), supporting the idea that the lag-1 correlation reflects subsequent La Niña events.

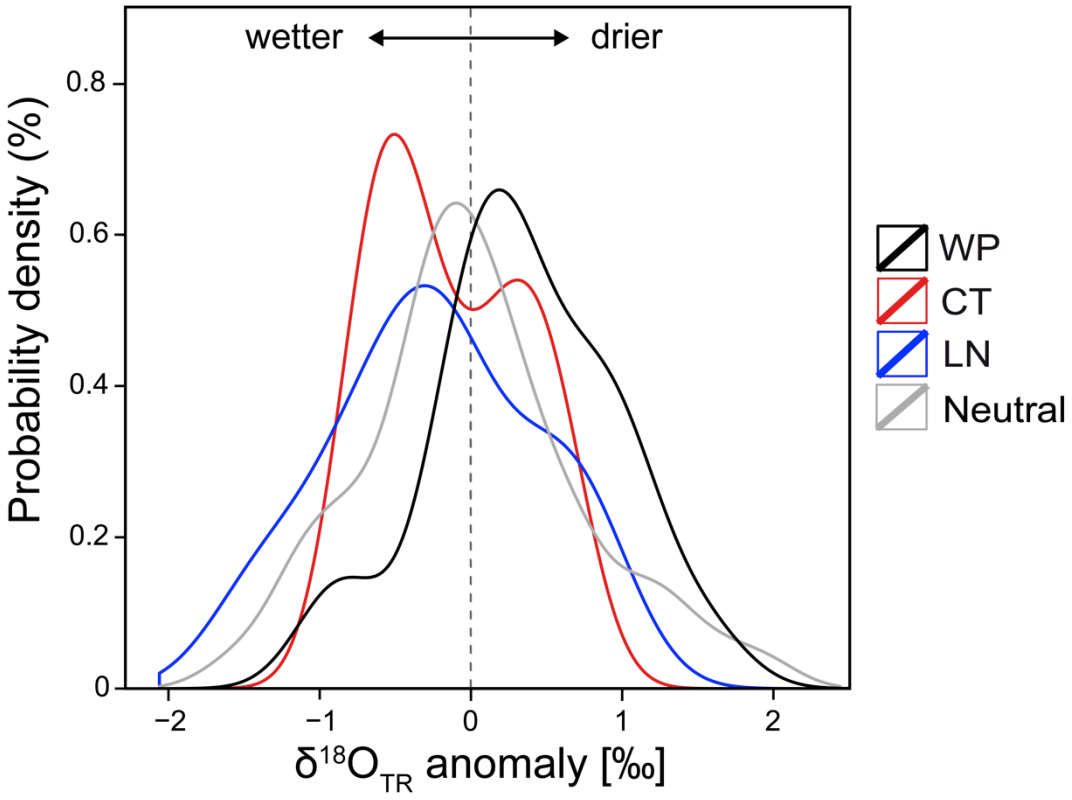

FIGURE 5.3 | Probability density function of tree-ring $\delta^{18}O$ variability from different ENSO types: Warm Pool El Niño (WP, black line), Cold Tongue El Niño (CT, red line), La Niña (LN, blue line) and neutral conditions (grey line). The January to February ($Jan_{n+1}Feb_{n+1}$) time-averaged indices are shown. Plotted are ±1 standard deviation values.

To further investigate expressions of ENSO variability in the $\delta^{18}O_{TR}$ record we performed spectral analysis (FIGURE 5.4A). Spectral analysis of the $\delta^{18}O_{TR}$ record reveals a broad peak at 2–4 years, falling within the classic ENSO bandwidth (Sarachik and Cane, 2010) as well as significant, decadal-to-multidecadal variability (12.5 years). Wavelet coherence analysis between the proxy record and WP El Niño (FIGURE 5.4B) and La Niña (FIGURE 5.4C) indicates that their coherence varies in time across most spectral bands. The periods of greatest coherence in time occur on inter-annual timescales (2-4 years), again spanning the classic ENSO bandwidth.

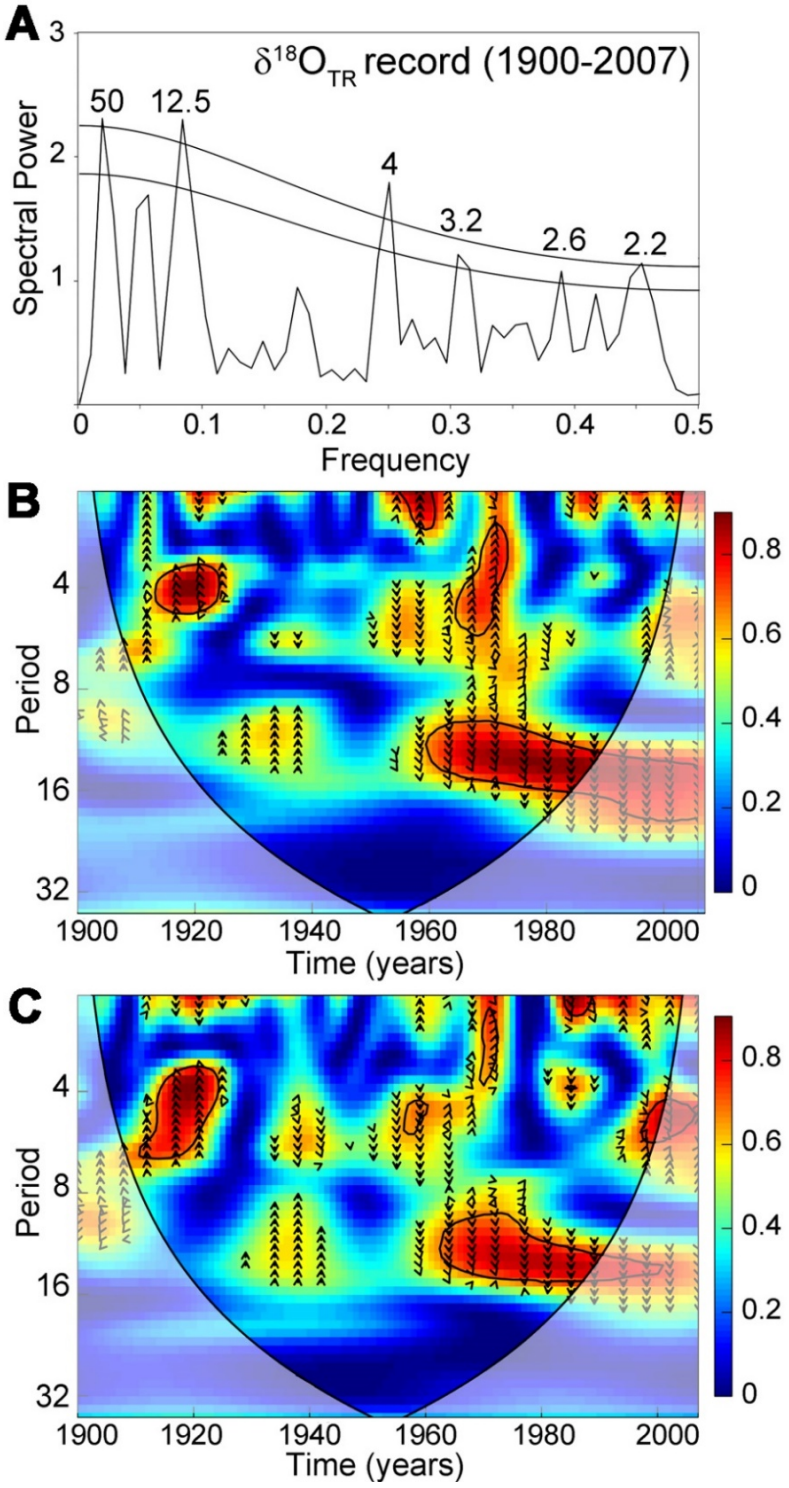

FIGURE 5.4 | (A) Spectral analysis (Schulz and Mudelsee, 2002) of the tree-ring $\delta^{18}O$ chronology from 1900 to 2007. 90% and 95% confidence levels are indicated. (B) Wavelet coherence transform comparing shared frequency between tree-ring $\delta^{18}O$ record and Warm Pool (WP) El Niño index (JF), and (C) La Niña index ($Jan_{n+1}Feb_{n+1}$) for 1900 to 2007. The wavelet coherence illustrating temporal frequency coherence between the time series at given periods. The thick black contour designates where time series share significant coherence (p=95%) and the cone of influence where edge effects might distort the picture is shown as a lighter shade. Arrows indicate the phase relationship between series with in-phase pointing right and antiphase pointing left.

5.4. Discussion

The positive correlation pattern between the $\delta^{18}O_{TR}$ record and the WP El Niño flavor, as well as the negative correlation with La Niña events, supports the conclusion in Schollaen et al. (2013) that the formation of annual $\delta^{18}O$ in Javanese teak trees is dominated by precipitation patterns. El Niño events are linked to drought conditions over the IMC coinciding with increased $\delta^{18}O$ values in the tree-ring proxy (FIGURES 5.2, 5.3). The opposite occurs during La Niña events. The PDFs illustrate a clear WP El Niño and a less strong La Niña signal, with really dry years linked to WP El Niños. In contrast, no clear CT El Niño signal is preserved in the $\delta^{18}O_{TR}$ record. The bimodality in the PDF illustrates the uncertainty in cases with no strong signal. The different seasonal rainfall signals (wet and dry season rainfall) in the $\delta^{18}O_{TR}$ record are damped in the annually resolved proxy due to seasonally alternating isotope signatures in $\delta^{18}O$ of precipitation (Schollaen et al., 2013). Thus, CT El Niño signals seem to be obscured when followed by a La Niña event. This is the case for the strong CT El Niño event in 1982/83 that was followed by a La Niña, resulting in a low $\delta^{18}O_{TR}$ value (FIGURES 5.2B, 5.2C). High-resolution intra-annual $\delta^{18}O_{TR}$ analyses help to disentangle the contrasting isotope effects of dry and rainy season rainfall patterns, as demonstrated in Schollaen et al. (2014). We conclude that the annually resolved tree-ring proxy is suitable for distinguishing between WP El Niño and La Niña, but not for CT El Niños. Overall, the strongest and most significant ENSO signal in the tree-ring proxy data is that of WP El Niño.

Our experiments show that the teleconnections described above are not stationary (FIGURES 5.2, 5.4). There is a drop in correlation in the first half of the 20th century. One can speculate this weakening teleconnection is related to the pattern of relatively weak and irregular ENSO activity in the middle of the 20th century (Tudhope et al., 2001). Arguably, there may be other factors (e.g. Indian Ocean Dipole Mode) determining wetter or drier conditions in this period and the ENSO phenomenon may play a secondary role. In recent decades, a climate regime transition has preceded periods of strong and sustained ENSO events (e.g. O'Kane et al., 2014), leading to a stronger ENSO fingerprint in the $\delta^{18}O_{TR}$ record. Furthermore Chang et al. (2004) reveal an interdecadal trend of increasing correlations between Indonesian monsoon rainfall and ENSO beginning in the late 1970s.

Several analyses of Indonesian rain gauge data show that Indonesian rainfall is poorly correlated with ENSO events during the wet monsoon season, but reveal highest coherence during the dry season and transition months prior to the wet season (June to November) (Haylock and McBride, 2001; Hendon, 2003). This is especially true for January, which has consistently insignificant correlations over Indonesia (1979–2002) (Chang et al., 2004). However, taking the IMC and surrounding oceanic rainfall into account, rainfall during the wet season is related to ENSO (see FIGURE 8a in Jourdain et al. (2013) and FIGURE 5.1 of this study). The $\delta^{18}O_{TR}$ record is a rainfall indicator for wet and dry season

rainfall, albeit largely dominated by the wet season signal (Schollaen et al., 2013). Note, that the "amount effect" leads to different isotopic signatures in $\delta^{18}O_{TR}$ values during wet and dry season. Thus, the dry season rainfall signal, which tends to have the highest coherence with ENSO, is damped in the annually resolved $\delta^{18}O_{TR}$ record by the following wet season signal. This may explain the low correlation between the tree-ring proxy and June to November ENSO indices. To distinguish the causes of inter-annual rainfall variability across Java future work needs to focus on high-resolution $\delta^{18}O_{TR}$ records.

5.5. Conclusions

In this study we used a $\delta^{18}O_{TR}$ chronology from teak (*Tectona grandis*) that correlates significantly with regional precipitation over Java (Schollaen et al., 2013) to examine various manifestations of ENSO. This is the first time a high-resolution $\delta^{18}O_{TR}$ record is used to detect signals of ENSO flavors in palaeoclimatic data as argued by Karamperidou et al. (submitted). These results indicate the significant potential for generating reconstructions of different ENSO flavors from the $\delta^{18}O_{TR}$ records in Indonesian teak. Such palaeoclimatic records may help answering the many remaining questions surrounding the diversity of ENSO activity. In addition, the conclusions of our study call for caution when doing model-proxy comparisons using ENSO indices that are not able to distinguish between the two flavors (e.g. single standard indices such as NINO3.4). Performing such comparisons may confound attempts to reconcile models with proxies.
More emphasis is needed on sampling long-term terrestrial $\delta^{18}O_{TR}$ records at seasonal resolution from eastern Indonesia to reveal a robust reconstruction of wet and dry season rainfall with its teleconnection to the different ENSO flavors.

Acknowledgements

Karina Schollaen was funded by the HIMPAC (HE 3089/4-1) and the CADY (BMBF, 03G0813H) project. Isotope analyses were funded by a Joint DFG/FAPESP Research Grant (HE3089/5-1). Christina Karamperidou is funded by NSF Award 1304910. We acknowledge the Bolin Centre's, Climate Research Summer School during which this project and collaboration was conceived.

Chapter 6

Synthesis

Palaeoclimatic records from tropical regions are still scarce and underrepresented. Thus, this thesis generates new stable isotope records ($\delta^{13}C/\delta^{18}O$) from a tropical tree-ring site in Indonesia to explore the potential of these records as climate proxies. In addition, novel techniques that facilitate and optimize the sampling preparation for tree-ring stable isotope analyses are introduced.

In the following summary section, the main findings of the thesis are shortly presented and generally discussed, along the defined *methodological approaches* and *research objectives* as stated in section 1.2. Furthermore, an overall conclusion is given and recommendations for possible future research avenues close the chapter.

6.1. Summary and General Discussion

Methodological approaches

Assessing the usefulness of UV-laser microdissection microscopes as a new high-resolution sampling tool for stable isotope research (*Chapter 2*)

This is the first time that UV-laser-based microscopic dissection systems were tested as a sampling tool for stable isotope studies on organic matter. The method uses thin wood cross-sections and allows serial isolation of tissue of any shape and from millimeter down to micrometer scale. On-screen pre-defined areas of interest were semi-automatically dissected and collected for mass spectrometric analysis whereby non-relevant tissues (e.g. resin ducts, wood rays) can be removed before stable isotope analysis. The use of cross-sections diminishes difficulties of cross-contamination when sampling tree rings with tight curvatures, non-parallel boundaries, varying fibre or vessel angles and/or irregular tree-ring width in radial direction. With this method a wood core sample is no longer sacrificed as only cross-sections are being used for IRMS. Remaining wood samples can be used for multidisciplinary approaches. High-resolution stable isotope analysis, quantitative wood anatomy, ring width or wood density analysis can now be performed on the same samples, minimizing uncertainties in the interpretation of results.

This UV-laser-based sampling method was particularly applied to disentangle the rainy and dry season rainfall signals in the annual tree-ring $\delta^{18}O$ record from the Indonesian study site (see Chapter 4). The obtained high-resolution tree-ring $\delta^{18}O$ profiles reflect both monsoonal rainfall patterns and reveal sensitivity to ENSO events. Furthermore, the novel sampling tool was tested on other tree species.

The application demonstrates that the introduced method allows for sampling plant tissue at ultrahigh resolution and unprecedented precision. The technique facilitates sampling not only for stable isotope analysis, but also other physical/chemical investigations and opens

the possibility to combine tree eco-physiological, wood anatomical and dendro-climatological studies.
Within this methodological approach I could demonstrate that the UV-laser-based microdissection system is a valuable method for high-precision sampling of thin wholewood cross-sections. To extend the usability of the UV-laser systems for dendroisotopic studies I focused further on the development of a method revealing thin cellulose cross-sections for UV-laser microdissection, since most tree-ring stable isotope studies prefer to analyze cellulose.

Establishment of an improved procedure of sample preparation for high-throughput stable isotope analysis of tree rings (*Chapter 3*)

I investigated a guideline for a modified method of cellulose extraction from wholewood cross-sections utilizing perforated teflon sheets as sample holders. This sampling design facilitates the possibility to extract numerous tree rings per sample at one step while the cell structure remains. Subsequent tree-ring dissection and sample collection for IRMS can be made in a single step without homogenization and by minimizing the efforts for weighing. Various coniferous and deciduous tree species can be applied and more precise tree-ring separation at inter- to intra-annual scale is revealed. With this fast and costumer friendly extraction method a real progress for stable isotope analysis on tree-ring cellulose is provided to much faster develop for example millennial-length palaeoclimate reconstructions.
Loader et al. (2013) highlight in a recent paper that higher levels of series replication than those typically adopted in isotope dendroclimatology (four to five trees, initially proposed by Leavitt and Long (1984)) may need to be considered if a representative regional environmental signal should be attained and used to reconstruct past climate conditions. With the new high-throughput cellulose extraction method this will not require a substantial increase in effort and time for sample preparation. Hence, the novel technique may facilitate the achievement of the required higher sample replication for isotope dendroclimatology. Furthermore, the question of whether or not cellulose extraction is required for stable (oxygen) isotope analysis on tree-ring chronologies may become redundant, as cellulose extraction and homogenization are no longer a time limiting step.
The obtained cellulose cross-sections can be treated with UV-laser-based microscopic dissection systems (Schollaen et al., 2014) or UV-laser ablation-IRMS (Schulze et al., 2004) to reveal high-resolution and very precise cellulose stable isotope data. I tested the practical application of using cellulose cross-sections along with UV-laser-based microscopic systems successfully on several tree species. The publication of results from a pilot study of intra-annually resolved cellulose $\delta^{18}O$ data of African baobab (*Adansonia* spp.) from Zimbabwe is in preparation.

Palaeoclimatological studies from Indonesia

Establishment of centennial well-replicated multiple tree-ring records (ring-width, $\delta^{13}C$, $\delta^{18}O$) from Java, Indonesia (*Chapter 4*)

A 294-year long tree-ring width chronology (AD 1714-2007) and 108-year long carbon and oxygen isotope chronologies (AD 1900-2007) of teak (*Tectona grandis*) from a study site in eastern Central Java were developed. The latter are the first well-replicated stable isotope records from 7 teak trees in that region. Although we used two more tree samples than typically used in isotope dendroclimatological studies (Leavitt and Long, 1984), the carbon isotope chronology slightly missed the threshold of an EPS ≥ 0.85 (Wigley et al., 1984) to be representative for the sampling site. However, the TRW and $\delta^{18}O$ chronologies are well intercorrelated and representative for the study site assuming that the established proxy records are well suitable to reconstruct climate variables of the past.

Assessment of statistical and mechanistic relationships between tree-ring series and climate variables for the 20th century *(Chapter 4)*

The highest correlation between the tree-ring series and climate variables is revealed with precipitation, as precipitation is mostly the limiting factor on tree growth at tropical sites with a typical equatorial climate. The climate response analysis with regional, monthly precipitation data reveals that all three tree-ring series are significantly correlated to rainfall, although during different monsoon seasons. Precipitation in the beginning of the rainy season is important for tree-ring width, confirming previous studies from D´Arrigo and co-workers. Compared to ring width, the stable isotope records reveal a higher correlation with rainfall amount, especially during portions of the peak rainy season. Furthermore, $\delta^{18}O_{TR}$ also responds to peak dry season rainfall. The correlations of opposite signs in $\delta^{18}O_{TR}$ reflect the distinct seasonal contrast of the isotope signatures in precipitation ($\delta^{18}O_{Pre}$) during the dry (^{18}O-enriched rain) and rainy (^{18}O-depleted rain) seasons, the so-called amount effect. Thus the annual $\delta^{18}O_{TR}$ record reflects the combination of two signals whereby the rainy season signal is dominant and stable in time. This is the first time that a $\delta^{18}O_{TR}$ record from tropical trees reveal correlations with dry and rainy season rainfall.

However, the correlations with climate are not as high and stable in time to be valuable using stable isotope chronologies to reconstruct past climate changes. For the carbon isotope record this may be due to the poor representativeness of the selected tree samples suggesting that higher sample replication is needed. In contrast, for the $\delta^{18}O_{TR}$ record this may be due to the seasonally alternating $\delta^{18}O_{Pre}$ signatures causing a damped dry and rainy season rainfall signal in the annually resolved $\delta^{18}O_{TR}$ record. Here, high-resolution intra-

annual $\delta^{18}O_{TR}$ data demonstrate the potential to distinguish clearly between both rainfall signals.

Establishment of highly resolved intra-annual $\delta^{18}O$ data to explain the transfer of precipitation signals into the tree rings of teak *(Chapter 2 and 4)*

We established highly resolved intra-annual $\delta^{18}O_{TR}$ data using UV-laser-based microscopic dissection systems (introduced in Chapter 2). The high-resolution intra-annual $\delta^{18}O_{TR}$ series explain the transfer of the dry and rainy season $\delta^{18}O_{Pre}$ signal into the tree rings of teak. A conceptual oxygen isotope model illustrating the hydrological conditions at the study site helps to interpret the high-resolution data (see FIG. 4.5A). Thus the first third of each tree ring present the $\delta^{18}O_{Pre}$ signature of the prior dry and early rainy season (^{18}O-enriched rain), while the following low $\delta^{18}O_{TR}$ values reveal the $\delta^{18}O_{Pre}$ signature of the main rainy season (^{18}O-depleted rain). Furthermore we could demonstrate that the intra-annual $\delta^{18}O_{TR}$ values are sensitive to rainfall extremes caused by ENSO. These seasonally alternating $\delta^{18}O$ signatures in precipitation provoke that the single monsoon footprints (dry/rainy season) are damped in the annual $\delta^{18}O_{TR}$ record.

Investigation of ENSO signals in the annual tree-ring $\delta^{18}O$ record *(Chapter 5)*

Indonesian rainfall is strongly linked to large-scale Indo-Pacific Ocean variability such as ENSO variations. Thus the annual tree-ring $\delta^{18}O_{TR}$ record was tested for ENSO signals whereby we distinguish between two ENSO types as recent studies have drawn attention to the existence of more than one “flavor" of El Niño (Ashok et al., 2007; Kug et al., 2009; Larkin and Harrison, 2005; Ren and Jin, 2011; Takahashi et al., 2011). The statistical analysis reveals a clear influence of Central Pacific (Warm Pool) El Niño events during the main rainy season while no clear signal of Eastern Pacific (Cold Tongue) El Niño events was found. Also correlations with La Niña events are revealed but with a weaker signal. To conclude, the $\delta^{18}O$ records indicate the significant potential for generating reconstructions of different ENSO flavors for the East Pacific region and illustrate the importance of considering ENSO flavors when interpreting palaeoclimatic data in the tropics.

6.2. Achievements

The studies comprising this thesis deliver:

1. The first study that tested UV-laser-based microscopic dissection systems for tree-ring research.
2. Evidence for the application of UV-laser-based microscopic dissection systems as a novel tool for high-resolution stable isotope analysis dissecting plant tissue at ultrahigh resolution and unprecedented precision.
3. A guideline for a modified cellulose extraction procedure that obtain thin cellulose laths directly from wholewood cross-sections optimizing the stable isotope analysis process in two ways: faster and costumer friendly extraction and precise tree-ring separation at annual to high-resolution scale.
4. The first well-replicated centennial stable isotope records ($\delta^{13}C$, $\delta^{18}O$) of teak from Java, Indonesia.
5. Results showing for the first time that a $\delta^{18}O_{TR}$ record from tropical trees reveals influence of dry and rainy season rainfall.
6. The first study that used a high-resolution tree-ring proxy record ($\delta^{18}O_{TR}$) to illustrate the importance of taking into account ENSO flavors when interpreting palaeoclimatic data from the Pacific region.

6.3. Concluding remarks and future prospects

My dissertation has advanced the applicability of novel techniques that facilitate and optimize high-resolution and high-throughput stable isotope analysis of tree rings. Together with other methodological development, for example simultaneous measurement of stable isotopes in tree-ring cellulose using high-temperature pyrolysis (Woodley et al., 2012; Helle 2010 - 8th International Conference on Dendrochronology, 13-18 June 2010, Rovaniemi, Finland; Loader et al. 2014 - 9th International Conference on Dendrochronology, 13-17 January 2014, Melbourne, Australia), the herein

presented novel techniques offer exciting new potential to improve precision, efficiency, quality and quality control of stable isotope analyses in tree-ring research. The methods offer many unexplored avenues of, in particular, multi-parameter research in dendroclimatology, as well as for research in high-resolution palaeoclimatology, in general. Multidisciplinary and long-term research programmes as for example TERENO (Terrestrial Environmental Observatories, http://teodoor.icg.kfa-juelich.de/) which aims to catalogue the long-term ecological, social and economic impact of global change at regional level, STReESS (Studying Tree Responses to extreme Events: a SynthesiS, http://streess-cost.eu/) which study tree response to extreme events among European countries or TRENCH (Tree-Ring Environmental Network for Climate Change Monitoring, http://tropicalmountainforest. org/) which aim to develop a tree-based indicator system for environmental change impacts on forest ecosystems in southern Ecuador, can widely benefit using these novel methods for studies on vulnerability, resilience and adaption of woody plants to past and present global change.

Apart from the new methodological achievements for tree-ring stable isotope studies this thesis contributed to a better understanding of the potential of stable isotope records from tropical teak trees in Indonesia as climate proxies. The research of this thesis provide new insights in using centennial stable isotope records from tropical trees to track climate signals, whereas it turned out that the $\delta^{18}O_{TR}$ record is the most valuable proxy for precipitation as it captures both monsoon seasons.

Reliable long-term precipitation data across the tropical Indo-Pacific region are urgently needed in this key region for ENSO since the IPCC state in its Fifth Assessment Report (IPCC, 2013) that the confidence of projected changes in ENSO, which will stay one of the dominant large-scale ocean-atmosphere phenomena with global impact, remains low for the 21st century. To use the potential of the herein presented tree-ring oxygen isotope record for precipitation reconstruction across the tropical Indo-Pacific region, further studies need to focus on the development of high-resolution stable isotope chronologies. Only seasonally resolved tree-ring $\delta^{18}O$ records can clearly distinguish between dry and

wet season rainfall signals allowing the reconstruction of seasonal rainfall variability and large-scale ocean-atmosphere phenomena like ENSO variations. The understanding of long-term palaeoclimate can be gained by researching old living tree samples as well as fossil teak remains from the Indonesian Archipelago. Existing multi-centennial teak TRW hronologies (e.g. Buckley et al., 2007; D'Arrigo et al., 1994) and further study sites with known subfossil teak trees offer the potential to continuously go back in time approximately 700 years (Jonathan Palmer and Paul Krusic, pers. communication) on inter- to intra-annual scale with a reasonable high sample replication. Those seasonally resolved tree-ring oxygen isotope records could allow us to reconstruct both local precipitation variability (monsoon signals) and large-scale ocean-atmosphere features (ENSO flavors). Hence, such high-resolution proxy from Indonesia will help to better understand the frequency and magnitude of extreme events over time being of particular relevance to societal concerns. Furthermore, I suggest to analyze cellulose instead of wholewood when establishing multi-centennial high-resolution $\delta^{18}O$ records from Indonesian teak as cellulose extraction is no longer the time limiting factor for sample preparation with the novel techniques presented in Chapter 3.

Future studies should consider a multi-proxy approach by the combination of different high-resolution proxy archives as tree rings, banded corals, laminated speleotherms or varved sediments. Thus, common extracted climate signals can be combined to provide more robust and long-term estimates of past climate conditions and thus may help to improve models simulating monsoon circulation changes over the Indo-Pacific region.

Closing words

To summarize, the research conducted throughout my PhD studies has deepened the knowledge on the potential of stable isotope records derived from Indonesian teak trees to track climate signals and to explain the transfer of precipitation signals into the tree ring. Furthermore, novel stable isotope techniques have been established, which may act as a basis for future tree-ring stable isotope studies on inter- to intra-annual scale. I wish that further scientific studies dealing with stable isotopes in tree rings will widely benefit from the application of the novel methods. Finally, I hope that this PhD study will motivate the palaeoclimate community to produce new and longer high-resolution proxy records to improve our understanding and the prediction of monsoon patterns, as most of the local population depends on monsoon rainfall for water and agricultural fertility.

Chapter 7

Appendix

Appendix A

Testing the influence of graphite and gypsum markings on stable isotope values ($\delta^{13}C$, $\delta^{18}O$) in tropical tree rings (*TRACE* Vol. 11, Proceedings of the DENDROSYMPOSIUM 2012: 85-87.)

Appendix B

A novel approach for the preparation of high-resolution stable isotope records from tropical tree rings (*TRACE* Vol. 11, Proceedings of the DENDROSYMPOSIUM 2012: 71-76.)

Appendix C

Toward multi-parameter records (ring width, $\delta^{13}C$, $\delta^{18}O$) from tropical tree-rings - A case study on *Tectona grandis* from Java, Indonesia (*TRACE* Vol. 9, Proceedings of the DENDROSYMPOSIUM 2010: 158-165.)

Appendix D

Tree-ring data: Annual tree-ring (ring width, $\delta^{13}C$, $\delta^{18}O$) chronologies from *Tectona grandis* of Central Java, Indonesia (07°52'S, 111°11'E)

Appendix A

Technical note:

Testing the influence of graphite and gypsum markings on stable isotope values ($\delta^{13}C$, $\delta^{18}O$) in tropical tree rings

This chapter was published in:
TRACE - Tree Rings in Archaeology, Climatology and Ecology, Vol. 11, Proceedings of the DENDROSYMPOSIUM 2012, 85-87.
Authored by Karina Schollaen and Gerhard Helle

GFZ - German Research Centre for Geosciences, Section 5.2 Climate Dynamics and Landscape Evolution, Telegrafenberg, 14473 Potsdam, Germany

Introduction

Tree-ring parameters (e.g. ring-width, stable isotopes) are one of the most important outputs from climate archives because of their precisely dated and annually resolved information. Tree-ring stable isotope records usually show higher signal strengths than tree-ring widths (e.g. Gagen et al., 2011; Schollaen et al., 2013). A careful wood surface preparation is an essential precondition for dendrochronological studies, since dating errors can not be corrected afterwards. Normally, when tree-ring samples are used for stable isotope analysis carbonaceous or oxygenic tools which could contaminate the stable isotope values, e.g. chalk or pencil, are avoided. However, the use of pencils and chalk aids the dating and dissection of samples, particularly when working with difficult tropical species. It is often necessary to highlight the contrast between different wood cell structures for a better detection of narrow or indistinct annual growth boundaries. Here, we tested a possible contamination with graphite and gypsum on stable isotope values ($\delta^{13}C$, $\delta^{18}O$) from wholewood Indonesian teak samples.

Material and Methods

The wood material used for the contamination test is part of a dendro-climatic isotope study of Teak trees, collected in the eastern part of Central Java, Indonesia (Schollaen et

al., 2013). All pre-treatment of the collected samples was carried out in the laboratory following standard procedures outlined in Stokes and Smiley (1968) and Schweingruber (1983). To improve the visibility of the tree-ring structure the surface of the core samples was cut with a microtome (WSL core microtome, Switzerland) or special knifes (NT Cutter BA-170). Fine chalk, which consists today only of gypsum (calcium sulfate: $CaSO_4$ x $2H_2O$), was rubbed into the pores to increase the visual contrast. Pencil strokes, which consist essentially of graphite, have been used for dating procedure (FIGURE A.1).

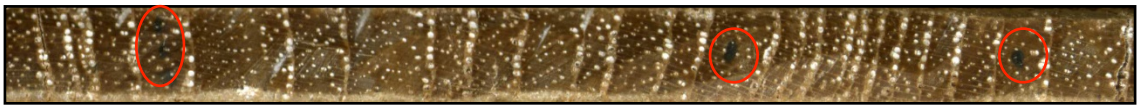

FIGURE A.1 | Wood surface from a teak core, contaminated with pencil strokes (graphite, red circle) to mark dating and chalk (calcium sulfate $CaSO_4$) to highlight wood anatomical features.

For stable isotope measurements seven different tree cores were chosen and the wholewood was analyzed for ~100 years (1900-2007). The tree rings from all cores were cut separately using a scalpel and grounded to assure homogeneity. Extractives, such as wood resins and oils, but also glue, pencil and chalk remains were removed from the wood with boiling de-ionized water and ethanol in a multiple sample isolation system for solids (Wieloch et al., 2011). Carbon isotope ratios were measured by combustion (at 1080°C) using an elemental analyser (Model NA 1500; Carlo Erba, Milan, Italy) coupled online to an Isotope Ratio Mass Spectrometer (IRMS, Isoprime Ltd. Cheadle Hulme, United Kingdom). Oxygen isotope ratios were measured using a high temperature TC/EA pyrolysis furnace (at 1340°C) coupled online to an IRMS (Delta V Advantage, Thermo Scientific, Bremen, Germany). Sample replication resulted in a reproducibility of better than ±0.1‰ for $\delta^{13}C_{TR}$ values and ±0.25‰ for $\delta^{18}O_{TR}$ values. The isotope ratios are given in the δ notation, relative to the standards V-PDB for $\delta^{13}C$ and V-SMOW for $\delta^{18}O$ (Craig, 1957).

Possible shifts of the original isotope values from pencil or chalk contaminants can be determined by:

$$\delta E_{TRC}\ [‰] = \frac{(MrTR \times \delta E_{TR}) + (MrC \times \delta E_C)}{MrTR + MrC} \qquad \text{(Equ. A.1)}$$

where

δE_{TRC}	is the $\delta^{13}C$ or $\delta^{18}O$ value of the contaminated wood sample,
$MrTR, MrC$	are the respective relative mass fractions of wood or contaminant,
δE_{TR}	is the original $\delta^{13}C$ or $\delta^{18}O$ value of the wood sample,
δE_C	is the $\delta^{13}C$ (graphite) or $\delta^{18}O$ (gypsum) of the contaminants.

To calculate the mass fraction of chalk in the wood samples the used chalk was weighted several times after highlighting 15 cm of the wood core surfaces. The repeated laboratory experiments gave a maximum contribution of chalk of 0.6% per tree ring. To simplify calculations, the mass fraction of graphite and chalk in the wood samples is estimated to be 1% (*MrC*), although the contribution is probably much lower. Thus, the relative mass fraction of wood is assumed to be 99% (*MrTR*).

Results and Discussion

TABLE A.**1** shows the results of the contamination tests. Calculations reveal that the graphite from pencil strokes ($\delta^{13}C_{Graphite}$=-26.25‰) has no significant influence (0.01‰) on the original carbon isotope ratio of the Teak wood ($\delta^{13}C_{TR}$=-25.22‰). The impact value is well below the measurement accuracy of the IRMS, which is ±0.1‰. The mean $\delta^{18}O$ value of chalk ($\delta^{18}O_{Gypsum}$=7.0‰) is far lower than typical $\delta^{18}O$ values of wood and thereby suggests a greater impact. However, the influence of chalk on the original oxygen isotope ratio of Teak ($\delta^{18}O_{TR}$ = 21.41‰) is -0.14‰ which is also within the analytical error of the oxygen isotope measurements (±0.25‰). In the worst case a possible analytical error of +0.25‰ to -0.39‰ could occur.

TABLE A.1 | Results from the contamination test of graphite and gypsum on tree-ring stable isotope values ($\delta^{13}C_{TR}$/ $\delta^{18}O_{TR}$).

	$\delta^{13}C_{TR}$	$\delta^{18}O_{TR}$	$\delta^{13}C_{Graphite}$	$\delta^{18}O_{Gypsum}$
mean (δE_{TR}/ δE_C) [‰]	-25.22	21.17	-26.25	7.0
δE_{TRC}[‰]	-25.23	21.27		
Impact value (δE_{TRC}- δE_{TR}) [‰]	-0.01	-0.14		

It should be noted that this error value represents the maximum effect of a contamination without any pre-treatment, i.e. extraction of impurities, which has been done here. It can be assumed that graphite and chalk residues have no significant influence on the original isotope ratios of the wood samples used in this study. Therefore, the use of carbonaceous or oxygenic tools (e.g. pencil and chalk) can be recommended for dendro-isotopic studies. In particular, when working with new or difficult tree species, the tools help to improve the dating and dissection of samples.

Acknowledgements

This project was funded by the CADY (BMBF, 03G0813H) and the HIMPAC (DFG, HE 3089/4-1) project. Furthermore, we thank Carmen Bürger for support in the laboratory.

Appendix B

Technical note:

A novel approach for the preparation of high-resolution stable isotope records from tropical tree rings

This chapter was published in:
TRACE - Tree Rings in Archaeology, Climatology and Ecology, Vol. 11, Proceedings of the DENDROSYMPOSIUM 2012, 71-76.
Authored by Karina Schollaen, Ingo Heinrich and Gerhard Helle

GFZ - German Research Centre for Geosciences, Section 5.2 Climate Dynamics and Landscape Evolution, Telegrafenberg, 14473 Potsdam, Germany

Introduction

Stable isotopes (carbon, oxygen and hydrogen) from tree-rings are widely used in climate and environmental studies (Dorado Liñán et al., 2012; Hennig et al., 2011; Leavitt et al., 2007; McCarroll and Loader, 2004; Saurer et al., 2008; Schleser et al., 1999b; Schollaen et al., 2013). Physiological processes affecting isotope fractionation such as stomatal conductance and photosynthetic rate react sensitively to climatic and environmental factors during the year. To extract valuable seasonal climatic and environmental information high-resolution stable isotope analyses of tree rings are needed. To date, the common method to prepare intra-annual isotope samples is to divide tree rings in tangential sections using a fixed-blade sledge microtome (e.g. Helle and Schleser, 2004a; Loader et al., 1995; Verheyden et al., 2005), a scalpel (e.g. Roden et al., 2009) or a twist drill (Fichtler et al., 2010). Thereby, the rings were subdivided into segments of equal widths along a radial direction and thickness of tangential sections varies from 20 µm to 180 µm. Accurate sample adjustment, as well as correct identification of tree-ring borders was provided by visual inspection using a binocular or microscope. Wood samples were ground to a fine powder and either cellulose was extracted or bulk wood samples were used, as recent studies on isotopic differences of bulk wood and cellulose extraction report little or no differences in the variability of the isotope signal (Borella et al., 1998; Loader et al., 2003; Taylor et al., 2008; Van de Water, 2002; Verheyden et al., 2005). Important for this

method is the selection of parallel rings with almost straight tree ring borders. As the curvature of growth rings varies under natural conditions, often only a limited number of consecutive rings per sample is suitable for high-resolution intra-annual isotope measurements. Another method for high-resolution stable isotope sampling is the use of a UV-laser ablation. Wood sample material from a tree core is extracted with an UV-laser leaving 40 µm-wide holes (Schulze et al., 2004). Ablated wood dust is then combusted to CO_2 at 700°C, separated from other gases and injected into an isotope ratio mass spectrometer.

Here, we tested a new UV-laser microdissection system from LEICA (www.leica-microsystems.com). Laser microdissection (LMD) is a specific form of laser-assisted microdissection that uses an UV cutting laser to isolate tissues of interest from thin sections of biological samples, which are collected by gravity below the sample. LMD is being applied widely in biomedical research and also in animal and plant research (e.g. Abbott et al., 2010; Nelson et al., 2006). We present the use of an UV-Laser Microdissection Microscope (LMD) to prepare reliable high-precisely intra-annual wood samples. The design and the handling of this UV-Laser Microdissection Microscope for dendrochronological research is described. Advantages and constraints are discussed on the basis of high resolution stable isotope analyses on woody plant material of teak (*Tectona grandis*) samples from Indonesia.

Samples and Methods

Sample preparation

The wood material selected is from living tropical teak trees (*Tectona grandis*) at Java (Indonesia) collected with increment cores of 5mm diameter. Firstly, the cores were cut in pieces of 5 cm length corresponding with the size of the object holders of the UV-Laser Microdissection Microscope. Secondly, transverse or cross-sections of approximately 500 µm thickness from sampled cores were cut with a core microtome (Gärtner and Nievergelt, 2010). To prepare the wood surface for an effective cutting process the sample lies some hours in a glycerin solution to make the surface soft. At last, the cross-sections were fixed on special object holders (FIGURE B.1), designed at the GFZ (German Research Centre for Geosciences) and treated under the LMD.

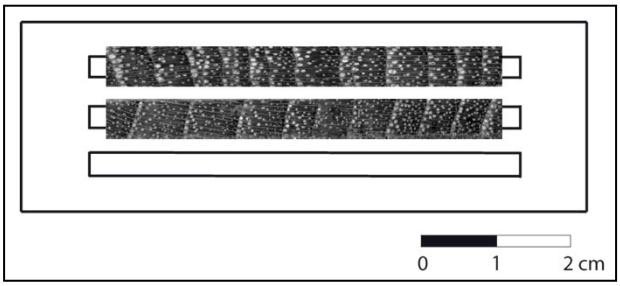

FIGURE B.1 | Object holder with wood samples. Tree-ring cross-sections are fixed between 2 metal frame slides, wherein the open area can be adapted to the height of the cross-sections.

UV-Laser Microdissection Microscope

The UV-Laser Microdissection Microscope from LEICA (LMD 7000) enables the analyses of cells or tissues and is frequently used in biomedical research. Biological samples are viewed under an upright microscope, dissected via an UV-laser coming from above and collected into tubes by gravity (FIGURE B.2).

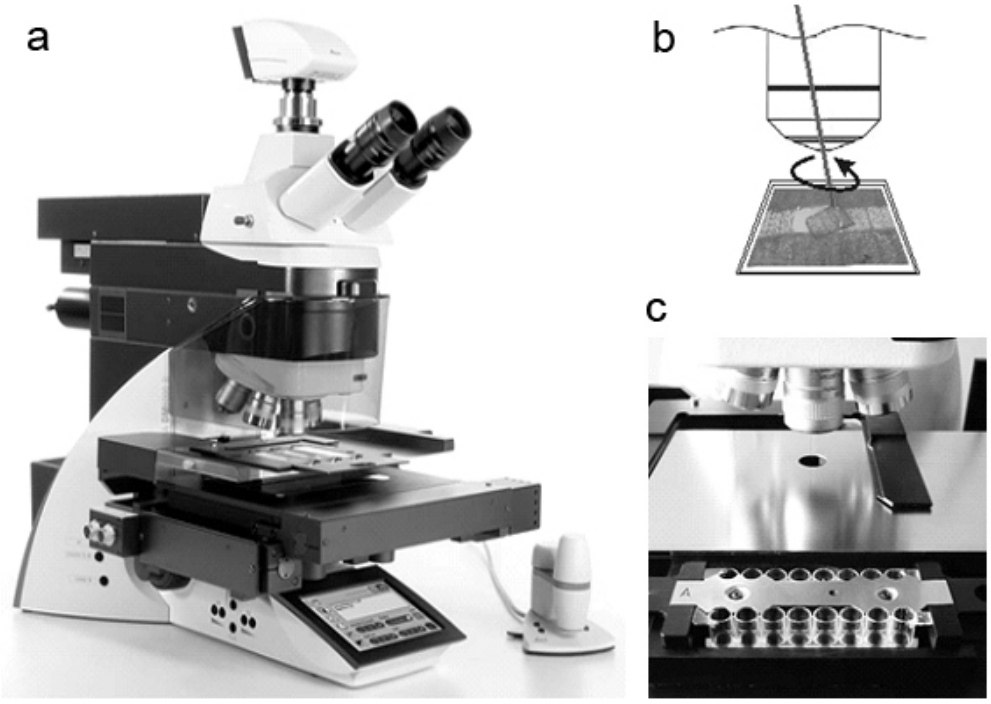

FIGURE B.2 | Leica LMD 7000, Research microscope with an UV-Microdissection Laser (A). Marked wood areas are cut by a moving laser (B) and fell down by gravity into tin or silver capsules standing in a collection device (C).

This UV-laser is able to cut fast and easy dissections of tree-rings or/and parts thereof with contact- and contamination-free specimen collection. Cutting lines can be drawn accurate by mouse or with a pen-screen and dissectioning of areas of any size or shape is possible. This allows to exclude irrelevant areas as resin ducts or rays. Furthermore, it is possible to

cut serial section or even to pool sample material, e.g. if the mass of the cut area is not sufficient for stable isotope measurements. The laser moves via optics and the cross-section sample stays fixed. The dissected wood samples can be collected directly in thin or silver capsules (for $\delta^{13}C$ or $\delta^{18}O$ measurements) and are ready for the mass spectrometry, if the mass of cutting areas is calculated in advance. The whole drawing and cutting process can be automatically documented (e.g. images, videos, database) for quality control.

Laser microdissection to capture high-resolution intra-annual tree-ring samples from Tectona grandis

The cross-sections of approximately 500 µm from teak cores are fixed in object holders and visualized under the microscope (magnification 5x, 10x). Several annual tree-rings were graphically subdivided into segments, with the number of segments per year varying depending on the tree-ring width and sample mass for following stable isotope measurements (range from 10 to 40 segments per year). The scheme of the intra-annual sampling process is illustrated in FIGURE B.3. Every drawn segment is dissected with the UV-laser and collected by gravity in single silver capsules standing in the collection holder ("8-well holder", Leica). The laser dissection process from wood segment selection to the cutting process was documented with an image-database (IM500).
Finally, the dissected and collected wood segments were given in the Isotope Ratio Mass Spectrometer (IRMS) for $\delta^{18}O$ measurements. The weight of dissected samples varies from 80 µg to 220 µg. The reduction in sample size down to 80mg can be reliably measured in our laboratory.

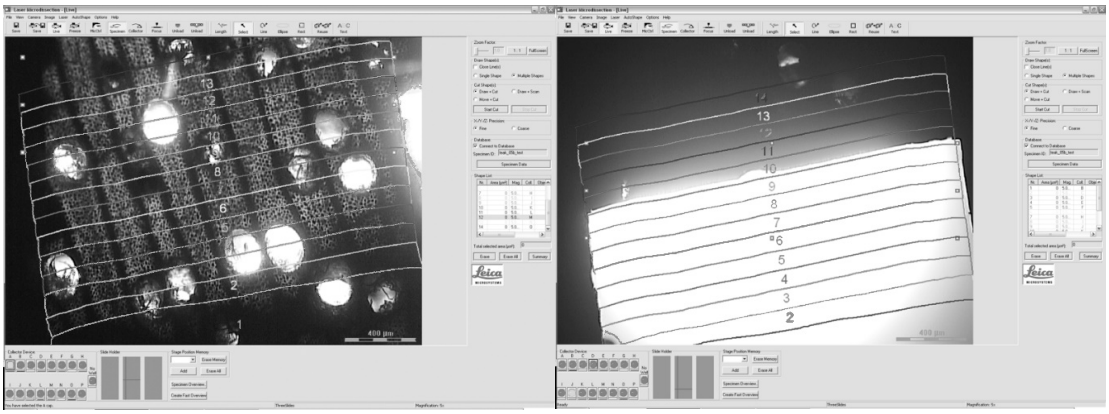

FIGURE B.3 | Left part: Selected segments (numbered 1,2,3, etc.) within one teak tree-ring for cutting process with an UV-Laser Microdissection Microscope (LMD 7000, Leica). Right part: Cutting process with the first 10 parts already cut and fallen down in separate collector devices.

Results and Discussion

High-resolution intra-annual $\delta^{18}O$ variations

The $\delta^{18}O$ profile shows a clear annual cyclicity (FIGURE B.4). Wood formation starts with a parenchyma band showing $\delta^{18}O$ values that are similar to the $\delta^{18}O$ values at the end of the previous ring. Afterwards the $\delta^{18}O$ values are rising up to a seasonal maximum appearing early in the growing season. This $\delta^{18}O$ maximum is followed by a decline to a seasonal minimum typically in the 2nd third of each tree ring before $\delta^{18}O$ is marginally rising again in the last third of the growing season. The annual $\delta^{18}O$ pattern follows the annual cycle in rainfall amount and its corresponding isotope signature at this site (Schollaen et al., 2013). High tree-ring $\delta^{18}O$ values during the start of the growing season represent the $\delta^{18}O$ signature in precipitation of the prior dry season. Low tree-ring $\delta^{18}O$ values reveal the $\delta^{18}O$ signature in precipitation of the main rainy season. To our knowledge, this is the first time that intra-annual $\delta^{18}O$ values in tropical trees can reflect the rainfall pattern over an entire year with distinct rainy and dry season signals.

As AD 1987 shows, less then 10 data points per tree ring are mostly not sufficient to produce reliable intra-annual variations. Minimum 10 data points per tree ring are recommended to illustrate high-resolution intra-annual stable isotope records.

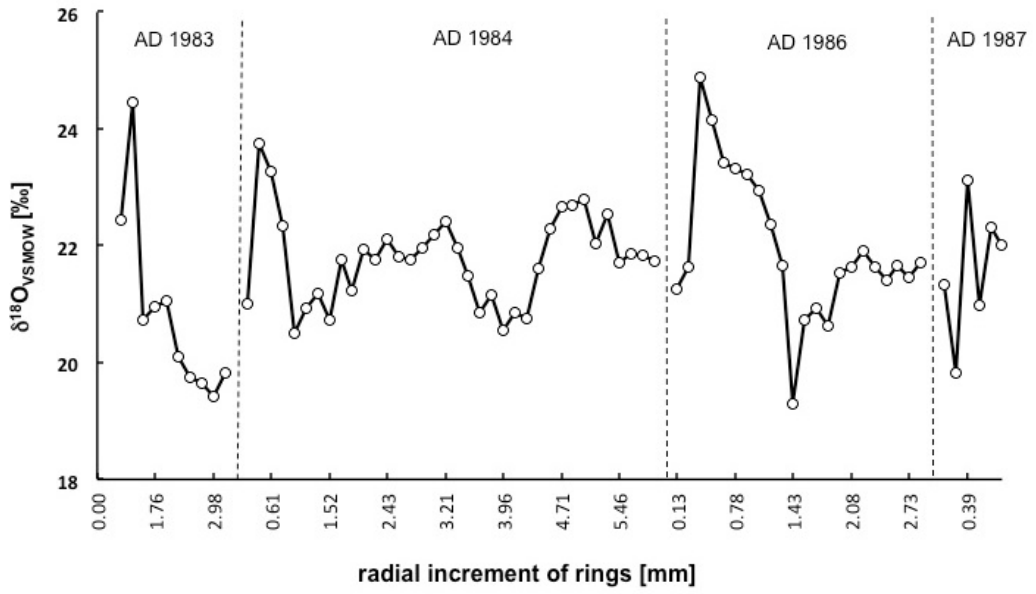

FIGURE B.4 | Intra-annual $\delta^{18}O$ variations from tree core 15b collected at Java, Indonesia, plotted vs. radial increment of the particular tree-ring. The data points represent the number of segments dissected per tree ring. This isotopic cycle is hypothesized to reflect the annual cycle in rainfall amount and humidity at this location (Schollaen et al., 2013).

Evaluation of the laser microdissection system from Leica (LMD 7000)

The automatic high precision laser dissection tool is a fast and reliable method for preparing high-resolution wood samples. The LMD can be used for inter-and intra-annual carbon and oxygen stable isotopes investigations on tree-rings. Our current measurement scheme contains 3 steps:
1. Preparation of thin cross-sections (max. 1000 µm thickness),
2. UV-laser microdissection of inter-or intra-annual wood sections and
3. Stable carbon and oxygen isotope analysis via Isotope Ratio Mass Spectrometry (IRMS).

There are several advantages using the LMD: Relevant cells/tissues can be selected on screen by pen, where else non-relevant tissues (e.g. resin ducts) can be removed. Any size and area can be dissected by the UV-laser and the complete selected sample is recovered. In addition, samples can be pooled and if desired cellulose extraction is possible after the cutting process. The use of thin cross-sections leaves the core intact and provides the opportunity for other dendrochronological investigations. Furthermore, there is a detailed documentation of dissecting and the cutting process. The laser dissection method avoids several disadvantages of the laser ablation method where spot size is limited, the loss of particles is >60 µm (dust filter) and no online monitoring of the laser ablation process is possible (Schulze et al., 2004).
Limitation of the LMD system is a non-automatic z-focus. When the selected shape does not fall down after the cutting process, a new cutting process must be started manually. The LEICA system uses high-precision optics to steer the laser beam using prisms along the desired cut lines on the tissue. This involves the limitation that the laser can only cut drawn lines/areas marked on the visible screen. If larger areas should be dissected a new shape must be drawn and a new cutting process must be started. However, pooling of selected specimen solve this limitation.

Conclusion and Applications

The automatic UV-laser dissection system (LMD7000, LEICA Microsystems) allows the user to cut samples of wood at unprecedented precision. Here, we tested the LMD tool as a fast and reliable method for preparing high-resolution intra-annual wood samples from tropical trees for standard stable isotope measurements. The new technique facilitates inter-and intra-annual tree-ring analysis and open various possibilities for wood anatomical and plant physiological studies. For instance, detailed assessment of carbon and oxygen isotope variability in wooden parts such as resin ducts, rays, fibres vessels or parenchyma cells are possible. Plant structure in relation to plant functioning by combining wood

anatomy and stable isotope analysis can be evaluated. Furthermore, the UV-laser microdissection system facilitates the establishment of long and continuous high-resolution isotope chronologies for high quality climate reconstructions. Multidisciplinary analyses (e.g. wood density, wood chemistry analyses) on the same wood sample are now possible with a complete recovery of the sample due to the use of thin cross-sections.

Appendix C

Research paper:

Toward multi-parameter records (ring width, $\delta^{13}C$, $\delta^{18}O$) from tropical tree-rings - A case study on *Tectona grandis* from Java, Indonesia

This chapter was published in:
TRACE - Tree Rings in Archaeology, Climatology and Ecology, Vol. 9, Proceedings of the DENDROSYMPOSIUM 2010, 158-165.
Authored by Karina Schollaen[1], Gerhard Helle[1], Ingo Heinrich[1], Burkhard Neuwirth[2], Oka Karyanto[3], Matthias Winiger[2]

[1]*GFZ - German Research Centre for Geosciences, Section 5.2 Climate Dynamics and Landscape Evolution, Telegrafenberg, 14473 Potsdam, Germany*
[2]*Department of Geography, University of Bonn, Meckenheimer Allee 166, D - 53115 Bonn, Germany*
[3]*Faculty of Forestry, Gadjah Mada University, Yogyakarta, Indonesia*

Introduction

Climate in Indonesia is mainly dominated by the equatorial monsoon system and tends to be linked to ENSO warm events which result in extensive droughts over the Indonesian archipelago (Hackert and Hastenrath, 1986). Hence, dendroclimatological studies from this region carry a great potential to improve land-based rainfall proxy records. The potential of tropical tree species as recorders of climate variability has not been fully exploited due to the frequent lack of visible, annual growth rings. However, as one of a few tropical tree species Teak (*Tectona grandis*) shows distinct annual growths boundaries. In earlier studies ring-width chronologies from Indonesian teak have been established and used for climatic reconstructions (e.g. Berlage, 1931; D'Arrigo et al., 1994; D'Arrigo et al., 2006). Multi-parameter studies, comprising wood anatomy or tree-ring stable isotopes, are still scarce in the tropics and the influence of climate and other environmental factors on tree-ring stable isotope ratios of Indonesian teak has not been studied in detail, yet. Here we present the first stable isotope ($\delta^{13}C$ and $\delta^{18}O$) records back to AD 1900 developed from Indonesian teak. These parameters as well as tree-ring width chronologies from the same

material were compared with climate data in order to test their potential for climate reconstructions.

Materials and Methods

Study site and climate conditions

The samples were collected in a lowland rain forest at an elevation of around 380 m a.s.l.. The study site, named Donoloyo, is located 90 km east of the city of Yogyakarta in the eastern part of Central Java, Indonesia (07°52'S, 111°11'E), as shown in FIGURE C.1.

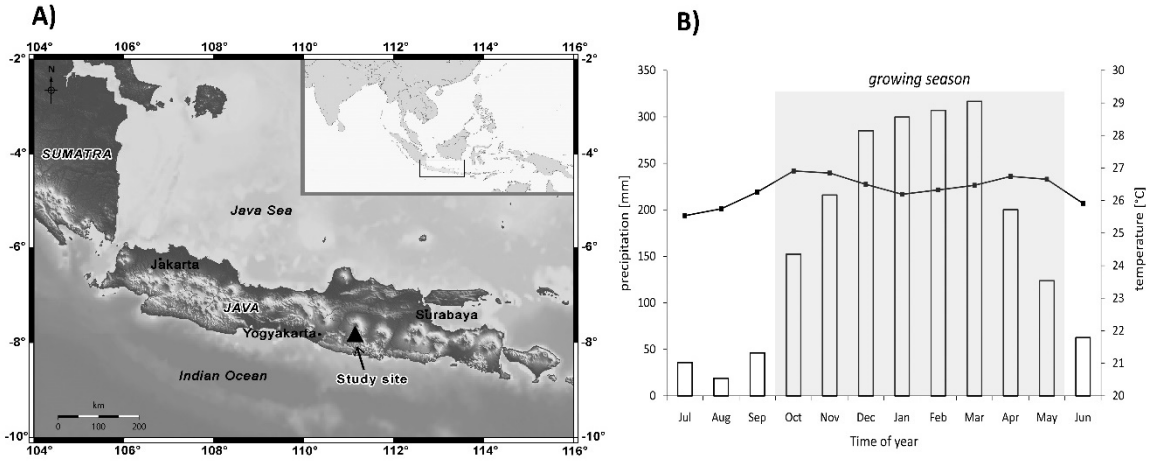

FIGURE C.1 | (A) Map showing the location of the study site (Donoloyo) in a lowland rain forest (380 m a.s.l.) in the eastern part of Central Java (07°52'S, 111°11'E). (B) Mean monthly precipitation (bars) and temperature (line) at the study site derived from gridded climate data (CRU TS 3.0, 1901-2006). The growing season is highlighted in grey.

The study site, among several others, was part of earlier investigations on ring width by D`Arrigo and co-workers. It revealed significant but comparatively low correlation between SST and growth (e.g. D'Arrigo et al., 2006). We re-sampled the site in November 2008 and initiated a stable isotope study in order to test whether or not the additional parameters provide better or different relationships to climate data than ring width have revealed in previous studies (Berlage, 1931; D'Arrigo et al., 1994; D'Arrigo et al., 2006; D'Arrigo et al., 2008).

In this study, gridded (0.5° x 0.5°) climate data, provided by the Climatic Research Unit of East Anglia University, Norwich, UK covering the time period 1901-2005 (CRU TS 3.0, Mitchell and Jones, 2005), were used for correlation analyses. The long-term mean annual values for precipitation and temperature are 2062 mm and 26.3°C, respectively. Precipitation is assumed to be the limiting factor for tree growth in the study area, because of a distinct seasonality, as well as well drained soil. Central and Eastern Java are

influenced by the equatorial monsoon climate which is characterized by a rainy season (north-west monsoon), persisting from November to April and a dry season (south-east monsoon) from May to October (FIGURE C.1B). The vegetation period (growing season) for *Tectona grandis* in Central and Eastern Java generally lasts approximately from the beginning of October to the end of May. Leaf flushing starts with the onset of the monsoon rains and flowering occurs toward the end of the rainy season. Approximately from June/July to September, that is, during the dry season, the species is leafless and consequentially in a state of cambial dormancy (Coster, 1927, 1928).

Sample material

For this study two cores each from 16 dominant *Tectona grandis* trees were collected. Ring widths were measured subsequently and cross-dated using the programmes TSAPWin (Rinn, 2005) and COFECHA (Holmes, 1983). The final tree-ring width chronology (TRW) is based on cores from 11 trees, 5 individuals were not included due to cross-dating problems. For dating purposes, we followed Schulman (1956) convention for the southern hemisphere, which assigns to each tree-ring the starting date of radial growth. All trees of our site chronology were, in average, older than 240 years, however, only the 19th and 20th centuries were investigated in this calibration study. This was done for allowing a direct comparison of raw values of ring-width and stable isotope records over a period in which any age-related growth trends can be neglected as being minor of higher order.

For the isotope analyses, five cores of different trees were chosen according to the following criteria: i) correct dating and high synchronicity of ring-width sequences as indicated by statistical parameters such as Gleichläufigkeit (GLK), Cross-Dating-Index and t-value, ii) good wood quality and iii) as few as possible problematic zones (such as false or narrow rings). For the period of AD 1900-2007 the entire annual rings from all cores were separated with a scalpel and finely ground to assure homogeneity. Resin extracted wood material was used instead of cellulose due to some very narrow rings which would have not provided sufficient amounts of cellulose for the conventional online IRMS determination of $\delta^{13}C$ and $\delta^{18}O$. However, recent research has shown that the cellulose extraction is not as crucial as had been suggested previously (Borella et al., 1998; McCarroll and Loader, 2004; Taylor et al., 2008; Verheyden et al., 2005). Consequently, only extractives, such as wood resins and oils, but also glue, pencil and chalk remains were removed from the wood with boiling de-ionized water and ethanol in a new multiple sample isolation system for solids (Wieloch et al., 2011). The $^{13}C/^{12}C$ and $^{18}O/^{16}O$ ratios were measured by combustion and low-temperature pyrolysis (at 1080°C), respectively, using an elemental analyzer (Model NA 1500; Carlo Erba, Milan, Italy) coupled to an IRMS (Isotope Ratio Mass Spectrometer; Micromass, Ltd. Manchester, UK). The results are given in the conventional δ notation relative to the international standards VPDB and

VSMOW. Sample replication resulted in a precision of better than ±0.1‰ for $\delta^{13}C$ values and ±0.25‰ for $\delta^{18}O$ values. Carbon isotope records are displayed as discrimination Δ, which is the shift between the carbon isotope ratios of the air relative to the isotope ratios of the tree-rings. Similarly, to the conventional δ notation in ‰, the discrimination Δ in ‰ follows as: $\Delta\ [‰] = (\delta^{13}C_{atm} - \delta^{13}C_{TR})/(1 + \delta^{13}C_{TR} \times 10^{-3})$. Hence, the records of Δ are free from the well-known trend of declining $\delta^{13}C_{atm}$-values due to fossil fuel burning and deforestation since AD 1850 (e.g. Helle and Schleser, 2004b).
The resulting series were compared with the CRU 3.0 (precipitation, air temperature) and HadSST2 gridded data sets (sea surface temperature, SST) (Rayner et al., 2006). Data from meteorological stations were acquired, but not used in this study due to short lengths and a lot of missing values.
In order to investigate the climate-proxy relationships, precipitation, air temperature and SST covering the periods 1901-2005 and 1901-2007, respectively, were compared with tree-ring data (TRW, Δ, $\delta^{18}O$) by calculating Pearson's correlation coefficient.

Results

Site chronologies

The three chronologies of tree-ring width (TRW), ^{13}C discrimination (Δ) and oxygen isotope ratio ($\delta^{18}O$) are shown in FIGURE C.2.
The top graph of FIGURE C.2 shows the dated ring width series along with the mean chronology. The series from 11 trees agree reasonably well (mean inter-series correlation of 0.54, GLK=69%, cf. TABLE C.1), and the EPS of 83% (slightly below the commonly adopted value of 85%) indicates that the chronology is replicated sufficiently back to AD 1800. However, the variability of the raw dataset is not stable over time with obvious periods of high scatter (1860-1880/1900-1920/1940-1970). Furthermore, a trend toward greater variability is visible over the second half of the 20th century. Although human influence cannot be excluded, a strong direct impact is very unlikely since the site is a protected area, used for seed collection since many years.
In the middle plot of FIGURE C.2, the carbon isotope chronology, presented as ^{13}C discrimination (Δ), derived from five individuals and selected according to the criteria described above, is displayed. The mean inter-series correlation is rather low (r=0.41) as well as the EPS value (EPS=0.64) (cf. TABLE C.1). Even without the outlier tree r and EPS increase only slightly to r=0.44 and EPS=0.67. For comparison, the EPS value for ring width of those five trees is of the same order, namely 0.68. The mean year-to-year variability of Δ is rather low (< 1‰, with few exceptions) as compared to the differences among the trees in mean Δ (2-4‰) and to tree-ring $\delta^{18}O$. This indicates that ecological

long-term changes seem to have a much stronger impact on Δ than short-term variations. Apart from this, one tree shows much higher ^{13}C discrimination than the others (see dashed line in FIGURE C.2). According to the model concept of carbon isotope fractionation during photosynthesis of C3-plants (Farquhar et al., 1982) high ^{13}C discrimination stands for a high ratio of c_i over c_a (c_i = leaf internal CO_2 concentration; c_a = atmospheric CO_2 concentration) due to a high stomatal conductance and/or a low assimilation rate. Interestingly, the tree with the higher ^{13}C discrimination is characterized by rather slow growth in general. A fact, that points to a strong impact of the assimilation rates on Δ. The averages of Δ of all the trees are relatively close for the first half of the 20th century. However, since the end of the 1950s two trees display a distinct increase in Δ, whereas two other trees show no changes and one a slight decline in Δ. This suggests that the individual tree responses are changing in time, probably due to differences in genetics or micro site conditions (e.g., nutrient supply).

TABLE C.1 | Descriptive statistics for the tree-ring width (TRW), ^{13}C discrimination (Δ) and oxygen isotope ($\delta^{18}O$) chronologies. CL: length of chronology; SD: standard deviation; GLK: Gleichläufigkeit; NET: see Esper et al. (2001); Cor: Series intercorrelation; AC1: first order serial autocorrelation

	Time-span	CL	# of trees	mean	SD	GLK [%]	NET	corr	EPS	AC1
TRW	1800-2007	208	11	1.69	1.22	69	0.64	0.54	0.83	0.64
Δ	1900-2007	108	5	19.02	0.37	64	0.41	0.41	0.64	0.54
$\delta^{18}O$	1900-2007	108	5	21.65	0.66	74	0.28	0.53	0.85	0.22

The results for oxygen isotopes ($\delta^{18}O$) from the same five individuals are shown in the bottom plot of FIGURE C.2. In contrast to ^{13}C discrimination, the individual series are quite well correlated (r=0.53, GLK=74%, EPS=0.85, cf. TABLE C.1) and the variability is rather stable throughout the entire 20th century.

Climate response

The climate response plots present Pearson's correlations between the stable isotope records and the climate data, respectively (FIGURE C.3). Correlations between TRW and climate are not shown here because they do not differ from previous analyses (D'Arrigo et al., 1994; D'Arrigo et al., 2006; D'Arrigo et al., 2008).

The Δ chronology (FIGURE C.3, 2nd row) shows no highly significant correlation with any climate parameter. However, the response to monthly and seasonal mean temperatures is mainly positive in sign, whereas precipitation of previous year`s October and November has a negative influence on ^{13}C discrimination.

We grouped and arranged the data according to the growing period of the trees, that is, October of the current year (date of the tree ring) to September of the following year.

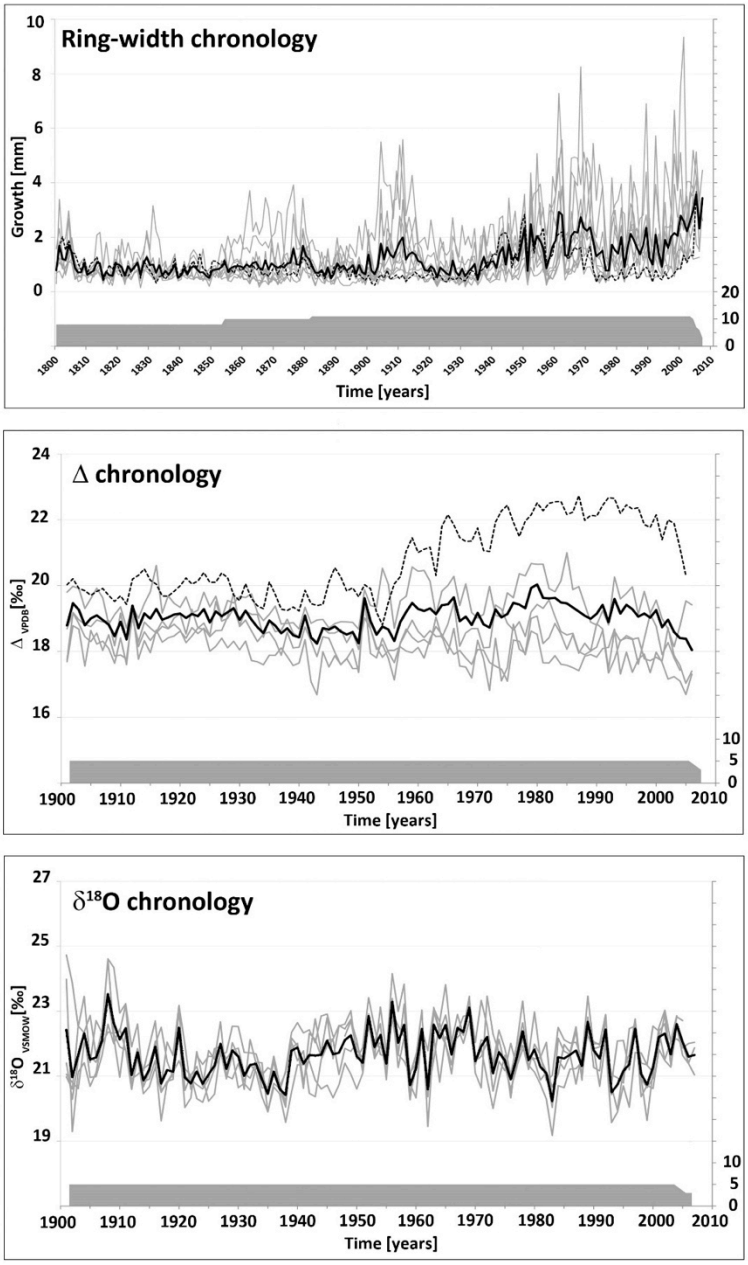

FIGURE C.2 | Raw tree-ring width and isotope chronologies and sample depth (thick black lines represent the mean chronology of each parameter). Note that the tree with rather high ^{13}C discrimination (Δ) is characterized by slow growth (dashed graphs in top and mid panel).

A climate response analysis of $\delta^{18}O$ (FIGURE C.3, 3th row), generally shows significant positive correlations with precipitation of the dry season and negative relationships with the wet season. Pre-season August, the driest month of the year directly before growth begins, displays the highest significance ($r=0.30$, for $p<0.01$). As for the growing period, precipitation in January has the strongest negative effect on tree-ring $\delta^{18}O$ at our site. The

relationships between $\delta^{18}O$ and temperature as well as SST show notable significance in some periods. The air temperature has some weak negative relationship with tree-ring $\delta^{18}O$, whereas SST shows no clear pattern of tree response.

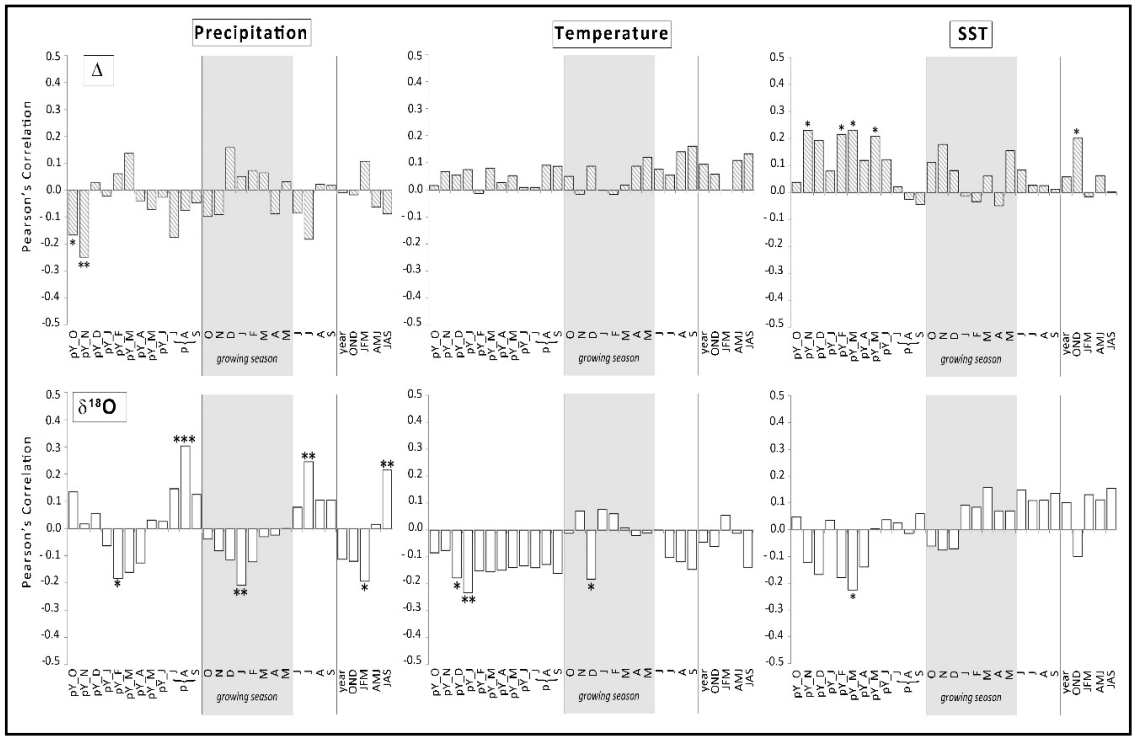

FIGURE C.3 | Correlations between Δ- and $\delta^{18}O$- records and climate data for the period 1901-2005. The diagrams for each climate parameter are separated into three parts by vertical lines. The left part displays the months (previous year October to current year September) prior to the actual growing period (grey shaded area), the middle parts shows the months of the actual growing period (October to September) and the right part depict seasonal means. Stars denote the significance levels: * 90% / ** 95% / *** 99%.

Discussion and Conclusions

We developed a 208-year long tree-ring width chronology (AD 1800-2007) and 108-year long carbon and oxygen isotope chronologies (AD 1900-2007) of *Tectona grandis* from a site of eastern Central Java.

Climate correlation tests show that tree growth is influenced by seasonal precipitation amounts and that it has a strong positive response to SST data which is a moisture indicator, similar to the results of previous studies from D'Arrigo et al. (1994); D'Arrigo et al. (2006).

The correlations between the carbon isotope record (Δ) and any of the three climate parameters were not highly significant. This may be due to the poor representativeness (low EPS and GLK) of the selected five sample trees. It may also be due to a very minor

influence of climatic quantities on the processes underlying carbon isotope variability, i.e., ^{13}C discrimination and carbon assimilation. More samples need to be analyzed and other environmental factors than climatic factors need to be studied to understand the carbon isotope variability at the Indonesian site.

Drought influenced sites very often showed good correlation between tree-ring $\delta^{13}C$ and precipitation in semi-arid or arid regions. However, during the vegetation period humid conditions persist at our site, and some kind of drought stress at the beginning or the end of the growing period may not have a significant impact.

Indeed, the $\delta^{18}O$ record shows notable significant correlation coefficients with precipitation of pre-season August (driest month) and current year January (wettest month). Interestingly, the correlations found are opposite in sign. Pre-season August has a positive relationship with tree-ring $\delta^{18}O$, while the correlation with January is negative. This is very likely because the rainfall of pre-season August reflects the highest $\delta^{18}O$ while precipitation in January is characterized by the lowest $\delta^{18}O$ signature of the year (FIGURE C.4). Hence, tree-ring $\delta^{18}O$ probably reflects the relative portion of August to January precipitation with subsequently changing isotope signatures derived from the so-called "amount effect" and/or changing origin of air moisture (e.g. Araguás-Araguás et al., 2000).

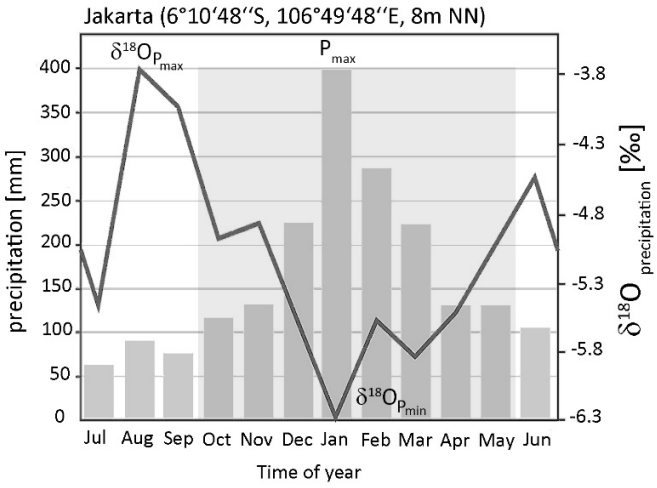

FIGURE C.4 | Average monthly precipitation sums (grey) and $\delta^{18}O_{Precip}$ in precipitation (black) for Jakarta/Indonesia. The grey shadow marks the growing season. (GNIP: http://www-naweb.iaea.org).

An influence of evapotranspiration on ^{18}O-enrichment of leaf water could not be detected, probably because the effects on tree-ring $\delta^{18}O$ act in the same direction as changes in $\delta^{18}O$ of precipitation under dry and wet conditions. Dry conditions result in high ^{18}O-enrichment in precipitation as well as in leaf water and wet conditions evoke the same effects in opposite direction. An influence of ground-water due to water uptake from deeper soil during the vegetation period seems to be unlikely since the soil at the site is well-drained and teak has a shallow root system.

In conclusion, the results of this calibration study point out that the isotope ratios of carbon and oxygen show weaker climate signals than tree-ring width, at least when only 5 trees are considered and the chronologies show relatively weak values of EPS and GLK etc. and thus more trees need to be analyzed. Furthermore, future efforts will focus on highly resolved intra-annual $\delta^{18}O$ studies which may provide more detailed insights into the influence of seasonally changing precipitation amounts and $\delta^{18}O_{Precip}$ on tree growth and tree-ring $\delta^{18}O$ records. This may improve land-based rainfall reconstructions based in multiple tree-ring parameters.

Acknowledgments

Many thanks to Rosanne D'Arrigo for providing some of the samples for this study and to Tomy Listyanto and Navis Rofii for their assistance in the field work. We are grateful to Carmen Bürger for support in the laboratory and Isabel Dorado, Thomas Wieloch and Katja Fregien for fruitful discussions. This study is funded by German Science Foundation (DFG) (HE3084-2).

Appendix D

Tree-ring data:

Annual tree-ring (ring width, $\delta^{13}C$, $\delta^{18}O$) chronologies from *Tectona grandis* of Central Java, Indonesia (07°52'S, 111°11'E)

Year	TRW	$\delta^{13}C_{TR}$			$\delta^{18}O_{TR}$
[AD]	[mm]	cor1[‰]	cor2[‰]	cor3[‰]	[‰]
2007	1.28	-23.63	-22.91	-21.72	21.43
2006	0.81	-24.31	-23.60	-22.44	21.61
2005	1.11	-24.61	-23.91	-22.77	21.92
2004	1.14	-24.51	-23.83	-22.72	22.34
2003	1.13	-24.82	-24.15	-23.07	21.42
2002	1.06	-25.20	-24.55	-23.49	21.81
2001	1.06	-24.83	-24.20	-23.12	21.78
2000	1.09	-25.26	-24.64	-23.59	20.93
1999	1.00	-25.19	-24.58	-23.54	20.42
1998	0.90	-25.25	-24.66	-23.64	20.68
1997	1.10	-25.30	-24.73	-23.75	21.58
1996	0.99	-25.41	-24.85	-23.88	20.83
1995	1.05	-25.58	-25.02	-24.08	20.36
1994	0.83	-25.34	-24.80	-23.88	20.39
1993	0.94	-25.67	-25.14	-24.24	19.75
1992	1.07	-24.95	-24.43	-23.54	21.65
1991	0.77	-25.26	-24.74	-23.86	21.18
1990	0.81	-25.12	-24.61	-23.75	21.15
1989	1.16	-25.23	-24.73	-23.88	22.15
1988	0.99	-25.12	-24.63	-23.80	21.02
1987	0.86	-25.34	-24.87	-24.07	20.99
1986	0.98	-25.45	-24.99	-24.22	21.01
1985	1.04	-25.50	-25.05	-24.29	21.13
1984	1.08	-25.59	-25.16	-24.42	21.44
1983	1.09	-25.74	-25.32	-24.60	19.90
1982	0.71	-25.67	-25.26	-24.56	20.58
1981	1.15	-25.64	-25.24	-24.55	20.86
1980	0.98	-25.99	-25.60	-24.92	21.35
1979	1.03	-25.81	-25.42	-24.78	21.30
1978	1.10	-25.50	-25.12	-24.49	22.18
1977	0.83	-25.47	-25.11	-24.50	21.22
1976	0.72	-25.59	-25.24	-24.65	20.67
1975	0.93	-25.45	-25.11	-24.53	20.94

Year	TRW	$\delta^{13}C_{TR}$			$\delta^{18}O_{TR}$
[AD]	[mm]	cor1[‰]	cor2[‰]	cor3[‰]	[‰]
1974	0.84	-25.35	-25.01	-24.45	21.16
1973	0.80	-25.44	-25.11	-24.56	20.40
1972	0.96	-25.45	-25.13	-24.60	21.40
1971	1.19	-25.23	-24.93	-24.41	20.98
1970	1.08	-25.48	-25.18	-24.67	20.66
1969	1.05	-25.14	-24.85	-24.36	22.25
1968	1.13	-25.36	-25.08	-24.61	21.98
1967	1.14	-25.24	-24.97	-24.51	21.81
1966	1.17	-25.74	-25.48	-25.02	21.11
1965	1.14	-25.66	-25.41	-24.97	21.63
1964	0.87	-25.62	-25.37	-24.94	21.72
1963	0.83	-25.37	-25.12	-24.70	22.38
1962	1.33	-25.38	-25.13	-24.72	20.24
1961	1.29	-25.59	-25.35	-24.94	21.83
1960	1.12	-25.43	-25.20	-24.80	21.02
1959	0.96	-25.74	-25.51	-25.13	20.15
1958	0.91	-25.46	-25.23	-24.85	21.89
1957	0.69	-25.26	-25.03	-24.66	21.18
1956	0.97	-24.81	-24.60	-24.23	22.57
1955	0.99	-24.87	-24.65	-24.29	20.97
1954	1.15	-25.00	-24.79	-24.43	21.46
1953	1.04	-24.99	-24.79	-24.43	21.26
1952	1.30	-25.09	-24.88	-24.53	22.06
1951	0.69	-25.57	-25.37	-25.03	20.97
1950	1.25	-24.58	-24.39	-24.05	20.92
1949	1.14	-24.81	-24.61	-24.28	21.62
1948	0.89	-24.86	-24.67	-24.34	21.42
1947	0.98	-24.90	-24.71	-24.38	20.88
1946	0.92	-25.05	-24.86	-24.54	21.14
1945	1.17	-24.94	-24.76	-24.44	21.72
1944	0.87	-25.03	-24.84	-24.53	20.96
1943	1.19	-24.60	-24.42	-24.11	21.15
1942	1.13	-24.83	-24.65	-24.34	21.11
1941	0.90	-25.37	-25.19	-24.89	21.02
1940	0.97	-24.76	-24.58	-24.28	21.36
1939	1.01	-24.84	-24.67	-24.36	21.40
1938	0.95	-25.00	-24.83	-24.53	19.87
1937	1.19	-24.92	-24.75	-24.45	20.14
1936	1.09	-25.14	-24.97	-24.67	20.85
1935	0.73	-25.16	-24.99	-24.70	20.07
1934	1.09	-24.84	-24.68	-24.39	20.48
1933	0.94	-24.91	-24.74	-24.46	20.96
1932	0.94	-25.21	-25.05	-24.77	20.98
1931	0.83	-25.42	-25.26	-24.99	20.78
1930	0.92	-25.09	-24.93	-24.66	21.38
1929	0.80	-25.33	-25.18	-24.91	21.39
1928	0.85	-25.35	-25.20	-24.94	20.87

Year	TRW	$\delta^{13}C_{TR}$			$\delta^{18}O_{TR}$
[AD]	[mm]	cor1[‰]	cor2[‰]	cor3[‰]	[‰]
1927	1.13	-25.27	-25.11	-24.86	21.27
1926	0.82	-25.50	-25.35	-25.10	20.75
1925	0.90	-25.11	-24.96	-24.71	20.55
1924	0.94	-25.50	-25.36	-25.11	20.64
1923	1.05	-25.24	-25.10	-24.86	20.79
1922	0.80	-25.45	-25.31	-25.07	20.41
1921	0.98	-25.27	-25.13	-24.90	20.58
1920	0.98	-25.42	-25.29	-25.06	21.82
1919	0.87	-25.39	-25.26	-25.03	20.60
1918	0.84	-25.32	-25.19	-24.97	20.83
1917	1.01	-25.20	-25.08	-24.86	20.21
1916	1.01	-25.46	-25.34	-25.13	21.53
1915	1.14	-25.23	-25.11	-24.90	20.77
1914	1.08	-25.44	-25.32	-25.12	20.48
1913	1.11	-25.02	-24.90	-24.70	21.11
1912	0.85	-25.47	-25.36	-25.17	20.58
1911	1.17	-24.73	-24.62	-24.43	21.77
1910	1.08	-25.18	-25.07	-24.89	21.40
1909	1.09	-24.79	-24.69	-24.50	21.95
1908	0.95	-25.12	-25.01	-24.84	22.94
1907	0.98	-25.30	-25.20	-25.03	21.67
1906	1.20	-25.35	-25.25	-25.08	21.28
1905	1.07	-25.23	-25.13	-24.97	20.86
1904	1.29	-25.03	-24.94	-24.78	21.78
1903	0.95	-25.46	-25.37	-25.21	21.54
1902	0.84	-25.67	-25.58	-25.43	20.44
1901	0.85	-25.26	-25.17	-25.02	21.45
1900	1.35	-25.08	-24.99	-24.85	22.65

Chapter 8

References

Abbott, E., Hall, D., Hamberger, B., Bohlmann, J., 2010. Laser microdissection of conifer stem tissues: Isolation and analysis of high quality RNA, terpene synthase enzyme activity and terpenoid metabolites from resin ducts and cambial zone tissue of white spruce (*Picea glauca*). BMC Plant Biology 10, 106.

Abram, N.J., Gagan, M.K., Cole, J.E., Hantoro, W.S., Mudelsee, M., 2008. Recent intensification of tropical climate variability in the Indian Ocean. Nature Geosci 1, 849-853.

Aldrian, E., Dümenil Gates, L., Widodo, F.H., 2007. Seasonal variability of Indonesian rainfall in ECHAM4 simulations and in the reanalyses: The role of ENSO. Theoretical and Applied Climatology 87, 41-59.

Aldrian, E., Susanto, R.D., 2003. Identification of three dominant rainfall regions within Indonesia and their relationship to sea surface temperature. International Journal of Climatology 23, 1435-1452.

Allan, J.R., 2000. ENSO and Climatic Variability in the Past 150 Years, In: Diaz, H.F., Markgraf, V. (Eds.), El Niño and the Southern Oscillation: Multiscale Variability and Global and Regional Impacts. Cambridge University Press, pp. 3-56.

Anchukaitis, K.J., Evans, M.N., Wheelwright, N.T., Schrag, D.P., 2008. Stable isotope chronology and climate signal calibration in neotropical montane cloud forest trees. Journal of Geophysical Research 113, G03030.

Araguás-Araguás, L., Froehlich, K., Rozanski, K., 1998. Stable isotope composition of precipitation over southeast Asia. Journal of Geophysical Research-Atmospheres 103, 28721-28742.

Araguás-Araguás, L., Froehlich, K., Rozanski, K., 2000. Deuterium and oxygen-18 isotope composition of precipitation and atmospheric moisture. Hydrological Processes 14, 1341-1355.

Ashok, K., Behera, S.K., Rao, S.A., Weng, H., Yamagata, T., 2007. El Niño Modoki and its possible teleconnection. Journal of Geophysical Research: Oceans 112, C11007.

Ashok, K., Yamagata, T., 2009. Climate change: The El Niño with a difference. Nature 461, 481-484.

Baker, P.J., Palmer, J.G., D'Arrigo, R., 2008. The dendrochronology of Callitris intratropica in northern Australia: annual ring structure, chronology development and climate correlations. Australian Journal of Botany 56, 311-320.

Ballantyne, A.P., Baker, P.A., Chambers, J.Q., Villalba, R., Argollo, J., 2010. Regional Differences in South American Monsoon Precipitation Inferred from the Growth and Isotopic Composition of Tropical Trees. Earth Interactions 15, 1-35.

Barbour, M.M., 2007. Stable oxygen isotope composition of plant tissue: a review. Functional Plant Biology 34, 83-94.

Barbour, M.M., Andrews, T.J., Farquhar, G.D., 2001. Correlations between oxygen isotope ratios of wood constituents of *Quercus* and *Pinus* samples from around the world. Australian Journal of Plant Physiology 28, 335-348.

Barbour, M.M., Walcroft, A.S., Farquhar, G.D., 2002. Seasonal variation in $\delta^{13}C$ and $\delta^{18}O$ of cellulose from growth rings of *Pinus radiata*. Plant Cell and Environment 25, 1483-1499.

Battipaglia, G., De Micco, V., Brand, W.A., Linke, P., Aronne, G., Saurer, M., Cherubini, P., 2010. Variations of vessel diameter and $\delta^{13}C$ in false rings of *Arbutus unedo* L. reflect different environmental conditions. New Phytologist 188, 1099-1112.

Battipaglia, G., Jäggi, M., Saurer, M., Siegwolf, R.T.W., Cotrufo, M.F., 2008. Climatic sensitivity of δ18O in the wood and cellulose of tree rings: Results from a mixed stand of *Acer pseudoplatanus* L. and *Fagus sylvatica* L. Palaeogeography, Palaeoclimatology, Palaeoecology 261, 193-202.

Bayona-Bafaluy, M., Blits, B., Battersby, B.J., Shoubridge, E.A., Moraes, C.T., 2005. Rapid directional shift of mitochondrial DNA heteroplasmy in animal tissues by a mitochondrially targeted restriction endonuclease. Proceedings of the National Academy of Sciences of the United States of America 102, 14392-14397.

Berlage, H.P., 1931. On the relationship between thickness of tree rings of Djati (teak) trees and rainfall on Java. Tectona 24, 939-953.

Biondi, F., 2001. A 400-year tree-ring chronology from the tropical treeline of North America. AMBIO: A Journal of the Human Environment 30, 162-166.

Biondi, F., Hartsough, P., Estrada, I., 2005. Daily Weather and Tree Growth at the Tropical Treeline of North America. Arctic, Antarctic, and Alpine Research 37, 16-24.

Boer, R.A.R.S., 2005. Agriculture drought in Indonesia, In: Boken, V.K., Cracknell, A.P., Heathcote, R.L. (Eds.), Monitoring and predicting agriculture drought: A global study, New York, pp. 330-344.

Boettger, T., Haupt, M., Knoller, K., Weise, S.M., Waterhouse, J.S., Rinne, K.T., Loader, N.J., Sonninen, E., Jungner, H., Masson-Delmotte, V., Stievenard, M., Guillemin, M.-T., Pierre, M., Pazdur, A., Leuenberger, M., Filot, M., Saurer, M., Reynolds, C.E., Helle, G., Schleser, G.H., 2007. Wood Cellulose Preparation Methods and Mass Spectrometric Analyses of $\delta^{13}C$, $\delta^{18}O$, and Nonexchangeable $\delta^{2}H$ Values in Cellulose, Sugar, and Starch: An Interlaboratory Comparison. Analytical Chemistry 79, 4603-4612.

Borella, S., Leuenberger, M., Saurer, M., Siegwolf, R., 1998. Reducing uncertainties in $\delta^{13}C$ analysis of tree rings: Pooling, milling, and cellulose extraction. Journal of Geophysical Research-Atmospheres 103, 19519-19526.

Borgaonkar, H.P., Sikder, A.B., Ram, S., Pant, G.B., 2010. El Niño and related monsoon drought signals in 523-year-long ring width records of teak (*Tectona grandis* L.F.) trees from south India. Palaeogeography, Palaeoclimatology, Palaeoecology 285, 74-84.

Braak, C., 1921-29. The climate of the Netherlands Indies. Meded. En Verh. Koninklijk Magnetisch en Meteorologisch Oberservatorium te Batavia 8, 257.

Braganza, K., Gergis, J.L., Power, S.B., Risbey, J.S., Fowler, A.M., 2009. A multiproxy index of the El Niño–Southern Oscillation, A.D. 1525–1982. Journal of Geophysical Research: Atmospheres 114, D05106.

Bräuning, A., Volland-Voigt, F., Burchardt, I., Ganzhi, O., Nauss, T., Peters, T., 2009. Climatic control of radial growth of *Cedrela montana* in a humid mountain rainforest in southern Ecuador. Erdkunde, 337-345.

Brendel, O., Iannetta, P.P.M., Stewart, D., 2000. A rapid and simple method to isolate pure alpha-cellulose. Phytochemical Analysis 11, 7-11.

Brienen, R., Wanek, W., Hietz, P., 2011. Stable carbon isotopes in tree rings indicate improved water use efficiency and drought responses of a tropical dry forest tree species. Trees - Structure and Function 25, 103-113.

Brienen, R.J.W., Helle, G., Pons, T.L., Guyot, J.L., Gloor, M., 2012. Oxygen isotopes in tree rings are a good proxy for Amazon precipitation and El Niño-Southern Oscillation variability. Proceedings of the National Academy of Sciences 109, 16957-16962.

Brienen, R.W., Zuidema, P., 2005. Relating tree growth to rainfall in Bolivian rain forests: a test for six species using tree ring analysis. Oecologia 146, 1-12.

Briffa, K., Jones, B., 1990. Basic chronology statistics and assessment, In: Cook, A.C., Briffa, K., Kairiukstis, L.A. (Eds.), Methods of Dendrochronology - Applications in the Environmental Sciences. Kluwer Academic Publ., Dordrecht, pp. 137-152.

Buckley, B.M., Anchukaitis, K.J., Penny, D., Fletcher, R., Cook, E.R., Sano, M., Nam, L.C., Wichienkeeo, A., Minh, T.T., Hong, T.M., 2010. Climate as a contributing factor in the demise of Angkor, Cambodia. Proceedings of the National Academy of Sciences 107, 6748-6752.

Buckley, B.M., Barbetti, M., Watanasak, M., Darrigo, R., Boonchirdchoo, S., Sarutanon, S., 1995. Dendrochronological investigations in Thailand. IAWA Journal 16, 393-409.

Buckley, B.M., Palakit, K., Duangsathaporn, K., Sanguantham, P., Prasomsin, P., 2007. Decadal scale droughts over northwestern Thailand over the past 448 years: links to the tropical Pacific and Indian Ocean sectors. Climate Dynamics 29, 63–71.

Cernusak, L.A., Aranda, J., Marshall, J.D., Winter, K., 2007. Large variation in whole-plant water-use efficiency among tropical tree species. New Phytologist 173, 294-305.

Chang, C.P., Wang, Z., Ju, J., Li, T., 2004. On the Relationship between Western Maritime Continent Monsoon Rainfall and ENSO during Northern Winter. J. Clim. 17, 665-672.

Charles, C.D., Cobb, K., Moore, M.D., Fairbanks, R.G., 2003. Monsoon–tropical ocean interaction in a network of coral records spanning the 20th century. Marine Geology 201, 207-222.

Cobb, K.M., Westphal, N., Sayani, H.R., Watson, J.T., Di Lorenzo, E., Cheng, H., Edwards, R.L., Charles, C.D., 2013. Highly Variable El Niño–Southern Oscillation Throughout the Holocene. Science 339, 67-70.

Collins, M., An, S.-I., Cai, W., Ganachaud, A., Guilyardi, E., Jin, F.-F., Jochum, M., Lengaigne, M., Power, S., Timmermann, A., Vecchi, G., Wittenberg, A., 2010. The impact of global warming on the tropical Pacific Ocean and El Niño. Nature Geosci 3, 391-397.

Cook, E., Kairiukstis, L.A., 1990. Methods of Dendrochronology. Applications in the Environmental Sciences. Kluwer, Dordrecht.

Cook, E.R., D'Arrigo, R.D., Mann, M.E., 2002. A Well-Verified, Multiproxy Reconstruction of the Winter North Atlantic Oscillation Index since A.D. 1400*. J. Clim. 15, 1754-1764.

Cook, E.R., Krusic, P.J., Peters, K., Holmes, R., 2012. Program ARSTAN version 41 (http://www.ldeo.columbia.edu/tree-ring-laboratory/resources/software).

Cook, E.R., Palmer, J.G., Ahmed, M., Woodhouse, C.A., Fenwick, P., Zafar, M.U., Wahab, M., Khan, N., 2013. Five centuries of Upper Indus River flow from tree rings. Journal of Hydrology 486, 365-375.

Cook, E.R., Peters, K., 1981. The smoothing spline: a new approach to standardizing forest interior tree-ring width series for dendroclimatic studies. Tree-Ring Bulletin 41, 45-53.

Coster, C., 1927. Zur Anatomie und Physiologie der Zuwachszonen- und Jahresringbildung in den Tropen. Ann. Jard. Bot. Buitenzong 37, 49-160.

Coster, C., 1928. Zur Anatomie und Physiologie der Zuwachszonen- und Jahresringbildung in den Tropen. Ann. Jard. Bot. Buitenzong 38, 1-114.

Craig, H., 1957. Isotopic standards for carbon and oxygen and correction factors for mass-spectrometric analysis of carbon dioxide. Geochimica et Cosmochimica Acta 12, 133-149.

Cropper, J.P., 1979. Tree-ring skeleton plotting by computer. Tree-ring Bulletin 39, 47-59.

Cullen, L.E., Grierson, P.F., 2006. Is cellulose extraction necessary for developing stable carbon and oxygen isotopes chronologies from Callitris glaucophylla? Palaeogeography, Palaeoclimatology, Palaeoecology 236, 206-216.

Cullen, L.E., MacFarlane, C., 2005. Comparison of cellulose extraction methods for analysis of stable isotope ratios of carbon and oxygen in plant material. Tree Physiology 25, 563-569.

D'Arrigo, R., Cook, E.R., Wilson, R.J., Allan, R., Mann, M.E., 2005. On the variability of ENSO over the past six centuries. Geophys. Res. Lett. 32, L03711.

D'Arrigo, R., Jacoby, G.C., Krusic, P., 1994. Progress in dendroclimatic studies in Indonesia. Terrestrial, Atmospheric and Oceanic Sciences 5, 349-363.

D'Arrigo, R., Smerdon, J.E., 2008. Tropical climate influences on drought variability over Java, Indonesia. Geophysical Research Letters 35, L05707.

D'Arrigo, R., Wilson, R., Palmer, J., Krusic, P., Curtis, A., Sakulich, J., Bijaksana, S., Zulaikah, S., Ngkoimani, L.O., Tudhope, A., 2006. The reconstructed Indonesian warm pool sea surface temperatures from tree rings and corals: Linkages to Asian monsoon drought and El Niño–Southern Oscillation. Paleoceanography 21, PA3005.

D'Arrigo, R., Allan, R., Wilson, R., Palmer, J., Sakulich, J., Smerdon, J.E., Bijaksanae, S., Ngkoimani, L.O., 2008. Pacific and Indian Ocean climate signals in a tree-ring record of Java monsoon drought. International Journal of Climatology 28, 1889-1901.

Dansgaard, W., 1964. Stable isotopes in precipitation. Tellus 16, 437-468.

Dawson, T.E., Mambelli, S., Plamboeck, A.H., Templer, P.H., Tu, K.P., 2002. Stable isotopes in plant ecology. Annual Review of Ecology and Systematics 33, 507-559.

De Micco, V., Battipaglia, G., Brand, W., Linke, P., Saurer, M., Aronne, G., Cherubini, P., 2012. Discrete versus continuous analysis of anatomical and $\delta^{13}C$ variability in tree rings with intra-annual density fluctuations. Trees 26, 513-524.

DeBoer, H.J., 1951. Treering measurements and weather Fluctuations in Java from A.D. 1514. Proc.K.Ned.Akad.Wetensch. 54, 194-209.

Dodd, J.P., Patterson, W.P., Holmden, C., Brasseur, J.M., 2008. Robotic micromilling of tree-rings: A new tool for obtaining subseasonal environmental isotope records. Chemical Geology 252, 21-30.

Dorado Liñán, I., Gutiérrez, E., Andreu-Hayles, L., Heinrich, I., Helle, G., 2012. Potential to explain climate from tree rings in the south of the Iberian Peninsula. Climate Research 55.

Douglass, A.E., 1935. Dating Pueblo Bonito and Other Ruins of the Southwest, Nat. Geog. Soc. Pueblo Bonito Series, Washington, D.C.

Ehleringer, J., Hall, A.E., Farquhar, G., 1993. Stable Isotopes and Plant Carbon-Water Relations. Academic Press, London.

Eilmann, B., Buchmann, N., Siegwolf, R., Saurer, M., Cherubini, P., Rigling, A., 2010. Fast response of Scots pine to improved water availability reflected in tree-ring width and $\delta^{13}C$. Plant, Cell and Environment 33, 1351-1360.

Emile-Geay, J., Cobb, K.M., Mann, M.E., Wittenberg, A.T., 2013. Estimating Central Equatorial Pacific SST Variability over the Past Millennium. Part II: Reconstructions and Implications. J. Clim. 26, 2329-2352.

Esper, J., Neuwirth, B., Treydte, K., 2001. A new parameter to evaluate temporal signal strength of tree-ring chronologies. Dendrochronologia 19, 93-102.

Evans, M.N., 2007. Toward forward modeling for paleoclimatic proxy signal calibration: A case study with oxygen isotopic composition of tropical woods. Geochemistry Geophysics Geosystems 8, Q07008.

Evans, M.N., Cane, M.A., Schrag, D.P., Kaplan, A., Linsley, B.K., Villalba, R., Wellington, G.M., 2001. Support for tropically-driven pacific decadal variability based on paleoproxy evidence. Geophysical Research Letters 28, 3689-3692.

Evans, M.N., Kaplan, A., Cane, M.A., 2002. Pacific sea surface temperature field reconstruction from coral $d^{18}O$ data using reduced space objective analysis. Paleoceanography 17, 7-1-7-13.

Evans, M.N., Schrag, D.P., 2004. A stable isotope-based approach to tropical dendroclimatology. Geochimica et Cosmochimica Acta 68, 3295-3305.

Farquhar, G.D., O'Leary, M.H., Berry, J.A., 1982. On the Relationship between Carbon Isotope - Discrimination and the Intercellular - Carbon Dioxide Concentration in Leaves. Aust. J. Plant Physiol. 9, 121-137.

Fend, F., Raffeld, M., 2000. Laser capture microdissection in pathology. Journal of Clinical Pathology 53, 666-672.

Feng, X., Epstein, S., 1995. Carbon isotopes of trees from arid environments and implications for reconstructing atmospheric CO_2 concentrations. Geochimica et Cosmochimica Acta 59, 2599-2608.

Ferrio, J.P., Voltas, J., 2005. Carbon and oxygen isotope ratios in wood constituents of *Pinus halepensis* as indicators of precipitation, temperature and vapour pressure deficit. Tellus B 57, 164-173.

Fichtler, E., Clark, D.A., Worbes, M., 2003. Age and long-term growth of trees in an old-growth tropical rain forest, based on analyses of tree rings and C-14. Biotropica 35, 306-317.

Fichtler, E., Helle, G., Worbes, M., 2010. Stable-Carbon Isotope Time Series from Tropical Tree Rings Indicate a Precipitation Signal. Tree-Ring Research 66, 35-49.

Fonti, P., von Arx, G., García-González, I., Eilmann, B., Sass-Klaassen, U., Gärtner, H., Eckstein, D., 2010. Studying global change through investigation of the plastic responses of xylem anatomy in tree rings. New Phytologist 185, 42-53.

Forster, T., Schweingruber, F.H., Denneler, B., 2000. Increment puncher - A tool for extracting small cores of wood and bark from living trees. Iawa Journal 21, 169-180.

Fowler, A.M., Boswijk, G., Lorrey, A.M., Gergis, J., Pirie, M., McCloskey, S.P.J., Palmer, J.G., Wunder, J., 2012. Multi-centennial tree-ring record of ENSO-related activity in New Zealand. Nature Clim. Change 2, 172-176.

Fritts, H.C., 1976. Tree Rings and Climate. Cambridge University Press, Cambridge, London.

Gagen, M., McCarroll, D., Loader, N., Robertson, I., 2011. Stable Isotopes in Dendroclimatology: Moving Beyond 'Potential', In: Hughes, M.K., Swetnam, T.W., Diaz, H.F. (Eds.), Dendroclimatology. Springer Netherlands, pp. 147-172.

Gärtner, H., Nievergelt, D., 2010. The core-microtome: A new tool for surface preparation on cores and time series analysis of varying cell parameters. Dendrochronologia 28, 85-92.

Gat, J.R., 1996. Oxygen and hydrogen isotopes in the hydrologic cycle. Annu. Rev. Earth Planet. Sci. 24, 225-262.

Gaudinski, J.B., Dawson, T.E., Quideau, S., Schuur, E.A.G., Roden, J.S., Trumbore, S.E., Sandquist, D.R., Oh, S.-W., Wasylishen, R.E., 2005. Comparative Analysis of Cellulose Preparation Techniques for Use with 13C, 14C, and 18O Isotopic Measurements. Analytical Chemistry 77, 7212-7224.

Gebrekirstos, A., Worbes, M., Teketay, D., Fetene, M., Mitlöhner, R., 2009. Stable carbon isotope ratios in tree rings of co-occurring species from semi-arid tropics in Africa: Patterns and climatic signals. Global and Planetary Change 66, 253-260.

Gehre, M., Geilmann, H., Richter, J., Werner, R.A., Brand, W.A., 2004. Continuous flow 2H/1H and 18O/16O analysis of water samples with dual inlet precision. Rapid Communications in Mass Spectrometry 18, 2650-2660.

Geiger, F., 1915. Anatomische Untersuchungen über die Jahresringbildung von Tectona grandis, In: Pfeffer, W. (Ed.), Jahrbücher für wissenschaftliche Botanik.

Gessler, A., Brandes, E., Buchmann, N., Helle, G., Rennenberg, H., Barnard, R.L., 2009. Tracing carbon and oxygen isotope signals from newly assimilated sugars in the leaves to the tree-ring archive. Plant, Cell & Environment 32, 780-795.

Gleixner, G., Danier, H.J., Werner, R.A., Schmidt, H.L., 1993. Correlations between the ^{13}C content of primary and secondary plant products in different cell comapartments and that in decomposing basidiomycetes. Plant Physiology 102, 1287-1290.

Green, J.W., Whistler, E., 1963. Wood Cellulose, Methods in Carbohydrate Chemistry III. Academic Press, New York, pp. 9-21.

Grießinger, J., Bräuning, A., Helle, G., Thomas, A., Schleser, G., 2011. Late Holocene Asian summer monsoon variability reflected by d18O in tree-rings from Tibetan junipers. Geophys. Res. Lett. 38, L03701.

Grinsted, A., Moore, J.C., Jevrejeva, S., 2004. Application of the cross wavelet transform and wavelet coherence to geophysical time series. Nonlin. Processes Geophys. 11, 561-566.

Hackert, E.C., Hastenrath, S., 1986. Mechanisms of Java Rainfall Anomalies. Monthly Weather Review 114, 745-757.

Harlow, B.A., Marshall, J.D., Robinson, A.P., 2006. A multi-species comparison of $\delta^{13}C$ from whole wood, extractive-free wood and holocellulose. Tree Physiology 26, 767-774.

Harrington, K.J., Higgins, H.G., Michell, A.J., 1964. Infrared Spectra of Eucalyptus regnans F. Muell. and Pinus radiata D. Don, Holzforschung - International Journal of the Biology, Chemistry, Physics and Technology of Wood, p. 108.

Hastenrath, S., 1991. Rainfall Anomalies in Indonesia, Climate dynamics of the tropics. Kluwer Academic Publishers, Dordrecht, The Netherlands, p. 488.

Haylock, M., McBride, J., 2001. Spatial Coherence and Predictability of Indonesian Wet Season Rainfall. J. Clim. 14, 3882-3887.

Heinrich, I., Touchan, R., Dorado Liñán, I., Vos, H., Helle, G., 2013. Winter-to-spring temperature dynamics in Turkey derived from tree rings since AD 1125. Climate Dynamics 41, 1685-1701.

Heinrich, I., Weidner, K., Helle, G., Vos, H., Banks, J.C.G., 2008. Hydroclimatic variation in Far North Queensland since 1860 inferred from tree rings. Palaeogeography, Palaeoclimatology, Palaeoecology 270, 116-127.

Helle, G., Schleser, G.H., 2004a. Beyond CO_2-fixation by Rubisco – an interpretation of $^{13}C/^{12}C$ variations in tree rings from novel intra-seasonal studies on broad-leaf trees. Plant, Cell and Environment 27, 367-380.

Helle, G., Schleser, G.H., 2004b. Interpreting climate proxies from tree-rings, In: Fischer, H., Floeser, G., Kumke,T., Lohmann, G., Miller, H., Negendank, J.F.W., von Storch, H. (Ed.), The KIHZ project: Towards a synthesis of Holocene proxy data and climate models, pp. 129-148.

Hendon, H.H., 2003. Indonesian Rainfall Variability: Impacts of ENSO and Local Air-Sea Interaction. J. Clim. 16, 1775-1790.

Hennig, K., Helle, G., Heinrich, I., Neuwirth, B., Karyanto, O., Winiger, M., 2011. Toward multi-parameter records (ring width, $\delta^{13}C$, $\delta^{18}O$) from tropical tree-rings - A case study on Tectona grandis from Java, Indonesia, TRACE 2010 Proceedings of the DENDROSYMPOSIUM 2010, Freiburg, Germany, pp. 158-165.

Hietz, P., Turner, B.L., Wanek, W., Richter, A., Nock, C.A., Wright, S.J., 2011. Long-Term Change in the Nitrogen Cycle of Tropical Forests. Science 334, 664-666.

Hietz, P., Wanek, W., Dunisch, O., 2005. Long-term trends in cellulose $\delta^{13}C$ and water-use efficiency of tropical Cedrela and Swietenia from Brazil. Tree Physiology 25, 745-752.

Holmes, R.L., 1983. Computer-assisted quality control in tree-ring dating and measurement. Tree-Ring Bulletin 43 69-78.

Huffman, G.J., Adler, R.F., Bolvin, D.T., Gu, G., 2009. Improving the global precipitation record: GPCP Version 2.1. Geophysical Research Letters 36, L17808.

Hughes, M.K., 2011. Dendroclimatology in High-Resolution Paleoclimatology, In: Hughes, M.K., Swetnam, T.W., Diaz, H.F. (Eds.), Dendroclimatology. Springer Netherlands, pp. 17-34.

IPCC, 2013. Climate Change 2013: The Physical Science Basis. Contribution of Working Group I to the Fifth Assessment Report of the Intergovernmental Panel on Climate Change, In: Stocker, T.F., Qin, D., Plattner, G.-K., Tignor, M., Allen, S.K., Boschung, J., Nauels, A., Xia, Y., Bex, V., Midgley, P.M. (Eds.). Cambridge University Press, Cambridge, United Kingdom and New York, NY, USA, p. 1535.

Jacoby, G.C., D'Arrigo, R.D., 1990. Teak (*Tectona grandis* L.F.), a tropical species of large-scale dendroclimatic potential. Dendrochronologia 8, 83-98.

Jones, P.D., Hulme, M., 1996. Calculating regional climatic time series for temperature and precipitation: Methods and illustrations. International Journal of Climatology 16, 361-377.

Jourdain, N., Gupta, A., Taschetto, A., Ummenhofer, C., Moise, A., Ashok, K., 2013. The Indo-Australian monsoon and its relationship to ENSO and IOD in reanalysis data and the CMIP3/CMIP5 simulations. Climate Dynamics 41, 3073-3102.

Kagawa, A., Nakatsuka, T., 2014. A novel method for extracting α-cellulose directly from tree-ring laths, 9th International Conference on Dendrochronology, Melbourne, Australia.

Kagawa, A., Nakatsuka, T., Zhang, C., Yasue, K., Helle, G., 2012. A method for extracting α-cellulose directly from tree-ring laths, TRACE 2012, Potsdam, Germany.

Kao, H.-Y., Yu, J.-Y., 2009. Contrasting Eastern-Pacific and Central-Pacific Types of ENSO. J. Clim. 22, 615-632.

Kaplan, A., Cane, M., Kushnir, Y., Clement, A., Blumenthal, M., Rajagopalan, B., 1998. Analyses of global sea surface temperature 1856–1991. Journal of Geophysical Research-Oceans 103, 18567-18589.

Karamperidou, C., Di Nezio, P.N., Timmermann, A., Jin, F.-F., Cobb, K., submitted. The response of ENSO flavors to mid-Holocene climate: Implications for proxy interpretation. Palaeoceanography.

Krepkowski, J., Bräuning, A., Gebrekirstos, A., Strobl, S., 2011. Cambial growth dynamics and climatic control of different tree life forms in tropical mountain forest in Ethiopia. Trees 25, 59-70.

Krepkowski, J., Gebrekirstos, A., Shibistova, O., Bräuning, A., 2013. Stable carbon isotope labeling reveals different carry-over effects between functional types of tropical trees in an Ethiopian mountain forest. New Phytologist 199, 431-440.

Kug, J.-S., Ham, Y.-G., 2011. Are there two types of La Nina? Geophysical Research Letters 38, L16704.

Kug, J.-S., Jin, F.-F., An, S.-I., 2009. Two Types of El Niño Events: Cold Tongue El Niño and Warm Pool El Niño. J. Clim. 22, 1499-1515.

Kumar, K.K., Rajagopalan, B., Hoerling, M., Bates, G., Cane, M., 2006. Unraveling the Mystery of Indian Monsoon Failure During El Niño. Science 314, 115-119.

Kürschner, W.M., van der Burgh, J., Visscher, H., Dilcher, D.L., 1996. Oak leaves as biosensors of late neogene and early pleistocene paleoatmospheric CO_2 concentrations. Marine Micropaleontology 27, 299-312.

Larkin, N.K., Harrison, D.E., 2005. On the definition of El Niño and associated seasonal average U.S. weather anomalies. Geophysical Research Letters 32, L13705.

Lau, N.-C., Nath, M.J., 2000. Impact of ENSO on the Variability of the Asian–Australian Monsoons as Simulated in GCM Experiments. J. Clim. 13, 4287-4309.

Laumer, W., Andreu, L., Helle, G., Schleser, G.H., Wieloch, T., Wissel, H., 2009. A novel approach for the homogenization of cellulose to use micro-amounts for stable isotope analyses. Rapid Communications in Mass Spectrometry 23, 1934-1940.

Leavitt, S.W., 1993. Seasonal $^{13}C/^{12}C$ changes in tree rings: species and site coherence, and a possible drought influence. Canadian Journal of Forest Research 23, 210-218.

Leavitt, S.W., 2010. Tree-ring C–H–O isotope variability and sampling. Science of the Total Environment 408, 5244-5253.

Leavitt, S.W., Chase, T.N., Rajagopalan, B., Lee, E., Lawrence, P.J., Woodhouse, C.A., 2007. Southwestern U.S. Drought Maps from pinyon tree-ring carbon isotopes. EOS 88 39-40.

Leavitt, S.W., Danzer, S.R., 1993. Method for Batch Processing Small Wood Samples to Holocellulose for Stable-Carbon Isotope Analysis. Analytical Chemistry 65, 87-89.

Leavitt, S.W., Long, A., 1982. Stable carbon isotopes as a potential supplemental tool in dendrochronology. Tree-Ring Bulletin 42, 49-55.

Leavitt, S.W., Long, A., 1984. Sampling strategy for stable carbon isotope analysis of tree rings in pine. Nature 311.

Lee, T., McPhaden, M.J., 2010. Increasing intensity of El Niño in the central-equatorial Pacific. Geophys. Res. Lett. 37, L14603.

Leuenberger, M., 2007. To what extent can ice core data contribute to the understanding of plant ecological developments of the past?, In: Dawson, T., Siegwolf, R. (Eds.), Stable isotopes as indicators of ecological change. Academic Press, London, pp. 211-234.

Li, Z.-H., Labbé, N., Driese, S.G., Grissino-Mayer, H.D., 2011. Micro-scale analysis of tree-ring $\delta^{18}O$ and $\delta^{13}C$ on α-cellulose spline reveals high-resolution intra-annual climate variability and tropical cyclone activity. Chemical Geology 284, 138-147.

Liang, W., Heinrich, I., Simard, S., Helle, G., Dorado Liñán, I., Heinken, T., 2013. Climate signals derived from cell anatomy of Scots pine in NE-Germany. Tree Physiology 33, 833-844.

Linsley, B.K., Wellington, G.M., Schrag, D.P., Ren, L., Salinger, M.J., Tudhope, A.W., 2004. Geochemical evidence from corals for changes in the amplitude and spatial pattern of South Pacific interdecadal climate variability over the last 300 years. Climate Dynamics 22, 1-11.

Loader, N.J., Robertson, I., Barker, A.C., Switsur, V.R., Waterhouse, J.S., 1997. An improved technique for the batch processing of small wholewood samples to a-cellulose. Chemical Geology 136, 313-317.

Loader, N.J., Robertson, I., L cke, A., Helle, G., 2002. Preparation of hollocellulose from standard increment cores for stable carbon isotope analysis. Swansea Geographer 37 1-9.

Loader, N.J., Robertson, I., McCarroll, D., 2003. Comparison of stable carbon isotope ratios in the whole wood, cellulose and lignin of oak tree-rings. Palaeogeography Palaeoclimatology Palaeoecology 196, 395-407.

Loader, N.J., Switsur, V.R., Field, E.M., 1995. High-resolution stable isotope analysis of tree rings: Implications of 'microdendroclimatology' for palaeoenvironmental research. The Holocene 5, 457-460.

Loader, N.J., Walsh, R.P.D., Robertson, I., Bidin, K., Ong, R.C., Reynolds, G., McCarroll, D., Gagen, M., Young, G.H.F., 2011. Recent trends in the intrinsic water-use efficiency of ringless rainforest trees in Borneo. Philosophical Transactions of the Royal Society B: Biological Sciences 366, 3330-3339.

Loader, N.J., Young, G.H., McCarroll, D., Wilson, R.J., 2013. Quantifying uncertainty in isotope dendroclimatology. The Holocene.

Managave, S.R., Sheshshayee, M., Bhattacharyya, A., Ramesh, R., 2010a. Intra-annual variations of teak cellulose $\delta^{18}O$ in Kerala, India: implications to the reconstruction of past summer and winter monsoon rains. Climate Dynamics, 1-13.

Managave, S.R., Sheshshayee, M.S., Borgaonkar, H.P., Ramesh, R., 2010b. Past break-monsoon conditions detectable by high resolution intra-annual $d^{18}O$ analysis of teak rings. Geophysical Research Letters 37, L05702.

Managave, S.R., Sheshshayee, M.S., Ramesh, R., Borgaonkar, H.P., Shah, S.K., Bhattacharyya, A., 2011. Response of cellulose oxygen isotope values of teak trees in differing monsoon environments to monsoon rainfall. Dendrochronologia 29, 89-97.

Mann, M.E., Gille, E., Overpeck, J., Gross, W., Bradley, R.S., Keimig, F.T., Hughes, M.K., 2000. Global Temperature Patterns in Past Centuries: An Interactive Presentation. Earth Interactions 4, 1-1.

McBride, J., 1999. Indonesia, Papua New Guinea, and tropical Australia: the southern hemisphere monsoon, In: Karoly, D., Vincen, t.D. (Eds.), Meteorology of Southern Hemisphere, Boston, pp. 89-98.

McCarroll, D., Loader, N.J., 2004. Stable isotopes in tree rings. Quaternary Science Reviews 23, 771-801.

McPhaden, M.J., Lee, T., McClurg, D., 2011. El Niño and its relationship to changing background conditions in the tropical Pacific Ocean. Geophysical Research Letters 38, L15709.

McPhaden, M.J., Zebiak, S.E., Glantz, M.H., 2006. ENSO as an Integrating Concept in Earth Science. Science 314, 1740-1745.

Mitchell, T.D., Jones, P.D., 2005. An improved method of constructing a database of monthly climate observations and associated high-resolution grids. International Journal of Climatology 25, 693-712.

Murphy, J.O., Whetton, P.H., Ritsema, A.R., 1989. A re-analysis of a tree ring chronology from Java. North-Holland, Amsterdam.

Nakatsuka, T., Zhang, C., Yasue, K., Kagawa, A., 2011. Extracting α-cellulose from tree-ring laths - a new method for tree ring stable isotope analysis, 2nd International Asian Dendrochronological Conference, Xian, China.

Nelson, T., Tausta, S.L., Gandotra, N., Liu, T., 2006. Laser microdissection of plant tissue: What You See Is What You Get. Annual Review of Plant Biology 57, 181-201.

Newman, M., Shin, S.-I., Alexander, M.A., 2011. Natural variation in ENSO flavors. Geophysical Research Letters 38, L14705.

Nock, C.A., Baker, P.J., Wanek, W., Leis, A., Grabner, M., Bunyavejchewin, S., Hietz, P., 2011. Long-term increases in intrinsic water-use efficiency do not lead to increased stem growth in a tropical monsoon forest in western Thailand. Global Change Biology 17, 1049-1063.

O'Kane, T.J., Matear, R.J., Chamberlain, M.A., Oke, P.R., 2014. ENSO regimes and the late 1970's climate shift: The role of synoptic weather and South Pacific ocean spiciness. Journal of Computational Physics 271, 19-38.

Ogée, J., Barbour, M.M., Wingate, L., Bert, D., Bosc, A., Stievenard, M., Lambrot, C., Pierre, M., Bariac, T., Loustau, D., Dewar, R.C., 2009. A single-substrate model to interpret intra-annual stable isotope signals in tree-ring cellulose. Plant, Cell & Environment 32, 1071-1090.

Ogle, N., McCormac, F.G., 1994. High-resolution $d^{13}C$ measurements of oak show a previously unobserved spring depletion Geophysical Research Letters 21, 2373-2375.

Olano, J.M., Arzac, A., García-Cervigón, A.I., von Arx, G., Rozas, V., 2013. New star on the stage: amount of ray parenchyma in tree rings shows a link to climate. New Phytologist 198, 486-495.

Pandey, K., Theagarajan, K., 1997. Analysis of wood surfaces and ground wood by diffuse reflectance (DRIFT) and photoacoustic (PAS) Fourier transform infrared spectroscopic techniques. European Journal of Wood and Wood Products 55, 383-390.

Pandey, K.K., 1999. A study of chemical structure of soft and hardwood and wood polymers by FTIR spectroscopy. Journal of Applied Polymer Science 71, 1969-1975.

Pandey, K.K., Pitman, A.J., 2003. FTIR studies of the changes in wood chemistry following decay by brown-rot and white-rot fungi. Int Biodeter Biodegr 52, 151-160.

Pfeiffer, M., Dullo, W.-C., Zinke, J., Garbe-Schönberg, D., 2009. Three monthly coral Sr/Ca records from the Chagos Archipelago covering the period of 1950–1995 A.D.: reproducibility and implications for quantitative reconstructions of sea surface temperature variations. International Journal of Earth Sciences 98, 53-66.

Pons, T., Helle, G., 2011. Identification of anatomically non-distinct annual rings in tropical trees using stable isotopes. Trees - Structure and Function 25, 83-93.

Ponton, S., Dupouey, J.L., Breda, N., Feuillat, F., Bodenes, C., Dreyer, E., 2001. Carbon isotope discrimination and wood anatomy variations in mixed stands of *Quercus robur* and *Quercus petraea*. Plant Cell and Environment 24, 861-868.

Poussart, P.F., Evans, M.N., Schrag, D.P., 2004. Resolving seasonality in tropical trees: multi-decade, high-resolution oxygen and carbon isotope records from Indonesia and Thailand. Earth and Planetary Science Letters 218, 301-316.

Poussart, P.F., Schrag, D.P., 2005. Seasonally resolved stable isotope chronologies from northern Thailand deciduous trees. Earth and Planetary Science Letters 235, 752-765.

Pumijumnong, N., 2013. Dendrochronology in Southeast Asia. Trees-Structure and Function 27, 343-358.

Pumijumnong, N., Eckstein, D., 2011. Reconstruction of pre-monsoon weather conditions in northwestern Thailand from the tree-ring widths of *Pinus merkusii* and *Pinus kesiya*. Trees - Structure and Function 25, 125-132.

Pumijumnong, N., Eckstein, D., Sass, U., 1995. Tree-ring research on *Tectona grandis* on northern Thailand. Iawa Journal 16, 385-392.

Quinn, T.M., Taylor, F.W., Crowley, T.J., 2006. Coral-based climate variability in the Western Pacific Warm Pool since 1867. Journal of Geophysical Research: Oceans 111, C11006.

Ram, S., Borgaonkar, H., Sikder, A., 2008. Tree-ring analysis of teak (*Tectona grandis* L.F.) in central India and its relationship with rainfall and moisture index. Journal of Earth System Science 117, 637-645.

Rayner, N.A., Brohan, P., Parker, D.E., Folland, C.K., Kennedy, J.J., Vanicek, M., Ansell, T.J., Tett, S.F.B., 2006. Improved Analyses of Changes and Uncertainties in Sea Surface Temperature Measured In Situ since the Mid-Nineteenth Century: The HadSST2 Dataset. J. Clim. 19, 446-469.

Ren, H.-L., Jin, F.-F., 2011. Niño indices for two types of ENSO. Geophysical Research Letters 38, L04704.

Riemer, T., 1994. Über die Varianz von Jahrringbreiten. Statistische Methoden für die Auswertung der jährlichen Dickenzuwächse von Bäumen unter sich ändernden Lebensbedingungen. Berichte des Forschungszentrums Waldökosysteme 121. Göttingen.

Rinn, F., 2005. TSAP - WinTM. Time Series Analysis and Presentation for Dendrochronology and Related Applications. Version 4.6, Heidelberg.

Rinne, K.T., Boettger, T., Loader, N.J., Robertson, I., Switsur, V.R., Waterhouse, J.S., 2005. On the purification of α-cellulose from resinous wood for stable isotope (H, C and O) analysis. Chemical Geology 222, 75-82.

Robert, E.R., Schmitz, N., Okello, J., Boeren, I., Beeckman, H., Koedam, N., 2011. Mangrove growth rings: fact or fiction? Trees 25, 49-58.

Robertson, I., Loader, N.J., Froyd, C.A., Zambatis, N., Whyte, I., Woodborne, S., 2006. The potential of the baobab (*Adansonia digitata* L.) as a proxy climate archive. Applied Geochemistry 21, 1674-1680.

Roden, J.S., Johnstone, J.A., Dawson, T.E., 2009. Intra-annual variation in the stable oxygen and carbon isotope ratios of cellulose in tree rings of coast redwood (*Sequoia sempervirens*). The Holocene 19, 189-197.

Roden, J.S., Lin, G., Ehleringer, J.R., 2000. A mechanistic model for interpretation of hydrogen and oxygen isotope ratios in tree-ring cellulose. Geochimica et Cosmochimica Acta 64, 21-35.

Rossi, L., Sebastiani, L., Tognetti, R., d'Andria, R., Morelli, G., Cherubini, P., 2013. Tree-ring wood anatomy and stable isotopes show structural and functional adjustments in olive trees under different water availability. Plant and Soil 372, 567-579.

Rossi, S., Anfodillo, T., Menardi, R., 2006. Trephor: A new tool for sampling microcores from tree stems. Iawa Journal 27, 89-97.

Sano, M., Buckley, B., Sweda, T., 2009. Tree-ring based hydroclimate reconstruction over northern Vietnam from *Fokienia hodginsii*: eighteenth century mega-drought and tropical Pacific influence. Climate Dynamics 33, 331-340.

Sano, M., Xu, C., Nakatsuka, T., 2012. A 300-year Vietnam hydroclimate and ENSO variability record reconstructed from tree ring $d^{18}O$. Journal of Geophysical Research 117, D12115.

Sarachik, E.S., Cane, M.A., 2010. The El Niño-Southern Oscillation Phenomenon. Cambridge University Press, London.

Sarris, D., Siegwolf, R., Körner, C., 2013. Inter- and intra-annual stable carbon and oxygen isotope signals in response to drought in Mediterranean pines. Agricultural and Forest Meteorology 168, 59-68.

Saurer, M., Cherubini, P., Reynolds-Henne, C.E., Treydte, K.S., Anderson, W.T., Siegwolf, R.T.W., 2008. An investigation of the common signal in tree ring stable isotope chronologies at temperate sites. J Geophys Res-Biogeo 113.

Saurer, M., Cherubini, P., Siegwolf, R., 2000. Oxygen isotopes in tree rings of *Abies alba* : The climatic significance of interdecadal variations. Journal of Geophysical Research 105, 12461-12470.

Saurer, M., Robertson, I., Siegwolf, R., Leuenberger, M., 1998. Oxygen Isotope Analysis of Cellulose: An Interlaboratory Comparison. Analytical Chemistry 70, 2074-2080.

Schleser, G.H., Helle, G., Lucke, A., Vos, H., 1999a. Isotope signals as climate proxies: the role of transfer functions in the study of terrestrial archives. Quaternary Science Reviews 18, 927-943.

Schleser, G.H., Helle, G., Lücke, A., Vos, H., 1999b. Isotope signals as climate proxies: the role of transfer functions in the study of terrestrial archives. Quaternary Science Reviews 18, 927-943.

Schollaen, K., Heinrich, I., Helle, G., 2014. UV-laser-based microscopic dissection of tree rings – a novel sampling tool for $\delta^{13}C$ and $\delta^{18}O$ studies. New Phytologist 201, 1045-1055.

Schollaen, K., Heinrich, I., Neuwirth, B., Krusic, P.J., D'Arrigo, R.D., Karyanto, O., Helle, G., 2013. Multiple tree-ring chronologies (ring width, $\delta^{13}C$ and $\delta^{18}O$) reveal dry and rainy season signals of rainfall in Indonesia. Quaternary Science Reviews 73, 170-181.

Schöngart, J., Junk, W.J., Piedade, M.T.F., Ayres, J.M., Hüttermann, A., Worbes, M., 2004. Teleconnection between tree growth in the Amazonian floodplains and the El Niño–Southern Oscillation effect. Global Change Biology 10, 683-692.

Schöngart, J., Piedade, M.T.F., Ludwigshausen, S., Horna, V., Worbes, M., 2002. Phenology and stem-growth periodicity of tree species in Amazonian floodplain forests. Journal of Tropical Ecology 18, 581-597.

Schubert, B.A., Jahren, A.H., 2011. Quantifying seasonal precipitation using high-resolution carbon isotope analyses in evergreen wood. Geochimica et Cosmochimica Acta 75, 7291-7303.

Schubert, B.A., Jahren, A.H., 2012. The effect of atmospheric CO_2 concentration on carbon isotope fractionation in C_3 land plants. Geochimica et Cosmochimica Acta 96, 29-43.

Schulman, E., 1956. Dendroclimatic Change in Semiarid America. University of Arizona Press, Tuscon, Arizona.

Schulz, M., Mudelsee, M., 2002. REDFIT: estimating red-noise spectra directly from unevenly spaced paleoclimatic time series. Computers & Geosciences 28, 421-426.

Schulze, B., Wirth, C., Linke, P., Brand, W.A., Kuhlmann, I., Horna, V., Schulze, E.D., 2004. Laser ablation-combustion-GC-IRMS - a new method for online analysis of intra-annual variation of $d^{13}C$ in tree rings. Tree Physiology 24, 1193-1201.

Schweingruber, F.H., 1983. Der Jahrring: Standort, Methodik, Zeit und Klima in der Dendrochronologie. Paul Haupt, Bern.

Schweingruber, F.H., Eckstein, D., Serre-Bachet, F., Bräker, O.U., 1990. Identification, presentation and interpretation of event years and pointer years in dendrochronology. Dendrochronologia 8, 9-38.

Shah, S.K., Bhattacharyya, A., Chaudhary, V., 2007. Reconstruction of June–September precipitation based on tree-ring data of teak (*Tectona grandis* L.) from Hoshangabad, Madhya Pradesh, India. Dendrochronologia 25, 57-64.

Skomarkova, M.V., Vaganov, E.A., Mund, M., Knohl, A., Linke, P., Boerner, A., Schulze, E.D., 2006. Inter-annual and seasonal variability of radial growth, wood density and carbon isotope ratios in tree rings of beech (*Fagus sylvatica*) growing in Germany and Italy. Trees-Structure and Function 20, 571-586.

Slotta, F., Riedel, F., Heußner, K.-U., Helle, G., 2014. The African Baobab – a high-resolution archive for climate variability of semi-arid Africa?, 9th International Conference on Dendrochronology, Melbourne, Australia.

Stahle, D.W., 1999. Useful strategies for the development of tropical tree-ring chronologies. IAWA 20, 249-253.

Stahle, D.W., Cleaveland, M.K., Therrell, M.D., Gay, D.A., D'Arrigo, R.D., Krusic, P.J., Cook, E.R., Allan, R.J., Cole, J.E., Dunbar, R.B., Moore, M.D., Stokes, M.A., Burns, B.T., Villanueva-Diaz, J., Thompson, L.G., 1998. Experimental Dendroclimatic Reconstruction of the Southern Oscillation. Bulletin of the American Meteorological Society 79, 2137–2152.

Sternberg, L.d.S.L.O.R., 2009. Oxygen stable isotope ratios of tree-ring cellulose: the next phase of understanding. New Phytologist 181, 553-562.

Stokes, M.A., Smiley, T.L., 1968. An Introduction to Tree-ring Dating. University of Arizona Press, Tuscon.

Sukanto, M., 1969. Climate of Indonesia, In: Arakawa, H. (Ed.), Climate of Northern and Eastern Asia.

Szymczak, S., Joachimski, M.M., Bräuning, A., Hetzer, T., Kuhlemann, J., 2011. Comparison of whole wood and cellulose carbon and oxygen isotope series from Pinus nigra ssp. laricio (Corsica/France). Dendrochronologia 29, 219-226.

Takahashi, K., Montecinos, A., Goubanova, K., Dewitte, B., 2011. ENSO regimes: Reinterpreting the canonical and Modoki El Niño. Geophysical Research Letters 38, L10704.

Taschetto, A.S., England, M.H., 2009. El Niño Modoki impacts on Australian rainfall. J. Clim. 22, 3167-3174.

Taylor, A.M., Renée Brooks, J., Lachenbruch, B., Morrell, J.J., Voelker, S., 2008. Correlation of carbon isotope ratios in the cellulose and wood extractives of Douglas-fir. Dendrochronologia 26, 125-131.

Therrell, M., Stahle, D., Ries, L., Shugart, H., 2006. Tree-ring reconstructed rainfall variability in Zimbabwe. Climate Dynamics 26, 677-685.

Torrence, C., Compo, G.P., 1998. A Practical Guide to Wavelet Analysis. Bulletin of the American Meteorological Society 79, 61-78.

Treydte, K.S., Schleser, G.H., Helle, G., Frank, D.C., Winiger, M., Haug, G.H., Esper, J., 2006. The twentieth century was the wettest period in northern Pakistan over the past millennium. Nature 440, 1179-1182.

Trouet, V., Esper, J., Beeckman, H., 2010. Climate/growth relationships of Brachystegia spiciformis from the miombo woodland in south central Africa. Dendrochronologia 28, 161-171.

Tudhope, A.W., Chilcott, C.P., McCulloch, M.T., Cook, E.R., Chappell, J., Ellam, R.M., Lea, D.W., Lough, J.M., Shimmield, G.B., 2001. Variability in the El Niño - Southern oscillation through a glacial-interglacial cycle. Science 291, 1511-1517.

Ummenhofer, C., D'Arrigo, R., Anchukaitis, K., Buckley, B., Cook, E., 2013. Links between Indo-Pacific climate variability and drought in the Monsoon Asia Drought Atlas. Climate Dynamics 40, 1319-1334.

Vaganov, E., Schulze, E.-D., Skomarkova, M., Knohl, A., Brand, W., Roscher, C., 2009. Intra-annual variability of anatomical structure and $\delta^{13}C$ values within tree rings of spruce and pine in alpine, temperate and boreal Europe. Oecologia 161, 729-745.

Van de Water, P.K., 2002. The effect of chemical processing on the $d^{13}C$ value of plant tissue. Geochimica et Cosmochimica Acta 66, 1211-1219.

Verheyden, A., Helle, G., Schleser, G.H., Dehairs, F., Beeckman, H., Koedam, N., 2004a. Annual cyclicity in high-resolution stable carbon and oxygen isotope ratios in the wood of the mangrove tree *Rhizophora mucronata*. Plant Cell and Environment 27, 1525-1536.

Verheyden, A., Kairo, J.G., Beeckman, H., Koedam, N., 2004b. Growth rings, growth ring formation and age determination in the mangrove *Rhizophora mucronata*. Annals of Botany 94, 59-66.

Verheyden, A., Roggeman, M., Bouillon, S., Elskens, M., Beeckman, H., Koedam, N., 2005. Comparison between $\delta^{13}C$ of α-cellulose and bulk wood in the mangrove tree *Rhizophora mucronata*: Implications for dendrochemistry. Chemical Geology 219, 275-282.

Visser, H., Molenaar, J., 1988. Kalman Filter Analysis in Dendroclimatology. Biometrics 44, 929-940.

Volland-Voigt, F., Bräuning, A., Ganzhi, O., Peters, T., Maza, H., 2011. Radial stem variations of Tabebuia chrysantha (Bignoniaceae) in different tropical forest ecosystems of southern Ecuador. Trees 25, 39-48.

Walcroft, A.S., Silvester, W.B., Whitehead, D., Kelliher, F.M., 1997. Seasonal Changes in Stable Carbon Isotope Ratios within Annual Rings of *Pinus radiata* Reflect Environmental Regulation of Growth Processes. Functional Plant Biology 24, 57-68.

Walter, H., Breckle, S.W., 1991. Ökologische Grundlagen in globaler Sicht. Fischer, Stuttgart.

Wan, H., Zhang, X., Zwiers, F.W., Shiogama, H., 2013. Effect of data coverage on the estimation of mean and variability of precipitation at global and regional scales. Journal of Geophysical Research: Atmospheres 118, 534-546.

Werner, C., Schnyder, H., Cuntz, M., Keitel, C., Zeeman, M.J., Dawson, T.E., Badeck, F.-W., Brugnoli, E., Ghashghaie, J., Grams, T.E.E., Kayler, Z.E., Lakatos, M., Lee, X., M´aguas, C., Ogée, J., Rascher, K.G., Siegwolf, R.T.W., Unger, S., Welker, J., L.Wingate, Gessler, A., 2012. Progress and challenges in using stable isotopes to trace plant carbon and water relations across scales. Biogeosciences 9, 3083–3111.

West, J.B., Bowen, G.J., Dawson, T.E., Tu, K.P., 2010. Isoscapes: Understanding movement, pattern, and process on Earth through isotope mapping Springer Science+Business Media B.V., London.

Wheeler, M.C., McBride, J.L., 2005. Australian-Indonesian monsoon, Intraseasonal Variability in the Atmosphere-Ocean Climate System. Springer Berlin Heidelberg, pp. 125-173.

Wieloch, T., Helle, G., Heinrich, I., Voigt, M., Schyma, P., 2011. A novel device for batch-wise isolation of a-cellulose from small-amount wholewood samples. Dendrochronologia 29, 115-117.

Wigley, T.M.L., Briffa, K.R., Jones, P.D., 1984. On the Average Value of Correlated Time-Series, with Applications in Dendroclimatology and Hydrometeorology. Journal of Climate and Applied Meteorology 23, 201-213.

Wilson, A.T., Grinsted, M.J., 1977. $^{12}C/^{13}C$ in cellulose and lignin as palaeothermometers. Nature 265, 133-135.

Wilson, R., Cook, E., D'Arrigo, R., Riedwyl, N., Evans, M.N., Tudhope, A., Allan, R., 2010. Reconstructing ENSO: the influence of method, proxy data, climate forcing and teleconnections. Journal of Quaternary Science 25, 62-78.

Wilson, R., Miles, D., Loader, N., Melvin, T., Cunningham, L., Cooper, R., Briffa, K., 2013. A millennial long March–July precipitation reconstruction for southern-central England. Climate Dynamics 40, 997-1017.

Wilson, R., Tudhope, A., Brohan, P., Briffa, K., Osborn, T., Tett, S., 2006. Two-hundred-fifty years of reconstructed and modeled tropical temperatures. Journal of Geophysical Research: Oceans 111, C10007.

Worbes, M., 1999. Annual growth rings, rainfall!dependent growth and long-term growth patterns of tropical trees from the Caparo Forest Reserve in Venezuela. Journal of Ecology 87.

Worbes, M., Blanchart, S., Fichtler, E., 2013. Relations between water balance, wood traits and phenological behavior of tree species from a tropical dry forest in Costa Rica—a multifactorial study. Tree Physiology 33, 527-536.

Wurster, C.M., Patterson, W.P., Cheatham, M.M., 1999. Advances in micromilling techniques: a new apparatus for acquiring high-resolution oxygen and carbon stable

isotope values and major/minor elemental ratios from accretionary carbonate. Computers & Geosciences 25, 1159-1166.

Xu, C., Sano, M., Nakatsuka, T., 2011. Tree ring cellulose d^{18}O of *Fokienia hodginsii* in northern Laos: A promising proxy to reconstruct ENSO? Journal of Geophysical Research 116, D24109.

Xu, C., Sano, M., Nakatsuka, T., 2013. A 400-year record of hydroclimate variability and local ENSO history in northern Southeast Asia inferred from tree-ring δ18O. Palaeogeography, Palaeoclimatology, Palaeoecology 386, 588-598.

Yeh, S.-W., Kug, J.-S., Dewitte, B., Kwon, M.-H., Kirtman, B.P., Jin, F.-F., 2009. El Niño in a changing climate. Nature 461, 511-514.

Yulihastin, E., Febrianti, N., Trismidianto, 2010. Impact of El Niño and IOD on the Indonesian Climate. National Institute of Aeronautics and Space (Lapan), Indonesia.

Zhu, M., Stott, L., Buckley, B., Yoshimura, K., Ra, K., 2012. Indo-Pacific Warm Pool convection and ENSO since 1867 derived from Cambodian pine tree cellulose oxygen isotopes. Journal of Geophysical Research 117, D11307.

Ziegler, H., 1995. Stable Isotopes in Plant Physiology and Ecology, In: Behnke, H.D., Lüttge, U., Esser, K., Kadereit, J., Runge, M. (Eds.), Progress in Botany. Springer Berlin Heidelberg, pp. 1-24.

Eidesstattliche Erklärung

Hiermit erkläre ich, dass ich die von mir vorgelegte Dissertation mit dem Titel "*Tracking climate signals in tropical trees - New insights from Indonesian stable isotope records*" selbstständig und nur unter Verwendung der angegebenen Quellen und Hilfsmittel angefertigt habe. Ich erkläre außerdem, dass diese Dissertation noch keiner anderen Fakultät oder Hochschule zur Prüfung vorgelegt wurde.

Declaration of Academic Honesty

I herewith declare, that I have prepared this thesis with the title "*Tracking climate signals in tropical trees - New insights from Indonesian stable isotope records*" on my own, using only the materials (devices) mentioned. This work has not been submitted to another examination office.

Potsdam, den 31. Januar 2014

Curriculum Vitae

This page contains personal data. It is thus not part of the online publication

Acknowledgements

It would not have been possible to write this thesis without the support of many people, to only some of whom it is possible to give particular mention here.
First of all I want to express my deep gratitude to my supervisors, Prof. Achim Brauer and Dr. Gerhard Helle, for supporting my PhD project. I thank Prof. Achim Brauer, the head of section 5.2 Climate dynamics and Landscape Evolution (GFZ), for guiding and encouraging me in every possible way and for providing an excellent working environment. I particularly thank Dr. Gerhard Helle for introducing me to the fascinating world of palaeoclimatology, for giving me the opportunity to work together in a great stable isotope laboratory and for your long-standing support since my diploma thesis. Your vast knowledge in the field of tree-ring stable isotopes, the careful reviewing of my manuscripts and the numerous discussions whenever necessary have been fundamental for the success of my work. You gave me valuable advices and at the same time you gave me the freedom to pursue my own ideas.

This thesis is the result of a close collaboration with excellent scientists and colleagues.

I would like to thank Dr. Ingo Heinrich, for reviewing several manuscripts and advising me in many ways. Thank you for keeping your door always open for questions and discussions!

I thank Heiko Baschek, Carmen Bürger and David Göhring for their invaluable support in the laboratory with a special thanks to Heiko for the very effective teamwork on the optimization of stable isotope techniques for high-resolution and high-throughput tree-ring isotope analysis.

A warm thank you goes to Paul Krusic for inspiring discussions during summer schools under the sun in Greece. I have learned a lot! I appreciate his efficient work on numerous manuscripts, significantly improving whatever I wrote and always within an incredible short time. Thank you for giving birth to the collaboration with Christina Karamperidou and Edward Cook, having enjoyable discussions about ENSO flavors.

Numerous colleagues have made life in the lab or behind the pc more fun: Thank you Tina, Sonia and Isabel for providing critical and valuable feedbacks during the last years. I thank Wei, Hagen, Thomas, Katja, Carola, Mandy, Antje, Franzi, Sandra and Julia for being great office and lab mates during my PhD time. I also thank numerous students who have worked with me in the lab. Our dendrolab owed lots of its charm to you, guys!

Furthermore, a lot of thanks goes to all the people of GFZ section 5.2 for creating a good working atmosphere. I particularly thank Christine Gerschke for guiding me through the administration of the GFZ, Markus Günzel for running my computer smoothly and Andreas Hendrich to make my figures more than perfect. Thanks to the all the section people for their help wherever necessary.

I am very grateful to my new colleagues from the AWI Potsdam, especially to Prof. Hans Hubberten and Prof. Hugues Lantuit, for their patience during the last month of finishing my thesis.

A special thank goes to Steffi and Tina for their support in many ways and the wonderful time we have together within and beyond the walls of the Telegrafenberg.

Zudem möchte ich mich noch bei meinen Freunden bedanken für ihr Interesse an meiner Arbeit, ihre Unterstützung und den Spaß den wir zusammen haben.

Schließlich danke ich besonders meiner ganzen Familie, v.a. meinen Eltern, Linda, Erika und Daniel für ihre stetige Unterstützung und Geduld. Ohne die Liebe und das unerschütterliche Vertrauen meiner Eltern, wäre ich weder eine „Diplom-Geographin“ geworden, noch hätte ich den Weg in die Forschung gefunden. Mein letzter und intensivster Dank geht an Uwe, für seine große Geduld, Liebe und Unterstützung. Danke, dass du dein Leben mit mir teilst!